REMARKS

Any fees that may be due in connection with the filing of this paper or with this application may be charged to Deposit Account No. 06-1050. If a Petition for Extension of time is needed, this paper is to be considered such Petition.

Claims 1-3, 6-10, 12-14, 22, 24, 31-34, 47, 50, 54-58, 61-80 and 82-110 are pending in this application. In the Preliminary Amendment and RCE filed January 28, 2008 (hereinafter, "RCE"), the claims were amended, in the interest of advancing prosecution, to specify that the therapeutic domain is a sialidase and the anchoring domain is a glycosaminoglycan (GAG) binding domain. The RCE is incorporated by reference herein in its entirety, and the claims are further amended herein. As amended, the claims specify that the compound has a sialidase domain containing a peptide or protein having sialidase activity, and an anchoring domain that binds to a glycosaminoglycan (GAG) on the surface of the target cell. In addition, new Claims 99-110, drawn to polypeptides containing a sialidase domain having sialidase activity and an anchoring domain that binds to a glycosaminoglycan (GAG) on the surface of a target cell, are added herein. Basis for the amended and added claims can be found in the claims as originally filed and in the specification, for example, at at page 4, lines 7-10 and 21-30; and at page 20, line 26 to page 21, line 30. No new matter is added.

In the RCE, Applicant also submitted that the withdrawal of Claim 80 as drawn to non-elected subject matter is improper. Claim 80, which is dependent on elected Claim 73, is a "combination" containing the "subcombination" of Claim 73. In the instant Office Action, the Examiner simply notes that Claims 50, 54-58, 80 and 82-93 "remain withdrawn." The Examiner provides no reason why the subject matter of Claim 80 is distinct from the elected Claim (Claim 73) on which it depends. Applicant respectfully resubmits that the withdrawal of Claim 80 from further consideration is improper (*see* discussion below), and asks that Claim 80 be examined with the remaining pending claims.

As noted in the RCE, method claims 50, 54-58 and 82-94, directed to non-elected subject matter, are retained for possible rejoinder upon allowance of product claims deemed allowable.

WITHDRAWAL OF CLAIM 80 FROM FURTHER CONSIDERATION AS BEING DRAWN TO NON-ELECTED SUBJECT MATTER

The Examiner includes Claim 80 among those that are withdrawn from further consideration as being drawn to non-elected subject matter. As noted in the RCE filed January 28, 2008, Applicant respectfully resubmits that the withdrawal is improper, and asks that Claim 80 be examined with the remaining pending claims.

Claim 80 as amended in the RCE is drawn to a delivery system containing the pharmaceutical formulation of Claim 73 and a nebulizer, an atomizer or a dropper bottle. Claims 80 and 73 are related as a combination (Claim 80) and subcombination (Claim 73). Inventions that are related as a combination and a subcombination are properly restrictable only if it can be shown that the combination as claimed does not require the particulars of the subcombination as claimed for patentability and the subcombination has utility by itself or in other combinations (MPEP §808.05(c)). In this instance, while the pharmaceutical formulation of Claim 73 (*i.e.*, the subcombination) can be used independently or in combination with components other than those specified in the delivery system of Claim 80, the combination of Claim 80, *i.e.*, the pharmaceutical formulation of Claim 73 combined with a nebulizer, an atomizer or a dropper bottle, requires the particulars of the pharmaceutical formulation of Claim 73 for patentability. Therefore, the two-way distinctness test set forth in MPEP §808.05(c) is not met, and Applicant asks that Claim 80 be examined with the remaining pending claims.

THE REJECTION UNDER 35 U.S.C. §112, FIRST PARAGRAPH- WRITTEN DESCRIPTION

Claims 1-3, 6-10, 12-14, 22, 24, 31-34, 47, 61-79 and 94-98 are rejected under 35 U.S.C. §112, first paragraph, as lacking adequate written description. The Examiner asserts that the specification does not adequately describe the structural and functional features commonly possessed by the genus of protein constructs containing a "therapeutic domain" that prevents pathogenic infection of a target cell by blocking entry of the pathogen into the cell, and an "anchoring domain" that binds to a molecule on the surface of the target cell. In support of this assertion, the Examiner alleges that the only exemplified constructs are those in which the therapeutic domain is the sialidase of SEQ ID NO: 8 or 9 and the anchoring domain is the GAG-binding domain of SEQ ID NOS: 2-7, and that these disclosed constructs are insufficient to put one of skill in the art in full possession of the claimed genus. He further alleges that no sequences that are "substantially homologous to" the disclosed sequences are described.

This rejection is traversed. First, in the interest of advancing the application to allowance, the claims were amended in the RCE filed January 28, 2008, to delete the phrase "substantially homologous to." Next, the claims as currently amended are drawn to a compound that includes "a sialidase domain comprising a peptide or protein having sialidase activity" and an "anchoring domain comprising a peptide or protein that binds to a glycosaminoglycan (GAG) on the surface of the target cell." As discussed below, both these protein domains, and their sequence-structure-activity correlations, are well-known in the art. Therefore, the description in the specification, when combined with the knowledge of those of skill in the art, leave no doubt that Applicant had possession of what is claimed.

Analysis

The specification lists numerous known sialidases. The specification also describes (and cites references to that effect) GAG-binding domains that have long been known to be present on a variety of proteins. No explicit recitation of each of their sequences, published in the various references cited in the application and/or in public databases such as Genbank, is necessary to establish their possession by Applicant for construction of the claimed compounds and their pharmaceutical formulations. The specification evidences Applicant's appreciation of the existence of each of these types of domains, already well-known to those of skill in the art, and their use in the construction of the presently claimed compounds. .

Applicant further disagrees that the specification is inadequately descriptive of sequences that are "substantially homologous to" those described. As the specification describes, for example, at page 7, line 30 to page 8, line 3, a substantially homologous sequence is one that essentially retains the activity of the reference sequence which, in this instance, is a protein of well-characterized activity such as a known sialidase or a GAG-binding domain. Nonetheless, in the interest of advancing prosecution, the present claims do not refer to "substantially homologous" sequences.

To satisfy the written description requirement, the application need only disclose sufficient relevant, identifying characteristics so that one of skill in the art would recognize that Applicant was in possession of the claimed subject matter. MPEP § 2163; *see also* University of California v. Eli Lilly, 119 F. 3d 1559, 1568, 43 USPQ2d 1398, 1406 (Fed. Cir. 1997); Enzo Biochem. Inc. v. Gen-Probe, 296 1316, 63 1609 (Fed. Cir. 2002).

Further, the standard for written description is an objective one, based on what one of skill in the art would recognize in the disclosure. In re Gosteli, 872 F.2d at 1012. The knowledge and level of skill in the particular art is a factor to be considered in determining the standard. It is not necessary to include in the specification that which those of skill in the art know; the specification is presumed to include all such knowledge.

Thus, whether a disclosure meets the written description required to establish possession of what is claimed depends, in part, on the knowledge of those skilled in the art. In the case of proteins, the knowledge of those skilled in the art includes sequence information and a known correlation between structure and function. It is Applicants' position that the sialidases and the GAG-binding domains have been so extensively studied as of the present application's priority date that there was an understood correlation between structure and function for each of these domains. It is also Applicants' position that given this knowledge available to those of skill in the art, and given the disclosure of the present application describing each of these domains, the present claims meet the written description requirement.

The courts have upheld the premise that when there is extensive or even adequate knowledge in the art regarding a technology (in this case, proteins), even one example may suffice to satisfy the written description requirement. In *Invitrogen Corporation v. Clontech Laboratories, Inc.* (429 F.3d 1052; Fed Cir (2005)), the court considered whether the following claim met the written description requirement.

> 1. An isolated polypeptide having DNA polymerase activity and substantially reduced RNaseH activity, wherein said polypeptide is encoded by a modified reverse transcriptase nucleotide sequence that encodes a modified amino acid sequence resulting in a polypeptide having substantially reduced RNaseH activity and wherein said nucleotide sequence is derived from an organism selected from the group consisting of a retrovirus, yeast, *Neurospora*, *Drosophila*, primates and rodents.

The patent disclosed the sequence of a MMLV DNA polymerase deletion mutant lacking RNaseH activity. In considering this claim, the trial court noted that at the time of the invention, the sequences of several reverse transcriptase genes were known and that it was known that several members of the reverse transciptase gene family shared significant homology. The trial court concluded the claim recited above met the written description requirement. This decision was appealed to the Court of Appeals for the Federal Circuit.

The appellant, citing *Fiers v. Revel* and *University of California v. Eli Lilly and Co.*,

argued that the trial court had erred in finding that the claim met the written description requirement. The appellant argued that the claim fails to meet the written description requirement because the claim is not limited to sequences recited in the specification or the claim. The Court of Appeals for the Federal Circuit upheld the trial courts decision that the claim meets the written description requirement. In doing so, the court stated that the challenger's reliance on *Fiers* and *Eli Lilly* was misplaced because the patent specification at issue in those cases did not disclose the sequence "of any embodiment of the DNA sequence claimed therein. Id. at 1073.

Thus, it is clear that the disclosure of even one embodiment of a recombinant gene encoding a mutant protein, when coupled with the knowledge of homologs in the prior art, can satisfy the written description requirement for even broad claims to modified proteins.

Similarly, *In Capon v. Eshhar v. Dudas*, the Court of Appeals for the Federal Circuit held that claims drawn to chimeric genes containing a sequence encoding a single-chain variable domain of an antibody and a sequence encoding the cytoplasmic, transmembrane and extracellular domains of a lymphocyte signaling protein, were adequately described in light of a few examples in the specification and the extensive knowledge in the art regarding the sequences and structures of each of the encoded domains.

In this instance, the detailed description in the specification of sialidases and GAG-binding amino acid sequences, including their sequences, structure, and correlation between their structure and function, the extensive knowledge in the art regarding the same, and the description in the specification of the resulting compounds and their properties, all clearly evidences possession of compounds containing a sialidase domain and a GAG-binding anchoring domain.

A. Sialidases

With regard to the sialidase domain, the specification provides extensive descriptions of many known sialidases, citing references and Genbank Accession numbers. At page 21, lines 3-22 and page 42, line 1 to page 45, line 27, the specification describes the cloning, sequencing and functional characterization of a number of bacterial, viral and human sialidases. Clearly, at the time the instant application was filed, many sialidases were known and fully characterized, not just the ones whose sequences are set forth in SEQ ID NOS. 8 and 9. The cited sections of the specification describe the types of linkages cleaved by these sialidases, and their substrate specificities. The same sections also describe how the sialidases

in general share about 20-30% sequence homology, but their overall fold is remarkably similar, especially in the catalytic region. The cited sections further describe standard assays to measure sialidase activity.

B. GAG-binding Domains

With regard to the GAG-binding domains, the specification at page 13, lines 11-26, describes and cites references describing a variety of proteins having domains that bind to heparin and/or heparan sulfate. The GAG-binding domains are distinct from the receptor binding or other such activities of the proteins. One such class of protein is the amphiregulins, and their GAG-binding domains also have long been known in the art (*see*, for example, Shoyab *et al.*, Thorne *et al.* and Johnson *et al.*, attached hereto as Appendix). Many classes of proteins were and are known to have GAG-binding domains; these include cell adhesion molecules, chemokines, glycoproteins of the extracellular matrix, polypeptide growth factors, secreted proteases and antiproteases, and proteins involved in lipoprotein uptake (*see* Lee *et al*, attached hereto as Appendix). The cited section of the specification describes exemplary sequences of GAG-binding domains that are known to have a high affinity for heparin (SEQ ID NOS: 2-7). Many such sequences have been identified, their binding affinities characterized, and consensus sequences deduced (*see*, for example, Verrecchio *et al.*, attached hereto as Appendix). As the specification describes, GAG-binding domains facilitate the binding of proteins to the cell surfaces of numerous cells, including respiratory epithelial cells, because GAGs such as heparin and heparan sulfate are ubiquitously present on cell surfaces. This property, and the fact that they are distinct from and do not interfere with other functions of a protein, make the GAG-binding domains suitable anchoring domains to deliver a domain of choice, such as a sialidase, to the surface of a cell.

C. Compounds that include a Sialidae Domain and a GAG-binding Domain

The specification describes the construction and optimization of compounds containing a sialidase domain and a GAG-binding anchoring domain (page 4, lines 26-30; page 21, line 23 to page 22, line 11; Example 6). Examples 4 and 5 describe how to clone, express, purify and select suitable sialidases, and assay for their activity. The specification describes in detail the various configurations in which the two domains (sialidase and GAG-binding), with or without a linker between them, can be arranged (page 9, line 13 to page 11, line 31). Given this characterization of such compounds in the specification, and given the

extensive knowledge in the art regarding the sequence and structure/function correlation of sialidase domains and GAG-binding domains as discussed above, one can readily use this information to identify and construct other compounds having similar properties.

Conclusion

As discussed above, the specification provides extensive descriptions of the individual domains (sialidase catalytic domain and GAG-binding domain) constituting the claimed compounds, construction of the compounds and assaying for their activities. In addition, as of the priority date of the present application, knowledge regarding the sequence, structure and structure/function correlation of sialidases and GAG-binding domains was already highly evolved, and it is Applicants' position that given the many known sialidase protein sequences, GAG-binding domain sequences and the recognition of consensus sequence patterns therein, and the known correlation between structure and function for each of these domains, the written description requirement has been met for the present claims.

In view of the forgoing, Applicant respectfully requests that the Examiner withdraw the rejections based on the written description requirement of 35 U.S.C. §112, first paragraph.

THE REJECTION UNDER 35 U.S.C. §112, FIRST PARAGRAPH- ENABLEMENT

Claims 1-3, 6-10, 12-14, 16-20, 22, 24, 31-34, 47, 61-79 and 94-98 are rejected under 35 U.S.C. §112, first paragraph, as not being enabled for their full scope. In particular, the Examiner alleges that the specification, "while being enabling for a compound or composition comprising a compound consisting of" therapeutic domain selected from among SEQ ID NO:8 and SEQ ID NO:9, and an anchoring domain selected from among the GAG-binding domains of SEQ ID NOS:2-7, does not reasonably provide enablement for a composition containing anchoring and/or therapeutic domains of "undetermined structure and function."

The Examiner further alleges that the disclosure is not sufficiently enabling for the full scope of the claims, which as pending encompass an "extremely large number" of fusion constructs. He states that the dependent claims 2-3, 6-10, 12-14, 22, 24, 31-34, 47, 61-79 and 94-98 identify specific target cells, therapeutic domains and anchoring domains, but allegedly "lack the complete structure of the compound in any single claim nor specify having a defined function with respect to a specific pathogen or in preventing any infection." (emphasis in quote)

With respect to pharmaceutical composition claims 47, 72, 73 and 76-79, it is alleged that the specification provides no teaching, nor is there any data, showing that the claimed fusion proteins are "associated with any of the known diseases or disorders or infections or can be treated or prevented" by administering the fusion constructs.

This rejection is traversed. As discussed above, the present claims specify the presence of a sialidase domain comprising a peptide or protein having sialidase activity; and an anchoring domain comprising a peptide or protein that binds to a glycosaminoglycan (GAG) on the surface of the target cell". Sialidases and GAG-binding domains are well known in the art. As discussed below, the teachings of the specification, when combined with the knowledge of those of skill in the art, render the specification more than adequately enabling for compounds containing these known domains.

As the present specification explains, sialic acid is a receptor for influenza viruses. Thus, treating the surface of respiratory epithelial cells with a sialidase can prevent influenza infections or interrupt early infections. The specification secribes a number of sialidases and describes how they can be tested for the ability to inhibit infection of cells by influenza virus. Attached are two publications, one by Malakhov *et al.* and the other by Belser *et al.*. These publications, which are discussed in greater detail below, demonstrate that a compound containing a sialidase domain and a GAG-binding anchoring domain is effective at preventing, treating or reducing the severity of infection by several influenza strains and avian influenza, as demonstrated in *in vitro* and *in vivo* model systems. The experiments described in these publications demonstrate that by following the teachings of the specification, one of skill in the art can make and test the claimed protein-based compositions, and one can observe a therapeutic effect in preventing and treating pathogenic infection.

Analysis

The inquiry with respect to scope of enablement under 35 U.S.C. §112, first paragraph, is whether it would require undue experimentation to make and use the subject matter as claimed. A considerable amount of experimentation is permissible, particularly if it is routine experimentation. The amount of experimentation that is permissible depends upon a number of factors, which include: the quantity of experimentation necessary, the amount of direction or guidance presented, the presence or absence of working examples, the nature of the invention, the state of the prior art, the relative skill of those in the art, the predictability

of the art, and the breadth of the claims. Ex parte Forman, 230 USPQ 546 (Bd. Pat. App. & Int'f 1986); see also In re Wands, 8 USPQ2d 1400 (Fed. Cir. 1988).

There is no requirement for disclosure of every species within a genus. Applicant is entitled to claims commensurate in scope with that which one of skill in the art could obtain by virtue of that which the Applicant has disclosed.

In this instance, a consideration of the factors enumerated in In re Wands, including: (a) the breadth of the claims, (b) the teachings of the specification regarding sialidases and GAG-binding domains, their sequences, structures, and corresponding activities, (c) examples describing the construction of compounds containing sialidase domains and GAG-binding domains and assaying for sialidase activity, (d) the extensive knowledge in the art, based on known sequences of sialidases (at least fifteen), regarding the consensus 3D structure (conserved catalytic fold) that is necessary for sialidase catalytic function, and the hundreds of known GAG-binding domains and the identification of consensus sequences that are needed for GAG-binding activity, (e) the high level of skill in the art regarding how to make, test and select compounds that retain sialidase catalytic activity and GAG-binding activity, and (f) the fact that identifying proteins belonging to a structurally and functionally well-characterized class is predictable given the extensive teachings of the instant application and the state of the art at the time of the effective date of the claims, leads to the conclusion that it would not require undue experimentation for one of skill in the art to make and use the subject matter as claimed.

The claims are directed to: (a) compounds that include a sialidase domain with sialidase activity, and a GAG-binding peptide anchoring domain, and (b) pharmaceutical compositions containing the compounds. As discussed above with respect to the rejection on grounds of alleged lack of written description, the specification teaches a number of known sialidases, their substrate specificities, and their conserved catalytic folds. The specification also teaches numerous classes of proteins that have GAG-binding domains, and provides the sequences of several exemplary GAG-binding domains. As the specification teaches, and as those of skill in the art knew, the knowledge in the art regarding the correlation between structure and catalytic function of the sialidases, the general knowledge in the art regarding sequence determinants of "3D" structure, and the knowledge regarding the correlation between sequence and binding activity of the GAG-binding domains (including the identification of consensus GAG-binding sequences collated from a number of classes of

proteins; *see* Verrecchio *et al.*, attached hereto as Appendix), was so extensive at the time of the application's priority date that by following the teachings of the specification, one of skill could readily identify sequences that contain the desired activities of these domains, and retain these activities in compounds that include both types of domains (sialidase and GAG-binding domains).

In addition to the above teachings, Examples 4 and 5 of the specification teach how to clone, express, purify and assay sialidases for selection of the optimal candidates for preparation of compounds containing a sialidase domain and a GAG-binding domain. Example 6 teaches how to construct, optimize and test the sialidase domain/GAG-binding domain constructs. By following the teachings of the specification, one can make a variety of compounds containing a sialidase domain and a GAG-binding anchoring domain, and test them in standard infectivity assays (as described, *e.g.*, in Example 2) for their ability to prevent or treat infection by a pathogen.

Therapeutic Effect of Compounds containing a Sialidase Domain and a GAG Binding Domain

The Examiner alleges that it is unpredictable which of the constructs produced as taught by the specification will actually have a therapeutic effect. Applicant respectfully submits that this is not the proper standard for enablement. To satisfy the requirement of enablement, a claim does not have to explicitly exclude every conceivable inactive variant. ("[I]t is not a function of the claims to specifically exclude either possible inoperative substances or ineffective reacting proportions". In re Application of Dinh-Nguyen, 492 F.2d 865 at 858-9 181 USPQ 46 (CCPA (1974)). Rather, the question is whether by following the teachings of the application, one of skill in the art can practice what is claimed with perhaps routine, but not undue, experimentation.

A number of bacterial and viral pathogens are known to use sialic acid receptors on target cells to bind and/or infect the target cells. Such pathogens include influenza virus, parainfluenza virus, paramyxoviruses, coronaviruses, rotaviruses, Sendai virus, reovirus, polyoma viruses and *Pseudomonas aeruginosa* (*see* Wassilewa, L., *Arch Virol* 54:299-305 (1977); Vlasak *et al.*, *Proc Natl Acad Sci USA* 85:4526-4529 (1988); Fukudome *et al.*, *Virology* 172:196-205 (1989); and Ramphal *et al.*, *Infect Immun* 41:339-44 (1983), of record). The specification teaches how compounds containing a sialidase domain to cleave sialic acid receptors on a target cell and a GAG-binding domain to anchor the sialidase to the target cell

can prevent binding and entry of a pathogen, such as influenza virus, which uses those sialic acid receptors to infect the target cell (specification at page 20, lines 28-29; page 22, lines 12-18; page 13, lines 10-15; page 21, line 23 to page 22, line 11). The specification teaches how to measure the sialidase activity of these compounds, and how to test them in infectivity assays. There is no reason why, given these teachings and the knowledge of those of skill in the art, one would not be able to obtain constructs having a therapeutic effect with perhaps reasonable, but not undue, experimentation.

Claims 47, 72, 73 and 77-79: With regard to the pharmaceutical composition claims 47, 72, 73, and 77-79, the Examiner asserts the lack of a working example demonstrating the therapeutic efficacy of one or more exemplary compounds containing a sialidase domain and a GAG-binding domain, as evidencing lack of enablement. Applicant takes exception to this. Working examples are not necessary for a showing of enablement; they are only one factor that goes to a consideration of enablement. The test is whether a consideration of all the Wands factors together lead to the conclusion that by following the teachings of the specification, one of skill in the art can make and use what is claimed in a manner that does not require a level of experimentation that is undue.

In this instance, the specification teaches the construction of compounds containing two well-known, well-characterized domains: a sialidase domain, and a GAG-binding domain. The specification teaches that the sialidase catalytic domain is a suitable for treating a variety of respiratory ailments in which infection is triggered *via* sialic acid receptors on a target epithelial cell surface. The specification further teaches that once the sialic acid receptor is cleaved, a pathogen, such as influenza virus, whose entry is mediated *via* these receptors, is unable to do so (page 20, lines 28-29; page 22, lines 12-18). The specification also teaches that a GAG-binding domain is a suitable domain to anchor the sialidase to the epithelial cells, which are ubiquitous expressors of heparin and heparan sulfate (types of GAGs) on the cell surface (page 13, lines 1015; page 21, line 23 to page 22, line 11).

The question that goes to enablement is whether by following these teachings, one of skill in the art can (1) construct a compound containing a sialidase domain and a GAG-binding anchoring domain; and (2) test its ability to prevent or treat pathogenic infection in a suitable assay. The specification has provided ample teachings to be able to do so. No actual working examples are necessary.

Although not needed, attached are two publications (Malakhov *et al.* and Belser *et al.*, attached hereto as Appendix) reporting experiments performed with an exemplary compound, one containing an *Actinomyces Viscosus* sialidase catalytic domain and a human amphiregulin GAG-binding domain. The experiments demonstrate that by following the teachings of the specification, one of skill in the art can make and test the claimed protein-based compositions, and one can observe a therapeutic effect in preventing and treating pathogenic infection.

Proteins containing a Sialidase domain and a GAG-binding domain can reduce infection by Human Influenza and Avian Flu in Animal Models

A) Malakhov *et al.*, *Antimicrob. Agents and Chemother.*, 50(4):1470-1479 (2006)

The ability of compounds containing a sialidase domain and a GAG-binding domain to protect against influenza infection was also tested in *in vivo* model systems. Attached is a publication by Malakhov *et al.*, demonstrating the *in vitro* and *in vivo* efficacy of two constructs containing a sialidase catalytic domain (A_vCD; amino acids 274-667 of *Actinomyces Viscosus* sialidase) and a human amphiregulin GAG-binding domain (AR; amino acids 125-145 of human amphiregulin). The constructs were as follows:

A_vCD-AR (DAS181; AR domain C-terminus to A_vCD domain); and

AR- A_vCD (DAS178; AR domain N-terminus to A_vCD domain)

Malakhov *et al.* demonstrate that a sialidase fusion protein containing a GAG-binding domain that anchors the fusion protein to a cell (DAS181) is ten times more effective at cleaving cellular sialic acid receptors than a sialidase fusion protein that does not contain a GAG-binding domain. Further, DAS181, which contains both the sialidase domain and the GAG-binding domain was found to: (i) protect cells from infection by a variety of influenza strains (increase cell viability post viral challenge); (ii) inhibit viral binding to the cells; and (iii) inhibit viral replication and infectivity) (Figure 3, Table 1).

The *preventative* and therapeutic activities of DAS181 were also tested *in vivo*, in a mouse model system. Mice exposed to DAS181 before being challenged with influenza virus strain H1N1 or at various times for up to 48 hours post viral challenge all showed a marked increase in survival, improved lung survival and lung pathology, and inhibition of virus titer in the lungs of infected animals (Figure 4, Table 5).

The DAS178 construct was then tested in ferrets, an animal model that most closely mimics the symptoms of human influenza. Ferrets exposed to DAS178 at various times beginning at 2 days prior to viral challenge with influenza strain H1N1 and ending at 5 days post viral challenge showed markedly improved protection against infection and diminished signs of illness and inflammation. Control animals treated with delivery vehicle alone and a viral challenge showed peak viral shedding at 1-2 days post viral challenge, followed by a gradual decrease in shedding. In contrast, only 3 out of 12 DAS178-treated ferrets showed viral shedding 1-2 days post viral challenge, and the nasal virus titer in these animals was hundred times less than that seen in the animals treated with delivery vehicle alone (Table 6).

B) Belser *et al., J. Infect. Dis.*, 196:1493-1499 (2007)

Applicant also provides herein a recent publication, Belser *et al.*, demonstrating the therapeutic efficacy of DAS181 (containing an *Actinomyces Viscosus* sialidase catalytic domain and a human amphiregulin GAG-binding domain as the anchoring domain; *see* description in Malakhov et al., discussed above). As shown in the publication, when mice were treated with the DAS181 construct prior to their exposure to a highly virulent lethal avian influenza virus, H5N1, 100% of the mice were protected from a fatal form of the disease, and 70% of the mice were protected from all forms of infection. In addition, the DAS181 compound was effective in treating the mice when the drug was administered 3 days after exposure to the virus, resulting in enhanced survival.

In light of the above experimental evidence, Applicant respectfully submits that the composition claims 47, 72, 73 and 77-79 are operative in their intended use as pharmaceuticals.

THE REJECTION OF CLAIMS 1-3, 6-10, 12-14, 22, 24, 31-34, 47, 61-79 AND 94-98 UNDER 35 U.S.C. §112, SECOND PARAGRAPH

Claims 1-3, 6-10, 12-14, 22, 24, 31-34, 47, 61-79 and 94-98 are rejected under 35 U.S.C. §112, second paragraph, as being indefinite in their recitation of the phrase "therapeutic domain." It is alleged that the meaning of the phrase is unclear. Without conceding the merits of this rejection, it is rendered moot by amending the claims to remove the phrase "therapeutic domain."

THE REJECTION OF CLAIMS 1-3, 5-10, 12-14, 16-20, 22-24, 31-34, 47, 61-79 AND 94-98 UNDER THE JUDICIALLY CREATED DOCTRINE OF OBVIOUSNESS-TYPE DOUBLE-PATENTING

Claims 1-3, 5-10, 12-14, 16-20, 22-24, 31-34, 47, 61-79 and 94-98 are provisionally rejected under the judicially created doctrine of obviousness-type double-patenting over claims 141-147, 149, 151, 162-169 and 171 of co-pending Application Serial No. 10/939,262. Without addressing its merits or conceding its propriety, this rejection will be addressed as appropriate upon indication that there is allowable subject matter in one or both applications.

* * *

In view of the amendment and remarks herein, allowance of the application is respectfully requested.

Please apply any charges or credits to Deposit Account No. 06-1050, referencing Attorney Docket No. 21865-0002001.

Respectfully submitted,

Date: 8 September 2008

/Anita L. Meiklejohn/
Anita Meiklejohn
Reg. No. 35,283

Fish & Richardson P.C.
225 Franklin Street
Boston, MA 02110
Telephone: (617) 542-5070
Facsimile: (617) 542-8906
email: seidman@fr.com

IN THE UNITED STATES PATENT AND TRADEMARK OFFICE

Applicant : Yu *et al.*
Serial No. : 10/718,986
Confirmation No.: 3664
Filed : November 21, 2003
Title : **BROAD SPECTRUM ANTI-VIRAL THERAPEUTICS AND PROPHYLAXIS**

Art Unit : 1652
Examiner : Saidha, Tekchand
Customer No.: 20985

Mail Stop Amendment
Commissioner for Patents
P.O. Box 1450
Alexandria, VA 22313-1450

APPENDIX

1) Shoyab *et al.*, *Science*, 243:1074-1076 (1989)

2) Thorne *et al.*, *Mol. Cell. Biol.*, 14:1635-1646 (1994)

3) Johnson *et al.*, *J. Biol. Chem.*, 269:27149-27154 (1994)

4) Lee *et al.*, *Proc. Natl. Acad. Sci. USA*, 88:2768-2772 (1991)

5) Verrecchio *et al.*, *J. Biol. Chem.*, 275:7701-7707 (2000)

6) Malakhov *et al.*, *Antimicrob. Agents and Chemother.*, 50(4):1470-1479 (2006)

7) Belser *et al.*, *J. Infect. Dis.*, 196:1493-1499 (2007)

THE JOURNAL OF BIOLOGICAL CHEMISTRY
Vol. 275, No. 11, Issue of March 17, pp. 7701–7707, 2000
Printed in U.S.A.

Design of Peptides with High Affinities for Heparin and Endothelial Cell Proteoglycans*

(Received for publication, July 12, 1999, and in revised form, December 3, 1999)

Angela Verrecchio‡, Markus W. Germann§, Barbara P. Schick¶, Brian Kung‡, Thomas Twardowski‖, and James D. San Antonio‡¶**

From the ‡Department of Medicine and the ¶Cardeza Foundation for Hematologic Research, §Kimmel Cancer Center, Jefferson Medical College of Thomas Jefferson University, Philadelphia, Pennsylvania 19107 and the ‖Department of Materials Engineering, Drexel University, Philadelphia, Pennsylvania 19104

Proteoglycan-binding peptides were designed based on consensus sequences in heparin-binding proteins: *XBBXBX* and *XBBBXXBX*, where *X* and *B* are hydropathic and basic residues, respectively. Initial peptide constructs included $(AKKARA)_n$ and $(ARKKAAKA)_n$ (n = 1–6). Affinity coelectrophoresis revealed that low M_r peptides (600–1300) had no affinities for low M_r heparin, but higher M_r peptides (2000–3500) exhibited significant affinities ($K_d \cong$ 50–150 nM), which increased with peptide M_r. Affinity was strongest when sequence arrays were contiguous and alanines and arginines occupied hydropathic and basic positions, but inclusion of prolines was disruptive. A peptide including a single consensus sequence of the serglycin proteoglycan core protein bound heparin strongly ($K_d \cong$ 200 nM), likely owing to dimerization through cysteine-cysteine linkages. Circular dichroism showed that high affinity heparin-binding peptides converted from a charged coil to an α-helix upon heparin addition, whereas weak heparin-binding peptides did not. Higher M_r peptides exhibited high affinities for total endothelial cell proteoglycans ($K_d \cong$ 300 nM), and ~4-fold weaker affinities for their free glycosaminoglycan chains. Thus, peptides including concatamers of heparin-binding consensus sequences may exhibit strong affinities for heparin and proteoglycans. Such peptides may be applicable in promoting cell-substratum adhesion or in the design of drugs targeted to proteoglycan-containing cell surfaces and extracellular matrices.

Proteoglycans (PGs)[1] are composed of a core protein to which are covalently attached one or more sulfated glycosaminoglycans (GAGs). PGs are ubiquitous components of cell surfaces and the extracellular matrix, and their GAG chains contribute to myriad biological functions, such as modulation of enzyme activities, regulation of cell growth, and control of assembly of the extracellular matrix (1). PGs are thus potential targets for therapeutic intervention. For example, heparin antagonists are needed to take the place of protamine, a heterogeneous, sometimes toxic protein mixture commonly used to neutralize the anticoagulant activity of heparin in humans (2, 3); in the design of drugs to be targeted to PG-rich tissues, such as cartilage (4); and to be used to promote cell adhesion in a variety of situations, *e.g.* by promoting binding of cells that express abundant amounts of PGs, such as endothelial cells (5), to synthetic vascular graft surfaces. To develop a rationale for the design of such reagents, it is useful to examine known features of protein structure required for high affinity interactions with GAGs. Thus, analysis of the structural features of many known heparin- and heparan sulfate (HS)-binding proteins has revealed the presence of conserved motifs, through which GAG binding has been postulated to occur. Cardin and Weintraub (6) identified two clusters of basic charge in known heparin-binding proteins in which amino acids tend to be arranged in the patterns *XBBXBX* or *XBBBXXBX*, where *B* represents an amino acid with basic charge, usually arginine or lysine, and *X* represents an uncharged or hydrophobic amino acid. Molecular modeling of these consensus sites predicts the arrangement of amino acids into either α-helices or β-strands. This allows for the clustering of noncontiguous basic amino acids on one side of the helix, thus forming a charged domain to which GAGs could bind. Indeed, for some but not all of the heparin-binding proteins, disruption of the heparin-binding consensus sequences hinders heparin binding. For example, chemical modification of the heparin-binding consensus site in thrombospondin (7) or site-directed mutagenesis of a heparin-binding sequence in fibronectin (8) eliminates or diminishes heparin binding affinity. Others have proposed a necessary distance of approximately 20 Å between basic amino acids for heparin binding, regardless of protein tertiary structure (9).

To date, few attempts have been made to use these concepts regarding the structural specificities of GAG-protein interactions to develop families of high affinity GAG- or PG-binding peptides. Thus, here we describe the design and characterization of high affinity heparin- and EC PG-binding peptides that were modeled from the proposed heparin-binding consensus sequences of native heparin-binding proteins.

EXPERIMENTAL PROCEDURES

Peptide Synthesis—Peptides were synthesized and purified by the University of Virginia Biomolecular Research Facility (Charlottesville, VA) or by Genosys Biotechnologies (The Woodlands, TX). Peptides were synthesized by standard solid phase synthesis using Fmoc (*N*-(9-fluorenyl)methoxycarbonyl) chemistry. Peptide molecular weight was verified by mass spectroscopy, and purity (>70%) was analyzed by high pressure liquid chromatography.

Preparation of Radiolabeled Heparin—Whole heparin from pig intes-

* This work was supported by the Landenberger Foundation, National Institutes of Health Grants HL 53590 (to J. D. S. A.) and HL 29282 (to B. P. S.), and the Drexel-Jefferson Seed-grant Program for Joint Research Projects (to J. D. S. A. and T. T.). The costs of publication of this article were defrayed in part by the payment of page charges. This article must therefore be hereby marked "*advertisement*" in accordance with 18 U.S.C. Section 1734 solely to indicate this fact.

** To whom correspondence should be addressed: Dept. of Medicine and the Cardeza Foundation for Hematologic Research, Thomas Jefferson University, 1015 Walnut St., Philadelphia, PA 19107. Tel.: 215-955-6121; Fax: 215-923-3836; E-mail: James.SanAntonio@mail.tju.edu.

[1] The abbreviations used are: PG, proteoglycan; ACE, affinity coelectrophoresis; CHAPS, 3-[(3-cholamidopropyl)dimethylammonio]-1-propanesulfonate; CS, chondroitin sulfate; EC, endothelial cell; ECM, extracellular matrix; GAG, glycosaminoglycan; HS, heparan sulfate; HUVEC, human umbilical vein endothelial cell; *R*, retardation coefficient; SG, serglycin; TFE, trifluoroethanol; MOPSO, sodium 3-(*N*-morpholino)-2-hydroxypropanesulfonate.

tinal mucosa (Sigma) was tyramine end-labeled and radiolabeled with $Na^{125}I$ (Amersham Pharmacia Biotech) to an average specific activity of $\sim 1.0 \times 10^7$ cpm/μg as described (10). Radiolabeled heparin was fractionated on Sephadex G-100 (Bio-Rad), and the final ~12% of material to elute was retained as the low M_r material of ≤6000 (11, 12).

Electrophoretic Analysis of Binding of Heparin and Human Umbilical Vein Endothelial Cell (HUVEC) PGs to Peptides—Binding of radiolabeled heparin and HUVEC PGs to peptides was studied by ACE as detailed elsewhere (13), because the heparin-protein binding affinities revealed by ACE match reasonably well with those obtained by other well established quantitative techniques for measuring binding interactions, *e.g.* (14–17). Briefly, peptides were dissolved in 1× ACE running buffer, 50 mM MOPSO (Sigma)/125 mM sodium acetate, pH 7.0, and serially diluted in running buffer at 2× concentrations. Peptides were then mixed 1:1 with 2% agarose/1% CHAPS (Roche Molecular Biochemicals) and loaded into wells of a 1% agarose gel. Radiolabeled heparin or HUVEC PGs were then loaded in a slot on the anode side of the gel and electrophoresed through the peptide-containing wells, toward the cathode. Gels were dried, and PG mobility was measured with a PhosphorImager (Molecular Dynamics, Sunnyvale, CA) by scanning each protein lane and determining the relative radioactivity content per 88-μm pixel through the length of the lane. Retardation coefficient (R) measurements, binding isotherm curve fittings, and apparent K_d value determinations were calculated as detailed previously (10, 13).

Some peptides were also analyzed by ACE for heparin binding under reducing conditions. Thus, after serial peptide dilution, β-mercaptoethanol was added at 5% to each peptide sample, and these were mixed 1:1 with 2% agarose/1% CHAPS/5% β-mercaptoethanol and added to the ACE gel sample wells as usual.

Binding analysis of peptides to enzymatically or chemically degraded PGs (see below) was carried out by ACE as detailed, except that PG samples included 6 M urea to denature any residual enzymes.

Cell Culture—HUVEC were isolated as detailed elsewhere (18) and were used up to passage seven. Cells were cultured on 0.2% gelatin-coated tissue culture flasks in normal culture medium composed of medium 199 (Life Technologies, Inc.), 10% fetal bovine serum (Mediatech Inc.), 80 μg/ml endothelial cell growth supplement isolated from bovine hypothalami as described (19), 50 μg/ml heparin (porcine intestinal mucosa, grade 1A, Sigma) 1% penicillin-streptomycin, and 0.1% fungizone.

Radiolabeling and Isolation of Total HUVEC PGs and GAGs—Exponentially growing, subconfluent HUVECs were labeled with 35 μCi/ml [^{35}S]Na_2SO_4 (ICN Pharmaceuticals, Costa Mesa, CA) in normal culture medium minus heparin for 12 h. Culture medium and cell layers were harvested separately. After removal of the medium, cells were washed with 2.0 ml of phosphate-buffered saline plus Ca^{2+}-Mg^{2+}. Medium and rinses were pooled and brought to 6 M urea, 10 mM EDTA, 1 mM phenymethylsulfonyl fluoride, 5 mM *N*-ethylmaleimide, 50 mM 6-aminocaproic acid, 5 mM benzamidine, and 1 μg/ml pepstatin A. Samples were stirred for 15 min at room temperature and then centrifuged at 10,000 rpm for 30 min to remove insoluble materials.

To the cell layer was added 2.0 ml of extraction solution, 6 M urea, 100 mM NaCl, 0.2% Triton X-100, 50 mM Tris-HCl, pH 7.0, and protease inhibitors as described above. Cells were scraped off the dishes, and the extracts were pooled and stirred for 5 min at room temperature and then centrifuged as described above.

Samples were concentrated on DEAE columns (DEAE Bio-Gel A agarose, Bio-Rad) equilibrated with low salt buffer, 0.1 M NaCl, 6 M urea, and 50 mM Tris-HCl, pH 7.0. Columns were rinsed with 10 ml of low salt buffer; flow-through was discarded. Bound PGs/GAGs were eluted with 3 ml of high salt buffer, 1.5 M NaCl, 6 M urea, and 50 mM Tris-HCl, pH 7.0. Eluted samples were dialyzed against distilled water, lyophilized, and stored at −20 °C until binding analysis.

Enzymatic Digestions of PGs—The contributions of PG GAG chain components to peptide binding affinities were assessed by selective enzymatic degradation of GAG chains prior to ACE analysis. [^{35}S]Na_2SO_4-labeled HUVEC PGs were digested with chondroitinase ABC or heparatinase I (Seikagaku America, Ijamsville, MD). PG samples were resuspended in 100 μl of enzyme buffer (chondroitinase buffer: 50 mM Tris-HCl, 30 mM sodium acetate, pH 8.0, 0.1 mM pepstatin A, 0.5 mg/ml bovine serum albumin, 10 mM *N*-ethylmaleimide, 1 mM phenylmethylsulfonyl fluoride, and 5 mM EDTA; heparatinase buffer: 50 mM Tris-HCl, 5 mM calcium acetate, pH 7.0, 0.5 mg/ml bovine serum albumin, and 1 mM phenylmethylsulfonyl fluoride). Samples were digested with 0.05 units/ml chondroitinase ABC at 37 °C for 3 h. Fresh enzyme was then added to the same concentration, and the incubation was continued for an additional 1 h. Heparatinase I was added to samples at 0.01 units/ml. Samples were incubated for 3 h at 43 °C, fresh enzyme was then added to the same concentration, and incubation was continued for an additional 1 h. All samples were then stored at −20 °C until binding analysis.

Chemical Degradation of PGs—The contributions of PG GAG chain components to peptide binding affinities were further assessed by selective chemical degradation. Total secreted HUVEC PGs were subjected to nitrous acid degradation as detailed (20), which selectively degrades HS GAG chains. Binding analysis to peptides was then measured by ACE.

β-Elimination of PGs—GAG chains were released from PG core proteins by alkaline borohydride reduction as detailed in Ref. 21.

Circular Dichroism Spectroscopy—CD spectra were recorded at 22 °C using a JASCO J-500C spectropolarimeter interfaced to a 486 PC. The path length of the CD cells was 0.5 mm, and the CD was expressed in terms of ellipticity [Θ] in degree·cm^2·dmol^{-1}. Samples were initially dialyzed to water to remove residual synthesis contaminants, lyophilized, and resuspended in water at 1 mg/ml, and the pH was adjusted to 7.0. Peptide concentrations of 0.1 or 0.2 mg/ml were analyzed. Typically, two scans were averaged for each spectrum. CD spectra of peptides in α-helical conformations were recorded in the presence of trifluoroethanol (TFE), which served as a positive control of peptides in α-helical conformations. To determine the effects of heparin on peptide conformation, solutions containing peptide plus heparin were prepared at various peptide:heparin ratios (w/w).

Analysis of Peptide Concentration—Concentrations of peptides used in CD were verified by one-dimensional NMR spectroscopy based on an internal 2,2-dimethylsilapentane-5-sulfonate standard. NMR experiments were recorded on a Bruker AMX 600 NMR spectrometer equipped with a 5 mm broadband inverse probe, using the XwinNMR 2.1 software package run on a Silicon Graphics INDY work station. One-dimensional proton spectra were acquired at 303 K using a 4 s relaxation delay and were processed with 0.5 Hz exponential line broadening. 250 μl of a 1 mg/ml peptide solution (as determined by weight) was lyophilized and dissolved in 405 μl of D_2O containing 0.123 mM 2,2-dimethylsilapentane-5-sulfonate. The degenerate arginine δCH_2 resonances at 3.2 ppm, ascertained by a total correlation spectroscopy experiment, were integrated and compared with the internal standard.

Peptide Length Calculations—Simple random walk statistics, neglecting contributions due to swelling, charge, and self-avoidance, were assumed to apply to peptides of type $(AKKARA)_n$ and $(ARKKAAKA)_n$, where n = 1–6, and used to calculate the average spatial separation of terminal amino acids and to estimate overall peptide size. Peptide size was calculated using the average end-to-end separation using the equation,

$$\langle r \rangle^2 = n l_c^2 \left(\frac{1 - \cos\theta}{1 + \cos\theta}\right)\left(\frac{1 - \overline{\cos\phi}}{1 + \overline{\cos\phi}}\right) \qquad \text{(Eq. 1)}$$

where <r> = average end-to-end distance, n = number of amino acid residues, l_c = average bond length, θ = average bond angle, and ϕ = rotation angle (22). The rotation angle was taken to equal either 0° for a fully extended molecule or 120° for bond rotation leading to a coiled structure. A perfect α-helix was assumed subsequent to binding with heparin, such that helical wheel diagrams, representing an 18/5 (residues/rotation) α-helix (23), could be constructed to visualize the position of and calculate the spacing for basic amino acids along the helix.

RESULTS

Peptide-Heparin Interactions—To design small peptides that exhibit high affinities for heparin and for the GAG components of PGs, peptide sequences were modeled after proposed heparin-binding consensus sequence motifs. Thus, a collection of peptides containing one of two consensus sequence motifs, either *XBBXBX* or *XBBBXXBX*, as well as various modifications of these, were synthesized (Table I). As peptides containing a single heparin-binding sequence often show little or no affinity for heparin (24), a strategy used here was to include consensus sequences in multiple copies within peptides. In initial studies, we selected for synthesis the sequences $(AKKARA)_n$ or $(ARKKAAKA)_n$, where n = 1–6. Alanine was included in the hydropathic positions because of its stabilizing activity on α-helices (25), and the basic amino acids were chosen to represent those

TABLE I

Heparin binding affinity of peptides containing heparin-binding consensus sequences

Peptides were analyzed for heparin-binding affinity by ACE, and K_d values of peptide-heparin interactions were calculated from binding plots as detailed under "Experimental Procedures." Each sample was tested for heparin-binding 3–11 times, with an average of 4 times. K_d represents an average of data obtained for all trials ± S.D.

Peptide sequence	M_r	K_d ± S.D.
		nM
XBBXBX tandem repeats		
AKKARA	644	Not detectable
$(AKKARA)_2$	1270	40,000 ± 18,000
$(AKKARA)_3$	1895	1,900 ± 210[a]
$(AKKARA)_4$	2520	174 ± 19
$(AKKARA)_5$	3146	94 ± 41[a]
$(AKKARA)_6$	3770	104 ± 32[a]
$(ARRAKA)_3$	1979	900 ± 170[b]
XBBBXXBX tandem repeats		
ARKKAAKA	843	Not detectable
$(ARKKAAKA)_2$	1668	6,200 ± 3,000
$(ARKKAAKA)_3$	2493	135 ± 54
$(ARKKAAKA)_4$	3318	42 ± 15[c]
$(ARKKAAKA)_5$	4143	51 ± 11[c]
$(ARRRAARA)_3$	2745	72 ± 22[d]
$(AKAAKKRA)_3$	2493	132 ± 93
XBBBXXBX tandem repeats with hydropathic position modifications		
$(AKRKKAAKA)_3$	2878	75 ± 41
$(GRKKGGKG)_3$	2325	200 ± 98[c]
$(LRKKLGKR)_3$	2959	105 ± 37
$(TRKKLGKI)_3$	2794	737 ± 350[c]
$(ARKKPAKA)_3$	2571	360 ± 127[c]
ARKKAAKAARKKPAKAARKKAAKA	2519	730 ± 340[c]
ARKKAAKARKKAKARKKAAKA	2351	450 ± 95[c]
ARKKAAKAAAAAARKKAAKAAAAAAARKKAAKA	3062	254 ± 137[c]
Native or modified serglycin sequences		
YPARRARYQWVRCKP	1948	187 ± 54
YPTQRARYQWVRCNP	1936	817 ± 170
YPARRARYQWVRAKP	1918	37,000 ± 6,700
AAARRARAAAARAKA	1482	72,000 ± 60,000

[a] $p < 0.01$ *versus* $(AKKARA)_4$.
[b] $p < 0.01$ *versus* $(AKKARA)_3$.
[c] $p < 0.01$ *versus* $(ARKKAAKA)_3$.
[d] $p < 0.05$ *versus* $(ARKKAAKA)_3$.

with the highest probability of occurrence in each basic position in the heparin-binding consensus sequences of native heparin-binding proteins (6). When single copies of either sequence were tested for heparin binding by ACE, no affinities were detected. In contrast, peptides containing two copies of the consensus sequence exhibited weak but detectable affinities for heparin (<6 μM), and peptides of higher molecular weight containing 4–6 copies of a consensus sequence showed a marked increase in heparin binding affinity (40–150 nM) (Fig. 1). The heparin binding affinity of both the 6-mer and 8-mer tandem repeat peptides reached a plateau as peptide length approached 30 amino acids ($(AKKARA)_5$, $K_d \cong 90$ nM; $(ARKKAAKA)_4$, $K_d \cong 40$ nM). Larger peptides ($(AKKARA)_6$ and $(ARKKAAKA)_5$) displayed similar affinities ($K_d \cong 100$ and 50 nM, respectively; Table I).

To define the sequence and conformational features of the tandem repeat peptides that confer their high affinity heparin binding characteristics, peptides containing variants of one of the consensus sequences first tested, $(ARKKAAKA)_3$, were synthesized. These included those in which alanines were replaced by other hydropathic residues, the spacings between consensus sequences were altered by removal or addition of alanine residues, or the potential of the peptides to form stable α-helices was inhibited by including proline residues at various positions. It was found that peptide affinity for heparin was decreased when alanine was replaced by glycine in all the hydropathic positions ($(ARKKAAKA)_3$, $K_d \cong 135$ nM; $(GRKKGGKG)_3$, $K_d \cong 200$ nM; $p < 0.01$); less conservative substitutions had varying effects on heparin binding affinity, *i.e.* for $(LRKKLGKR)_3$, $K_d \cong 105$ nM, affinity was unaffected; for

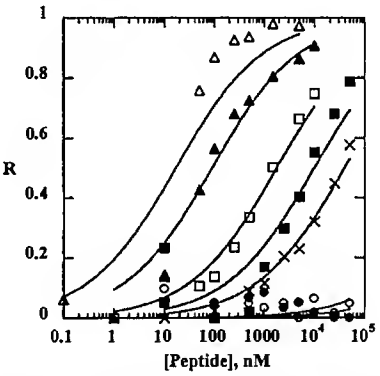

FIG. 1. **Calculation of heparin binding affinities of peptides containing heparin-binding consensus sequences.** Retardation coefficients (R) for the migration of low M_r ^{125}I-tyramine-heparin through peptides were determined from ACE gel electrophoretograms and are plotted against peptide concentration as detailed under "Experimental Procedures." Smooth curves represent nonlinear least-squares fits to the equation $R = R_\infty/(1+ (K_d/[\text{peptide}])^n)$. Peptides containing single consensus sequences (AKKARA (●) or ARKKAAKA (○)) do not bind heparin with a measurable affinity; in contrast, significant heparin binding was seen with peptides containing multiple heparin-binding consensus sequences and increased as a function of peptide M_r. ×, $(AKKARA)_2$ ($K_d \cong 40$ μM); ■, $(ARKKAAKA)_2$ ($K_d \cong 6$ μM); □, $(AKKARA)_3$ ($K_d \cong 2$ μM); ▲, $(ARKKAAKA)_3$ ($K_d \cong 135$ nM); △, $(ARKKAAKA)_4$ ($K_d \cong 40$ nM).

$(TRKKLGKI)_3$, $K_d \cong 740$ nM ($p < 0.01$), affinity was decreased (Table I).

Two peptides were synthesized in which the spacings be-

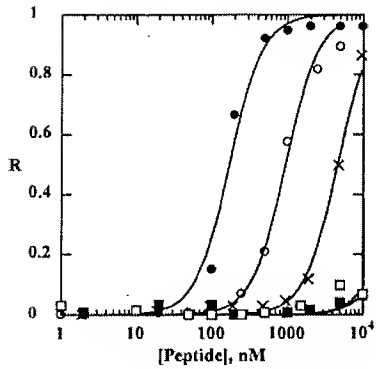

FIG. 2. **Calculation of heparin binding affinities of SG peptides.** *R* values for the migration of low M_r ^{125}I-tyramine-heparin through peptides containing sequences native to the mouse (YPARRARYQWVRCKP (●)) or human (YPTQRARYQWVRCNP (○)) SG PG core proteins were determined from ACE gel electrophoretograms as detailed under "Experimental Procedures." SG peptides displayed relatively strong affinities for heparin ($K_d \cong 200$ and 900 nM for the mouse and human peptides, respectively), in comparison to peptides of similar size that contain multiple repeats of heparin-binding consensus sequences (*e.g.* $(AKKARA)_3$, $K_d \cong 2000$ nM, and $(ARKKAAKA)_2$, $K_d \cong 6000$ nM; Table I). Peptide AAARRARAAAARAKA (■) displayed negligible heparin binding affinity ($K_d \cong 75$ μM), indicating the importance of the nonbasic residues to heparin binding. YPARRARYQWVRCKP-heparin binding in the presence of β-mercaptoethanol (YPARRARYQWVRCKP + β-mercaptoethanol (×)) was decreased by over 20-fold ($K_d \cong 4$ μM). Replacement of cysteine by alanine in the mouse SG peptide (YPARRARYQWVRAKP (□)) further reduced heparin binding affinity ($K_d \cong 36$ μM).

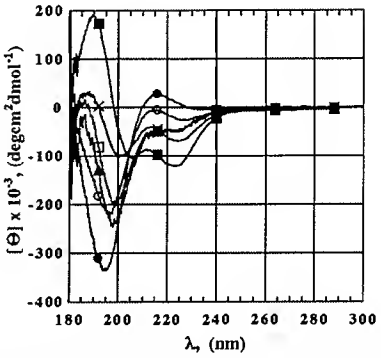

FIG. 3. **CD spectroscopy of $(AKKARA)_6$ in the presence or absence of low M_r heparin.** CD spectra measurements of $(AKKARA)_6$ in the absence of heparin (1:0 (●)) reveal peaks at 195 and 216 nm and a crossover at 210 nm, indicative of an extended charged coil conformation. Upon heparin addition (1:0.25 (○) or 1:0.50 (×)), the peptide conformation is altered, and at a 1:1 peptide-heparin ratio (■), the peptide becomes α-helical with characteristic α-helical peaks at approximately 190, 207, and 222 nm. Excess heparin (1:2 (□) or 1:4 (▲)) disrupts this interaction, and the spectra resemble that of a protein in a random coil conformation. Spectra are heparin and/or blank (water) corrected.

tween adjacent consensus sequences were altered. Both increasing(ARKKAAKA-AAAA-ARKKAAKA-AAAA-ARKKAAKA) and decreasing (ARKKAAKA-RKKAAKA-RKKAAKA) the distance between consensus sequences resulted in decreased heparin binding affinity ($K_d \cong 250$ and 450 nM, respectively). Inclusion of prolines also decreased the heparin binding affinity, the degree of which was influenced by their position and number. Thus, the heparin binding affinity decreased to 360 nM when prolines were present in each tandem repeat in place of an alanine $((ARKKPAKA)_3)$; however, a weaker affinity was obtained when a single proline was substituted in the center of a series of three heparin-binding consensus sequences (ARKKAAKA-ARKKPAKA-ARKKAAKA, $K_d \cong 730$ nM; Table I).

Other peptides synthesized and studied include sequences native to the mouse (YPARRARYQWVRCKP) and human (YPTQRARYQWVRCNP) serglycin (SG) core proteins, which contain a single and a partial consensus sequence, respectively. These showed significant affinities for heparin ($K_d \cong$ 200–900 nM; Table I and Fig. 2), despite their small sizes (about 2000 Da). To elucidate the basis for the strong heparin binding features of these peptides, the ability of the basic residues to sustain high affinity binding was tested by studying a peptide that contained all of the basic residues of the mouse sequence in their native positions but in which all other residues were changed to alanines (AAARRARAAAARAKA). A 350-fold decrease in heparin binding affinity ($K_d \cong 72$ μM) for this peptide indicated that the number and arrangement of basic residues in the mouse sequence was not sufficient for high affinity binding and suggests the importance of one or more of the other nonbasic residues (Fig. 2). We next tested whether the C-terminal cysteine in the mouse SG peptide may promote peptide dimer formation, thereby influencing heparin binding affinity. Thus, heparin binding was tested by ACE under reducing conditions, and it was found that this treatment yielded negligible heparin binding. Likewise, when the cysteine residue was replaced by an alanine in the native mouse SG sequence, YPARRARYQWVRAKP, heparin binding affinity was again negligible; both results are consistent with the potential cross-linking function of the cysteine residues (Fig. 2).

CD—The intrinsic structural properties of the peptides were explored using CD spectroscopy. Short peptides of known heparin-binding proteins containing heparin-binding consensus sequences have previously been shown to fold into α-helical conformations. In doing so, the basic amino acids locate to one face of the helix and thus are potentially exposed for binding. Peptides that displayed weak $((AKKARA)_2)$, moderate $((AKKARA)_4)$, and strong $((AKKARA)_5$ and $(AKKARA)_6)$ heparin binding affinities were analyzed by CD to characterize their degree of α-helical contents and propensities to form an α-helix. All peptides exhibit very similar spectra with peaks at 195 and 216 nm and a crossover at 210 nm (for example, see Fig. 3, $(AKKARA)_6$, 1:0 (●), and Fig. 4, $(AKKARA)_2$, 1:0 (●)). These spectra are indicative of an extended charged coil conformation that was previously reported for charged poly-L-lysines and poly-L-arginines (26).

Intrinsic CD of the peptides shows that they do not adopt α-helical conformations. To explore the conformational repertoire of the peptides and to record CD spectra for the α-helical conformations, peptides were analyzed by CD in the presence of the nonpolar solvent TFE. Nonpolar solvents are known to increase the degree of α-helicity of a peptide in solution by enhancing hydrogen bonding and electrostatic interactions (27). CD of $(AKKARA)_6$ at 0.1 mg/ml containing 0, 10, 20, 30, 40, and 50% TFE (v/v) was measured. At TFE concentrations >30%, with an apparent maximal effect induced at 40% TFE, the peptide assumes an α-helical conformation, with classic α-helical peaks at 206 and 220 nm and a crossover at 197 nm (data not shown).

The CD spectra of $(AKKARA)_6$ recorded in the presence of increasing amounts of heparin (Fig. 3) demonstrate that a change from a charged coil conformation displayed in the absence of heparin (1:0) occurs upon heparin addition (1:0.25, 1:0.50, and 1:1). Heparin induces a similar α-helical conformation at a 1:1 peptide:heparin ratio that was obtained in the presence of >30% TFE, with classic α-helical peaks at 190, 207, and 222 nm. At higher heparin concentrations (1:2 or 1:4) the α-helical form is lost, and the spectrum resembles that of a random coil structure. This ability of excess GAG to disrupt the

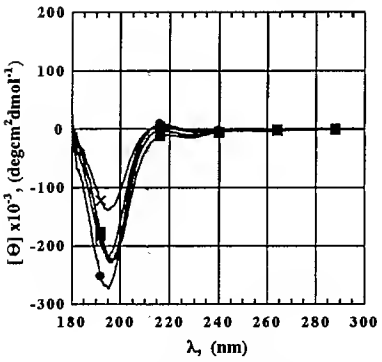

FIG. 4. **CD spectroscopy of $(AKKARA)_2$ in the presence or absence of low M_r heparin.** The CD spectra measurements of $(AKKARA)_2$ in the absence of heparin (1:0 (●)) indicate a charged coil conformation (peaks at 195 and 216 nm, crossover at 210 nm). However, in contrast to the heparin-induced conformational change seen for the high affinity heparin-binding peptide $(AKKARA)_6$, $(AKKARA)_2$, which binds heparin weakly, remains a charged coil in the presence of heparin (1:0.25 (○), 1:0.50 (×), 1:0.75 (■), and 1:1 (□)).

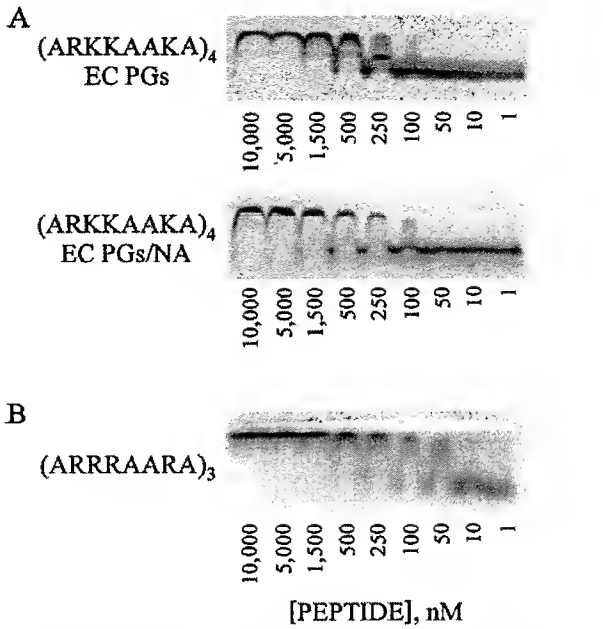

FIG. 5. **ACE analysis of the interactions between peptides containing heparin-binding consensus sequences and HUVEC PGs.** ACE gel images as obtained by a PhosphorImager in which EC PGs/GAGs (*A*) or heparin (*B*) was fractionated through peptides. In *A*, at least two populations of high affinity PG/GAG, seen as two bands of radiolabeled material migrating with different mobilities, are visible at peptide concentrations of ≤50 nM. At a peptide concentration of 250 nM (near the $K_d \cong 300$ nM), a separation of the PG/GAG species is evident as a broad smear throughout the lane and as a sharp band that migrates approximately half way down the lane, indicating heterogeneity in size, charge density, and/or peptide binding interactions of the PG/GAG population. PG/GAG samples in which HS PGs have been chemically degraded by nitrous acid (*EC PGs/NA*) also displayed high binding affinity ($K_d \cong 300$ nM), implying that chondroitin/dermatan sulfates that remain in the sample bind the peptide strongly. In contrast to the heterogeneity seen in *A*, *B* shows that heparin migrates as a single broad band of radiolabeled material.

α-helical conformation of a polypeptide in solution has been reported previously (26).

This same heparin effect is not obtained for the weak heparin-binding peptide $(AKKARA)_2$ (Fig. 4). In the absence of heparin (1:0), the peptide assumes a similar charged coil conformation as that observed for $(AKKARA)_6$ but fails to display α-helical character in the presence of heparin (1:0.25, 1:0.50, 1:0.075, or 1:1).

Peptide-PG Interactions—The interactions between consensus sequence peptides and PGs were also examined. For these experiments, total PGs were isolated from HUVEC cultures, because HUVECs have been shown to express a variety of types of HS and CS PGs, including, for example, syndecans, perlecan, glypican, and biglycan (28, 29). Thus, cell layer-associated and secreted $[^{35}S]SO_4$-radiolabeled PGs were purified by extraction with urea, and those PGs retained on DEAE after a 0.1 M NaCl rinse were studied for their binding to $(ARKKAAKA)_4$ by ACE (Fig. 5*A*, *EC PGs*). This peptide exhibited significant affinity for secreted HUVEC PGs, although the average affinity was somewhat weaker than that exhibited by the peptide for heparin (PG $K_d \cong 300$ nM; heparin $K_d \cong 50$ nM). Similar affinities were obtained for cell layer-associated PGs (data not shown). Inspection of ACE gels in which secreted PGs were fractionated through peptides demonstrated the presence of at least two populations of PG evident as two distinct bands of radiolabeled material migrating through the peptide lanes with different mobilities (Fig. 5*A*, *EC PGs*). This difference in migration rate could indicate heterogeneity of the PG in size or charge. In contrast to the heterogeneity seen in Fig. 5*A*, Fig. 5*B* shows that heparin migrates as a single band of radiolabeled material.

Thus, to ascertain which GAG chains, as well as which PG component (*i.e.* core protein, GAG chains, or both), were responsible for peptide binding, total HUVEC PGs were subjected to various chemical and enzymatic degradations. Samples were then tested for their ability to bind to $(ARKKAAKA)_4$. PGs in which HS GAGs were chemically degraded by nitrous acid or enzymatically degraded by heparatinase I were able to maintain comparable affinity for the peptide as was displayed by the total PG sample (Fig. 5*A*, *EC PGs/NA*, and Fig. 6). PGs in which CS GAG chains were digested with chondroitinase ABC were also able to maintain comparable affinity for the peptide. Release of GAG chains from cores by borohydride reduction resulted in a 3–4-fold diminished affinity (Fig. 6).

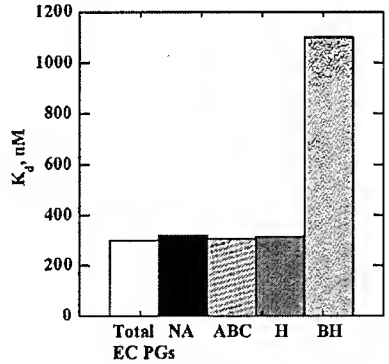

FIG. 6. **Affinity of $(ARKKAAKA)_4$ for HUVEC PGs and PG components.** The peptide was analyzed for binding affinity to HUVEC PGs/GAGs by ACE, and the K_d values of the peptide-PG/GAG interactions were calculated from binding plots as detailed under "Experimental Procedures." Similar affinities (~300 nM) were obtained for total PGs, for PG samples devoid of HS GAGs via nitrous acid treatment (*NA*) or heparatinase I digestion (*H*), and for PGs devoid of CS GAGs via chondroitinase ABC digestion (*ABC*). Liberation of GAG chains from the core protein by borohydride reduction (*BH*) of total PGs caused a 3-fold reduction in affinity ($K_d \cong 1200$ nM).

DISCUSSION

The goal of this study was to design high affinity heparin- and PG-binding peptides; the strategy we used was to incorporate into their structure copies of sequences proposed to bind heparin in native proteins. Our approach was also based on the fact that truncation of peptide structure without loss of activity

can sometimes be achieved by constraining or manipulating peptide conformation (30). In the case of apolioprotein E and apolipoprotein B-100, heparin-binding sites are believed to form α-helices upon heparin binding, and molecular modeling illustrates that basic amino acids in the binding sites align to one side of the helix to form a region of high positive charge through which heparin binding occurs (6). Thus, in our design of heparin-binding peptides, we also incorporated structural features conducive to stable α-helicity.

In our initial experiments, families of peptides were synthesized that contained single or multiple copies of heparin-binding consensus sequences. When their heparin binding was examined by ACE, peptides containing single sequences showed no measurable affinity for heparin. This result is as expected because peptides carrying single heparin-binding sequences found in native proteins often fail to display significant heparin binding (24), but they may contain multiple consensus sequences that come into proximity upon protein folding or multimerization, thereby enhancing heparin binding through cooperativity (31). In contrast, the affinity of peptides $(AKKARA)_n$ or $(ARKKAAKA)_n$ ranged from weak ($K_d \cong 6-40$ μM) at $n = 2$ to strong ($K_d \cong 50-100$ nM) at $n = 3-6$. These latter affinities are in the range of those displayed by heparin-binding proteins such as basic fibroblast growth factor ($K_d \cong 10$ nM) or type I collagen ($K_d \cong 100-200$ nM) (10). However, the fact that the peptides are roughly 4 times smaller than basic fibroblast growth factor and 100 times smaller than type I collagen highlights their significant heparin binding abilities. The affinity appeared to plateau at $n \geq 5$, or 36–40 amino acids, suggesting that peptides of approximately 30–32 amino acids were of sufficient length to occupy all available binding sites on low M_r heparin and that additional amino acid residues beyond this did not contribute to heparin binding due to a lack of available ligand. However, this hypothesis cannot be tested without knowing the M_r distribution of the heparin used in these experiments. Alternatively, one can speculate on the basis of coil and helix calculations that basic residue spacings within the peptides may account for both the increase and plateau in binding affinity observed for the larger peptides. The random walk calculations confirm that peptides of 20 residues are on the order of the same size as low M_r heparin, with an average 6,000 M_r, and have sufficient length to form a stable α-helix. Helical wheel constructions (not shown) illustrated that in peptides of ≥24 amino acids, basic residues occupy locations primarily to one side of the helix. The basic residues show three consistent spacings, estimated at approximately 10–12-, 20–24-, and 45–50-Å separations, with uncertainty being introduced primarily by the assumption of an ideal 18/5 helix. These spacings between basic amino acids could facilitate binding to sulfated heparin disaccharides, based on a 5.5-Å spacing between monosaccharide units, a distance predicted from spacing that occurs in CS (32). This is consistent with work by others who report a necessary 20–24-Å distance between basic amino acids for optimal heparin binding (9). Peptides of >36 amino acids do not exhibit a further increase in the number of basic residues aligning to one side of the helix in this 10- or 20-Å spacing; thus, the additional basic amino acids in the larger peptides may not contribute to a further increase in heparin binding affinity.

Other experiments examined heparin binding by peptides including sequences native to proteins that contain a single or partial heparin-binding consensus sequence. Results again suggested the critical nature of peptide M_r and number of consensus sequences to heparin binding. Thus, surprisingly, a strong heparin binding affinity was displayed by a peptide corresponding to the mouse SG proteoglycan core protein containing a single consensus sequence, YPARRARYQWVRCKP ($K_d \cong 200$ nM). However, the affinity was diminished over 200-fold by disulfide reduction or replacement of the cysteine with alanine, thus implying that its strong heparin binding relies on peptide dimerization and that the other residues flanking the consensus sequence were of little consequence. Indeed, others have shown that inclusion of cysteines near peptide termini to promote disulfide bond formation may improve peptide-ligand binding (30); our results suggest this to be a simple strategy to greatly enhance the affinity of peptides for heparin. SG, cerebroglycan (with PRRLRL) (33), and perlecan (with TRRFRD) (34) are among the few PGs that contain heparin-binding consensus sequences on their core proteins. Interestingly, the SG core protein, which carries many heparin chains, migrates at twice its predicted molecular weight on PAGE gels under reducing conditions (35), suggesting dimerization. This could result from GAG chains of one PG binding to the core protein of another or from core-core associations through disulfide bonding. The potential physiological function of such PG-PG interactions remains to be explored.

Additional consensus sequence peptides were designed to determine other aspects of peptide structure important to heparin binding. Including glycine in place of alanine in the hydropathic positions weakened heparin binding, and peptides in which arginine was included in all basic positions displayed higher affinity for heparin than did those containing arginines and lysines. The latter is consistent with work showing a higher affinity interaction of arginine-heparin and arginine-HS than lysine-heparin or lysine-HS (36). This suggests that the heparin binding characteristics of the peptides developed here may rely on amino acid type and arrangement in addition to ionic interactions. Inclusion of prolines within or between consensus sequence motifs weakened affinity for heparin, possibly as a result of alterations in peptide secondary conformation; this issue was investigated in our CD experiments. Finally, changing the spacing between consensus motifs weakened affinity for heparin; however, sequence orientation did not appear to influence binding ability as long as the motifs were contiguous and in one orientation.

Molecular modeling of consensus sequences in native heparin-binding proteins predicts their presence within α-helical regions (6). Additionally, GAG-directed conformational changes on polypeptides such as poly-L-lysine and poly-L-arginine have been identified (26, 37, 38). Aqueous solutions of these polypeptides at neutral pH were shown by CD to adopt charged coil conformations and to display α-helical conformations in the presence of heparin. Our results showed that peptides of the type $(AKKARA)_n$ have charged coil conformations at neutral pH. In the presence of heparin, however, a peptide that showed high affinity for heparin, $(AKKARA)_6$, underwent a conformational change to an α-helix. In the presence of excess heparin, a further conformational change produced a random coil structure. In contrast, a peptide that displayed weak heparin binding, $(AKKARA)_2$, failed to undergo any conformational change. Thus, the solution conformation of a peptide and its propensity to change conformation in the presence of heparin may be an indication of its ability to bind to heparin strongly. These data and those from experiments examining the effects of including prolines in peptides, which are known to disrupt the α-helical conformation, suggest that peptide secondary structure facilitates heparin binding.

Here we also examined the interaction between the high affinity heparin-binding peptide $(ARKKAAKA)_4$ and EC PGs. Results showed that ECs secreted several types of PGs/GAGs that displayed significant affinities for $(ARKKAAKA)_4$ ($K_d \cong 300$ nM). ACE gel images revealed the resolution of multiple

PG/GAG species after their migration through the peptide-containing lanes, suggesting heterogeneity in PG/GAG charge, size, and/or binding affinities. It was found that the CS PGs or HS PGs likely bind the peptide similarly, because affinity was maintained even after treatment of total PGs with nitrous acid, which selectively degrades HS GAGs, heparatinase I, or chondroitinase ABC. The free GAG chains had 3–4-fold lower affinity than the intact PGs. Thus, the core proteins of certain EC PGs may either contribute to binding directly or act as a tether to bring multiple GAGs into proximity for cooperative binding. Similar observations have been made previously for cartilage PG-type II collagen interactions (39) and SG-type I collagen interactions (40, 41). Our results are inconsistent with carbohydrate sequence selectivity in the binding of these peptides with EC PGs, because similar affinities for peptides were displayed by either total EC PGs or its CS PG fraction.

Of note is that the heparin-binding peptides designed here incorporate concatamers of heparin binding consensus sequences, which should rarely, if ever, appear in native proteins. Nonetheless, the proposed characteristics of heparin-binding motifs in proteins, as set forth by Cardin and Weintraub (6) based on their theoretical analysis of putative heparin-binding domains of native proteins, hold true with our model peptides. Thus, our data suggest that peptides containing the Cardin and Weintraub heparin-binding consensus sequences may show a selective advantage in heparin binding over certain other sequences that do not fit their criteria.

In summary, optimally active heparin-binding peptides should include multiple sequences of the types $(XBBXBX)_n$ and $(XBBBXXBX)_n$. Sequence number and peptide M_r are the most critical features; peptides should be of at least approximately 30 residues, which could be decreased to 15 if cysteine is included near either terminus to promote dimerization. Peptides should contain contiguous sequence arrays, without intervening residues between sequences. Alanine, which stabilizes α-helical conformation, should occupy the hydropathic residue positions, and arginine should occupy the basic positions. The high affinity PG- or GAG-binding peptides developed here, or derivatives thereof, could prove useful as tools for the promotion of cell-substratum attachment of PG-expressing cells, in the targeting of drugs to PG-expressing cells and PG-rich extracellular matrices, or as antagonists of GAG-mediated actions, *e.g.* neutralization of the anticoagulant activity of heparin.

Acknowledgment—We thank Dr. Eric Wickstrom of Thomas Jefferson University for the use of the JASCO 500C spectropolarimeter.

REFERENCES

1. Jackson, R. L., Busch, S. J., and Cardin, A. D. (1991) *Physiol. Rev.* **71**, 481–539
2. Racanelli, A., Fareed, J., Walenga, J. M., and Coyne, E. (1985) *Semin. Thromb. Hemostasis* **11**, 176–189
3. DeLucia, A., Wakefield, T. W., Andrews, P. C., Nichol, B. J., Kadell, A. M., Wrobleski, S. K., Downing, L. J., and Stanley, J. C. (1993) *J. Vasc. Surg.* **18**, 49–58
4. Hascall, V. C., Heinegard, D. K., and Wight, T. N. (1991) in *Cell Biology of Extracellular Matrix* (Hay, E. B., ed) pp. 149–172, Plenum Press, New York
5. Vargas, F. F., Osorio, H. M., Basilio, C., De Jesus, M., and Ryan, U. S. (1990) *Membr. Biochem.* **9**, 83–89
6. Cardin, A. D., and Weintraub, H. J. R. (1989) *Arteriosclerosis* **9**, 21–32
7. Lawler, J., and Hynes, R. O. (1986) *J. Cell Biol.* **103**, 1635–1648
8. Barkalow, F. J. B., and Schwartzbauer, J. E. (1991) *J. Biol. Chem.* **266**, 7812–7818
9. Margalit, H., Fischer, N., and Ben-Sasson, S. A. (1993) *J. Biol. Chem.* **268**, 19228–19231
10. San Antonio, J. D., Slover, J., Lawler, J., Karnovsky, M. J., and Lander, A. D. (1993) *Biochemistry* **32**, 4746–4755
11. Jordan, R., Beeler, D., and Rosenberg, R. (1979) *J. Biol. Chem.* **254**, 2902–2913
12. Laurent, T. C., Tengblad, A., Thunberg, L., Hook, M., and Lindhal, U. (1978) *Biochem. J.* **175**, 691–701
13. Lee, M. K., and Lander, A. D. (1991) *Proc. Natl. Acad. Sci. U. S. A.* **88**, 2768–2772
14. San Antonio, J. D., Lander, A. D., Karnovsky, M. J., and Slayter, H. S. (1994) *J. Cell Biol.* **125**, 1179–1188
15. San Antonio, J. D., Karnovsky, M. J., Gay, S., Sanderson, R. D., and Lander, A. D. (1994) *Glycobiology* **4**, 327–332
16. McPherson, J. M., Sawamura, S. J., Condell, R. A., Rhee, W., and Wallace, D. G. (1988) *Collagen Rel. Res.* **1**, 65–82
17. Tsilibary, E. C., Koliakos, G. G., Charonis, A. S., Vogel, A. M., Reger, L. A., and Furcht, L. T. (1988) *J. Biol. Chem.* **263**, 19112–19118
18. Gimbrone, M. A. (1976) in *Progress in Hematology and Thrombosis* (Collen, B. S., ed) Vol. III, pp. 1–28, W. B. Saunders, Philadelphia
19. Maciag, T., Cerundolo, J., Ilsley, S., Kelley, P. R., and Forand, R. (1979) *Proc. Natl. Acad. Sci. U. S. A.* **76**, 5674–5678
20. Shively, J. E., and Conrad, H. E. (1976) *Biochemistry* **15**, 3932–3942
21. Iozzo, R. V., and Muller-Glauser, W. (1985) *Cancer Res.* **45**, 5677–5687
22. Hiemenz, P. C. (1984) *Polymer Chemistry: The Basic Concepts*, Jwang Yuan Publishing Co., New York
23. Wunderlich, B. (1973) *Macromolecular Physics 1*, Academic Press, New York
24. Conrad, H. E. (1998) *Heparin-Binding Proteins*, Academic Press, San Diego
25. Ferran, D. S., Sobel, M., and Harris, R. B. (1992) *Biochem.* **31**, 5010–5016
26. Gelman, R. A., Rippon, W. B., and Blackwell, J. (1973) *Biopolymers* **12**, 541–558
27. Adler, A. J., and Fasman, G. D. (1971) *J. Phys. Chem.* **75**, 1516–1526
28. Mertens, G., Cassiman, J., Van den Berghe, H., Vermylen, J., and David, G. (1992) *J. Biol. Chem.* **267**, 20435–20443
29. Jarvelainen, H. T., Kinsella, M. G., Wight, T. N., and Sandell, L. J. (1991) *J. Biol. Chem.* **266**, 23274–23281
30. Starovasnik, M. A., Braisted, A. C., and Wells, J. A. (1997) *Proc. Natl. Acad. Sci. U. S. A.* **94**, 10080–10085
31. Huntington, J. A., Olson, S. T., Fan, B., and Gettins, P. G. (1996) *Biochemistry* **35**, 8495–8503
32. Doyle, B. B., Hukins, D. W. L., Hulmes, D. J. S., Miller, A., and Woodhead-Galloway, J. (1975) *J. Mol. Biol.* **91**, 79–99
33. Stipp, C. S., Litwack, E. D., and Lander, A. D. (1994) *J. Cell Biol.* **124**, 149–160
34. Murdoch, A. D., Dodge, G. R., Cohen, I., Tuan, R. S., and Iozzo, R. V. (1992) *J. Biol. Chem.* **267**, 8544–8557
35. Perin, J.-P., Bonnet, F., Maillet, P., and Jolles, P. (1988) *Biochem. J.* **255**, 1007–1013
36. Fromm, J. R., Hileman, R. E., Caldwell, E. E. O., Weiler, J. M., and Linhardt, R. J. (1995) *Arch. Biochem. Biophys.* **232**, 279–287
37. Gelman, R. A., and Blackwell, J. (1973) *Arch. Biochem. Biophys.* **159**, 427–433
38. Gelman, R. A., and Blackwell, J. (1974) *Biopolymers* **13**, 139–156
39. Toole, B. (1976) *J. Biol. Chem.* **251**, 895–897
40. Schick, B. P., Pestina, T. I., San Antonio, J. D., Stenberg, P. E., and Jackson, C. W. (1997) *J. Cell. Physiol.* **172**, 87–93
41. Schick, B. P., and Jacoby, J. A. (1995) *J. Cell. Physiol.* **165**, 96–106

Analysis of Affinity and Structural Selectivity in the Binding of Proteins to Glycosaminoglycans: Development of a Sensitive Electrophoretic Approach

MK Lee, and AD Lander

PNAS 1991;88;2768-2772
doi:10.1073/pnas.88.7.2768

Proc. Natl. Acad. Sci. USA
Vol. 88, pp. 2768–2772, April 1991
Biochemistry

Analysis of affinity and structural selectivity in the binding of proteins to glycosaminoglycans: Development of a sensitive electrophoretic approach

MATTHIAS K. LEE* AND ARTHUR D. LANDER*†‡

*Department of Biology and †Department of Brain and Cognitive Sciences, Massachusetts Institute of Technology, Cambridge, MA 02139

Communicated by Phillip A. Sharp, December 13, 1990

ABSTRACT **Members of several families of cell surface and secreted proteins bind glycosaminoglycans (GAGs), the structurally heterogeneous polysaccharides found on proteoglycans. To understand the physiological significance of the interactions of proteins with GAGs, it is critical that relationships between GAG structure and binding be analyzed. It is particularly important that interactions depending on common structural features of GAGs (e.g., size, charge density, and disaccharide repeat unit) be distinguished from those mediated by specific sequences of carbohydrate modification. Gathering the information needed to make such distinctions has so far been difficult, however, partly because structurally homogeneous samples of GAGs are lacking but also because of technical difficulties associated with performing and interpreting assays of protein–GAG binding. We describe an electrophoretic method useful for both measuring affinity and evaluating structural selectivity in protein–GAG binding. Data are presented on the binding of the GAG heparin to the protease inhibitor antithrombin III, the acidic and basic fibroblast growth factors, and the extracellular matrix protein fibronectin. Results obtained with fibronectin are consistent with a model in which high-affinity binding ($K_d \sim 34$ nM) is mediated through the recognition of specific carbohydrate sequences.**

Proteins that bind glycosaminoglycans (GAGs) include many cell adhesion molecules, glycoproteins of the extracellular matrix, polypeptide growth factors, secreted proteases and antiproteases, and proteins involved in lipoprotein uptake (1, 2). In the tissue environments in which these proteins are found, GAGs are present as side chains of proteoglycans and exhibit diversity in length, disaccharide composition, and patterns of N- and O-sulfation.

For most GAG-binding proteins, the relationship between GAG structure and binding affinity is poorly understood. For some, all that is known is that a high concentration of salt is required to elute them from heparin-agarose columns; sometimes the relative abilities of GAGs of different classes (e.g., heparan sulfate, chondroitin sulfate, dermatan sulfate, keratan sulfate, etc.) to compete away such binding has also been measured (e.g., refs. 3 and 4). Those direct measurements of affinity that have been made have often required derivatization or immobilization of either protein or GAG (e.g., refs. 5–7); such measures may inhibit (e.g., by blocking sites of interaction) or artificially enhance (e.g., by favoring multivalent interactions) binding. Quantifying binding is also impeded by the fact that most GAG–protein K_d values are thought to be in the range of 5–500 nM, where the possibility of rapid dissociation kinetics argues against the use of many types of binding assays that involve separation and washing of bound complexes. In addition, measurements that have been made of GAG–protein affinity have usually measured the average affinity of a protein for the structurally heterogenous set of binding sites represented by any GAG sample. Selectivity of a protein for specific sequences of carbohydrate modification is, therefore, not readily appreciated, despite the fact that such selectivity exists and is, in at least one case, of considerable physiological importance (8).

Below, experiments are presented in which the principle of affinity electrophoresis (9) was exploited to analyze protein–GAG binding. The technique described is referred to as affinity coelectrophoresis (ACE) because both protein and GAG are permitted to migrate freely during electrophoresis (typically, in affinity electrophoresis, as in affinity chromatography, one ligand is physically immobilized). The method uses small amounts of material and can yield values of the affinity constant even when dissociation is rapid (e.g., when affinity is low). Experiments are presented in which ACE was used to identify and isolate a subpopulation of heparin molecules to which fibronectin binds selectively. Some of these data have been presented in abstract form (10, 11).

MATERIALS AND METHODS

Materials. Low-melting-point agarose (SeaPlaque) and GelBond were purchased from FMC, heparin (grade I, from porcine intestinal mucosa) was from Sigma, chondroitin sulfate (from shark cartilage) was from Fluka, bovine serum albumin (crystalline) was from ICN, and human plasma fibronectin (FN) was from New York Blood Center (New York). Basic fibroblast growth factor (bFGF) and acidic fibroblast growth factor (aFGF) were purified from bovine brain (12). Human antithrombin III (AT) was the generous gift of Robert Rosenberg (M.I.T.). β-Nerve growth factor was generously donated by Randall Pittman (University of Pennsylvania).

Heparin was substituted with fluoresceinamine to a level of 15.7 ng/μg (13) and radioiodinated to a specific activity of 110,000 cpm/ng (14). A portion of the ^{125}I-labeled fluoresceinamine-heparin (^{125}I-F-heparin) was fractionated by gel filtration [on Sephadex G-100 in 50 mM sodium 3-(*N*-morpholino)-2-hydroxypropanesulfonate) (Mopso), pH 7.0/125 mM sodium acetate] and the last 10.8% of the radioactive material to elute ($0.57 < K_{av} < 0.76$) was pooled as a low molecular weight (LMW) fraction. This fraction was estimated to contain heparin chains of $M_r \leq 6000$ (3, 15–18).

Electrophoretic Analysis of Binding. Low-melting-point agarose (1%) was prepared in either of two electrophoresis buffers: 50 mM sodium Mopso, pH 7.0/125 mM sodium acetate/0.5% 3-[(3-cholamidopropyl)dimethylammonio]-1-

The publication costs of this article were defrayed in part by page charge payment. This article must therefore be hereby marked "*advertisement*" in accordance with 18 U.S.C. §1734 solely to indicate this fact.

Abbreviations: ACE, affinity coelectrophoresis; aFGF and bFGF, acidic and basic fibroblast growth factor, respectively; AT, antithrombin III; CHAPS, 3-[(3-cholamidopropyl)dimethylammonio]-1-propanesulfonate; ^{125}I-F-heparin, ^{125}I-labeled fluoresceinamine-heparin; FN, fibronectin; GAG, glycosaminoglycan; LMW, low molecular weight; Mopso, 3-(*N*-morpholino)-2-hydroxypropanesulfonic acid.

‡To whom reprint requests should be addressed.

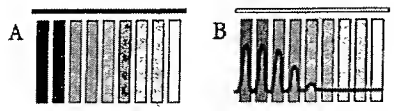

FIG. 1. Schematic representation of a gel before and after electrophoresis. Proteins are cast at various concentrations into nine rectangular zones within an agarose gel (*A*); the dark line at top represents a slot into which labeled GAG is introduced. During electrophoresis, GAGs migrate through the rectangular zones but are slowed by binding to proteins. This produces a series of peaks (*B*), from which an affinity constant may be derived (see text).

propanesulfonate (CHAPS) (buffer A) or 50 mM sodium Mopso, pH 7.0/125 mM NaCl/0.5% CHAPS (buffer B). A Teflon comb consisting of nine parallel bars, each 45 × 4 × 4 mm and held rigidly together with a spacing of 3 mm between bars, was placed onto GelBond film fitted to a Plexiglas casting tray (75 × 100 mm) with the long axis of the bars parallel to the long dimension of the tray. A Teflon strip (66 × 37 × 1 mm) was stood on edge with its long dimension parallel to the short dimension of the casting tray, at a distance of 4 mm from one edge of the Teflon comb. Tabs extending from the Teflon strip enabled it to be held upright by tape affixed to the casting tray. Typically, 19 ml of agarose were poured hot (>70°C) to achieve a cooled gel ≈4 mm thick. Removal of the comb and strip resulted in a gel containing nine 4 × 45 mm rectangular wells adjacent to a 66 × 1 mm slot (Fig. 1*A*).

Protein samples (typically 350 μl) were prepared in electrophoresis buffer at twice the desired concentrations. Samples were mixed with an equal volume of melted 2% (wt/vol) agarose at 37°C, pipeted into the appropriate rectangular wells, and allowed to gel. After submerging a protein-loaded gel in the electrophoresis chamber (Hoefer SuperSub) containing buffer minus CHAPS, ≈190 μl of ^{125}I-F-heparin [4 ng/ml in electrophoresis buffer containing 0.5% bromphenol blue and 6% (wt/vol) sucrose] was added to the 66 × 1 mm slot.

Typically, electrophoresis was performed at 60–70 V (2–2.4 V/cm) for 0.75–2 hr, with currents of ≈330 mA (in buffer A). Buffer was recirculated, and a flow of cold tap water through the coolant ports of the apparatus was used to maintain buffer temperature at 20–25°C. Endpoints were determined by the position of the bromphenol blue, which migrated about half as rapidly as heparin. Gels were air-dried and autoradiographed against preflashed film at −80°C. In some experiments, ^{125}I-F-heparin was recovered from gels by electroelution in 0.75 mM NaOAc/0.25 mM sodium Mopso, pH 7, concentrated 2-fold using a SpeedVac evaporator (Savant), and retested for binding using ACE.

RESULTS

Demonstration of Protein–GAG Binding. At neutral pH, the electrophoretic mobilities of most proteins are much lower than those of GAGs. Consequently, the binding of proteins to GAGs should, in most cases, retard GAG electrophoresis. To determine whether this effect could be exploited to quantify protein–GAG binding, a method was devised for electrophoresing labeled GAGs though zones containing multiple protein samples. Briefly, special combs were used to create agarose gels of the configuration shown in Fig. 1*A*. The long rectangles represent wells into which proteins in molten low-gelling-temperature agarose (at 37°C) could be introduced and allowed to gel. The dark line at the top of Fig. 1*A* indicates where samples of labeled GAGs were introduced. The position of the anode is at the bottom. Fig. 1*B* presents the expected experimental results when the nine wells contain a single GAG-binding protein at a series of concentrations decreasing from left to right: at sufficiently high protein concentrations, migration of the GAG front (thick black line) is retarded in a dose-dependent manner. The protein-free spaces between the wells facilitate measurement of the changes in mobility associated with each protein concentration.

Fig. 2*A* shows that the predicted pattern was indeed obtained when ^{125}I-F-heparin was electrophoresed at neutral pH and physiological ionic strength through zones containing a known heparin-binding protein, bFGF. In response to bFGF concentrations of up to 35 nM, heparin mobility was reduced up to 88%. The effect was specific, in that even much higher concentrations of nerve growth factor (a protein of similar size and isoelectric point to bFGF) had no effect on ^{125}I-F-heparin mobility (Fig. 2*B*).

An assumption made in predicting the simple pattern shown in Fig. 1*B* was that all heparin molecules behave more or less identically. The data in Fig. 2 *A* and *B* support this assumption. In contrast, experiments performed with a different heparin-binding protein, AT, illustrate the type of pattern that can result when heparin molecules do not behave identically (Fig. 2*C*). In this case, the migrating heparin front was split by AT into two distinct fronts, one of which was progressively slowed by AT concentrations ≥5 nM, whereas the other was shifted only slightly by AT at 1 μM. The same result was obtained with a size-selected LMW fraction of ^{125}I-F-heparin (Fig. 2*D*). A large excess of unlabeled heparin

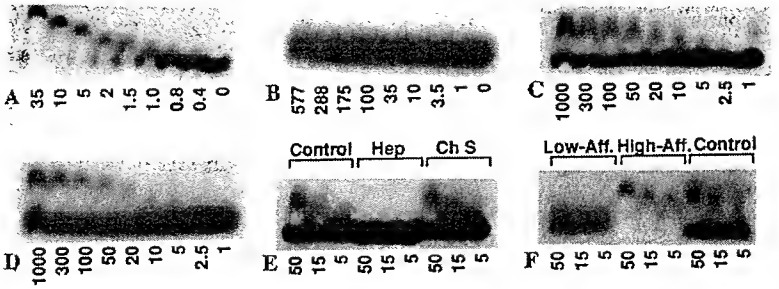

FIG. 2. (*A–D*) Autoradiographs of gels in which ^{125}I-F-heparin was electrophoresed through zones containing bFGF (*A*), β-nerve growth factor (*B*), and AT (*C* and *D*). Protein concentrations are in nM. (*B* and *D*) Size-selected LMW heparin was used. (*E*) Inhibition of binding of ^{125}I-F-heparin to AT by unlabeled heparin. In this experiment, a gel was cast with three sample slots, each opposite three of nine rectangular zones. Equal amounts of ^{125}I-F-heparin were introduced into each slot. In the central slot, unlabeled heparin (1 mg/ml) was mixed with the labeled sample; in the slot at right, unlabeled chondroitin sulfate (1 mg/ml) was added. Concentrations of AT are in nM. (*F*) Recovery and analysis of heparin with high and low affinity for AT. A set of three sample slots was prepared as in *E*. Into the slot at left was loaded material isolated from LMW ^{125}I-F-heparin that had previously migrated through AT-containing agarose without retardation (lanes Low-Aff.). Material that had been retarded by AT was isolated and loaded in the central slot (lanes High-Aff.). Control ^{125}I-F-heparin was loaded in the slot at right. Concentrations of AT are shown in nM.

readily blocked the effects of AT on heparin mobility, but an equal concentration of chondroitin sulfate did not (Fig. 2*E*).

These results fit with what is known about the properties of AT, one of the most studied GAG-binding proteins: AT binds a subset of heparin molecules, with subtleties of carbohydrate sequence, rather than heparin chain length, providing the basis for selectivity (19). To confirm that the two heparin fronts observed in ACE gels containing AT actually result from the fractionation of heparin into distinct species with different binding properties, a gel similar to the one shown in Fig. 2*D* was electrophoresed and pieces of agarose were cut out of locations where the two heparin fronts were well separated. The pieces were then melted, and their contents were retested for binding to AT. The results (Fig. 2*F*) confirm that separable fractions of heparin account for the pattern in Fig. 2*D*.

Measurement of Binding Affinity. In general, heparin's mobility in any protein-containing environment should be the average of the mobilities of protein-bound heparin and free heparin, weighted according to the fraction of time that heparin molecules spend in the bound and free states. To quantify protein-induced shifts in mobility, it is convenient to introduce a unitless number, the retardation coefficient R [$R = (M_o - M)/M_o$, where M_o is the mobility of free heparin and M is heparin's observed mobility through a protein-containing zone]. Provided that heparin and protein form a 1:1 complex, R at any protein concentration should be proportional to the amount of heparin bound. Moreover, if R_∞ is taken to represent the value of R seen at full saturation (i.e., at an arbitrarily high concentration of binding protein), then R/R_∞ should be equivalent to the fractional saturation. Accordingly, experimental values of R should vary with protein concentration according to the Scatchard equation; specifically, a plot of $R/[\text{protein}]_{\text{free}}$ vs. R should yield a straight line with a slope of $-1/K_d$ and a y intercept of R_∞/K_d. If the concentration of heparin is small compared to K_d, plotting $R/[\text{protein}]_{\text{total}}$ vs. R should yield the same plot.

Two such plots are shown in Fig. 3. The data for bFGF binding to LMW heparin (Fig. 2*A*) fit a line implying a K_d of 2 nM. For AT binding to LMW heparin, values of R obtained from Fig. 2*D* also fit a line, implying a K_d of 16 nM (Fig. 3*B*). Straight lines also fit the data obtained for the binding of unfractionated heparin to bFGF and AT, and for the binding of heparin to aFGF and serum albumin (data not shown). These findings are summarized in Table 1. Results with two buffer systems that differed in their major anion (chloride vs. acetate) did not differ significantly.

Characterization of Heparin Binding to FN. FN is a major glycoprotein of the extracellular matrix and a component of plasma (20, 21). FN binds heparin and heparan sulfate (3, 22, 23), whereupon alterations in its structural properties and ability to bind other molecules can be detected (e.g., refs. 24–26). Recent evidence indicates that the attachment of epithelial cells and fibroblasts to FN is mediated, in part, by cell surface heparan sulfate (27, 28).

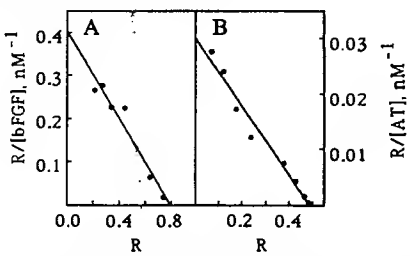

FIG. 3. Graphic analysis of binding of bFGF to LMW heparin (*A*) and binding of AT to the high-affinity fraction of LMW heparin (*B*). The lines drawn imply K_d values of 2 nM for bFGF and 16 nM for AT.

Plasma FN, a disulfide-linked dimer, is eluted from heparin-Sepharose between 0.3 and 0.5 M NaCl (29). Two distinct heparin-binding fragments of FN have been identified and mapped. Yamada *et al.* (3) used a filter-binding assay to measure the binding of [^{3}H]heparin to FN and obtained a biphasic Scatchard plot, suggestive of two component affinities (K_d values of 4.2 nM and 110 nM), but were unable to determine whether their data reflected differences in the affinity of heparin for two distinct sites on FN or the presence of subspecies of heparin that bind FN with different affinities. In addition, values of K_d were derived assuming that heparin molecules contain only one binding site for FN. This assumption may not be valid, especially given that particularly long heparin chains (average M_r, 12,000) were used in that study (3).

Analysis of the heparin–FN interaction by ACE is shown in Fig. 4*A*. At high FN concentrations, LMW ^{125}I-F-heparin was observed to shift to a single very low mobility, implying that essentially all heparin molecules bind FN. At somewhat lower FN concentrations, however, the labeled material migrated not as a discrete band but as a diffuse smear. It seemed likely that this smear represented the fractionation of individual heparin molecules according to differences in affinity for FN.

To test this possibility, LMW ^{125}I-F-heparin was electrophoresed through a single zone of 125 nM FN. The gel was then cut transversely into segments, and fractions were pooled representing the leading 26% of the ^{125}I-F-heparin (pool 1, "weakly retarded heparin") and the trailing 26% (pool 2, "strongly retarded heparin"). The samples were heated to 100°C for 10 min (to denature FN) and labeled heparin was recovered by electroelution. The resulting material was retested for binding to FN. As shown in Fig. 4 *B* and *C*, the ACE patterns for pools 1 and 2 were distinctly different from each other and considerably less diffuse than those of the starting material.

Graphical analysis of the patterns in Fig. 4 *B* and *C* is shown in Fig. 5. The data from pool 1 yield a linear plot, suggesting a K_d of 640 nM. Pool 2 yields an apparently discontinuous plot—two line segments with similar slopes (implying K_d values of 32 and 36 nM). Examination of Fig. 4*C* indicates how the result for pool 2 arises: with increasing FN concentration, heparin's mobility decreases, levels off at $R \approx 0.5$,

Table 1. Measurement of protein affinities for heparin and LMW heparin

Protein	Heparin	K_d, nM
bFGF	Unfractionated	2.2
	LMW	2.0
	LMW	3.1*
AT	Unfractionated, HA	11
	LMW, HA	16
	LMW, HA	12*
	Unfractionated, LA†	≈6000
aFGF	LMW	91
Plasma FN	LMW, HA‡	34
	LMW, LA‡	640
Nerve growth factor	LMW	>600§
Serum albumin	LMW	4300

Measurements were made in buffer A except for those indicated by an asterisk, which were made in buffer B. HA and LA refer to strongly retarded (high affinity) and weakly retarded (low affinity) fractions, respectively, as isolated from ACE gels (see text). As described in the *Discussion*, correct values of K_d for bFGF may be lower by as much as 0.8 nM.

†Estimated from data in Fig. 2*C* and the assumption that R_∞ for low-affinity heparin will be the same as that observed for high-affinity heparin.

‡From the experiment described in Figs. 4 and 5.

§Highest concentration tested.

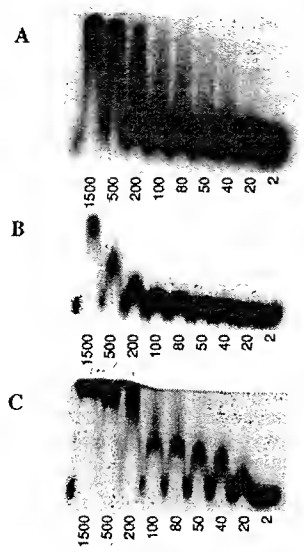

FIG. 4. Analysis of heparin–FN binding. (*A*) Electrophoresis of ^{125}I-F-heparin through zones containing FN (concentrations in nM, based on a molecular weight of 440,000). In contrast to the examples in Fig. 1, the migrating heparin front becomes broadly smeared at protein concentrations between 50 and 500 nM. (*B* and *C*) After electrophoresis of ^{125}I-F-heparin in the presence of 125 nM FN, the 26% of labeled material that was retarded least (pool 1) and the 26% of labeled material that was retarded most (pool 2) were recovered by electroelution and retested for binding to FN. The patterns produced by pool 1 (*B*) and pool 2 (*C*) are distinctly different.

and then shifts again, leveling off at $R \approx 0.8$. This behavior is most easily explained by the known tendency of FN to self-aggregate when concentrated (see ref. 30). Thus, the first shift (to $R \approx 0.5$) may represent saturation of heparin by single FN molecules, whereas the second shift (to $R \approx 0.8$) reflects aggregation of FN molecules into oligomers (which, being larger, more strongly retard heparin's mobility). In support of this view, studies in which trace amounts of ^{125}I-labeled FN were electrophoresed in the presence of unlabeled FN showed that the mobility of FN in 2% agarose undergoes a concentration-dependent decrease (consistent with aggregation) in the expected range (10–200 nM) (unpublished observations).

Thus the data in Figs. 4 and 5 indicate that LMW heparin is heterogeneous and that classes of heparin molecules that differ by as much as 20-fold in affinity for FN can be isolated. To test whether this difference in affinity depends on heparin size (chain length), pools 1 and 2 were compared by gel

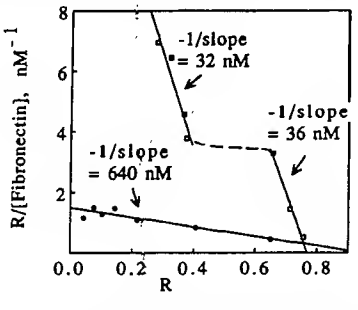

FIG. 5. Graphic analysis of data in Fig. 4 *B* and *C*. Weakly retarded heparin (●) yields a linear plot implying a K_d value of 640 nM. Strongly retarded heparin (□) yields a discontinuous plot with two line segments that imply K_d values of 32 nM and 36 nM. The discontinuity apparently reflects oligomerization of FN at high concentrations (see text).

filtration on Sephadex G-75 in 10 mM Mopso, pH 7.0/125 mM sodium acetate/4 M urea. The size distributions of molecules in pools 1 and 2 were largely overlapping, with those of pool 1 being slightly smaller ($K_{av} = 0.250$) and those in pool 2 slightly larger ($K_{av} = 0.162$) than the LMW heparin from which both pools were derived ($K_{av} = 0.235$) (data not shown). To assess whether the molecules in pools 1 and 2 differed greatly in charge density (a reflection of the degree of sulfation), their electrophoretic mobilities in 1% agarose (containing no binding proteins) were compared. The mobilities obtained for the two pools were identical: $5.6 \pm 0.03 \times 10^{-8}$ m^2/V·s for pool 1 and $5.6 \pm 0.05 \times 10^{-8}$ m^2/V·s for pool 2 (in buffer A at 25°C).

DISCUSSION

We report here the development of an affinity-electrophoretic technique, ACE, for studying GAG–protein interactions. Binding is measured at physiological pH and ionic strength and under conditions in which interacting molecules are freely mobile. ACE can in principle be used to measure binding between any two macromolecules, provided that the complex they form has an electrophoretic mobility different from that of at least one of its components. In practice, this difference should be large enough that distances migrated by bound and free ligand are distinguishable within reasonable time. In some of the experiments described above, it was possible to achieve sufficient separations with electrophoresis of the GAG front through only 20 mm of gel; in no experiment was electrophoresis through >50 mm necessary. These distances required short electrophoresis times at modest field strengths (e.g., 2.4 V/cm for 1–2 hr). Also, because electrophoresis was carried out in a gel of small width and height, little material was required. For example, to measure binding of heparin to AT in Fig. 2*E*, only 400 pmol of protein and 75 fmol of GAG were used. Considering that ACE can measure affinities when dissociation rates are fast and that other techniques for doing so [e.g., equilibrium gel filtration (31, 32)] can require large amounts of material, the sensitivity of ACE seems particularly good.

Accurate determination of affinity constants using ACE requires that the following conditions be met. (*i*) The radiolabeling of one component should not affect binding. (*ii*) The physical properties of the gel should not affect binding. (*iii*) The kinetics of association and dissociation should be rapid compared to the time of electrophoresis. In the experiments reported here, heparin was substituted with <1 fluoresceinamine per molecule and radioiodinated (14); the possibility that labeling interfered with binding is argued against by ACE experiments on the binding of intact proteoglycans (labeled by protein radioiodination) to FN and the binding of heparan sulfate (metabolically labeled) to AT, which have yielded results similar to those reported here (ref. 11; T. Kojima, G. Marchildon, and R. Rosenberg, personal communication). Also, electrophoresis was performed using a highly porous matrix (1% agarose) to minimize effects of sieving on molecular interactions, and electrophoresis times were long (1–2 hr) compared with likely kinetic constants.

As shown in Figs. 3 and 5, it is convenient to analyze ACE data by plotting $R/[\text{protein}]_{total}$ vs. R and to obtain an apparent value of K_d from the slope. Strict validity of this procedure has the following three requirements.

(*i*) **Concentration of GAG Is Much Less Than the K_d.** Use of the total, rather than the free, concentration of protein in the Scatchard equation is convenient, because it does not require the concentration of labeled heparin to be known accurately. This substitution is valid as long as the total concentration of heparin is sufficiently low. Otherwise, deviations from linearity at low values of R will occur, leading to a possible overestimation of K_d (by an amount no greater than the heparin concentration itself). The results in Table 1 were

obtained using heparin at 4 ng/ml, which for LMW heparin chains (estimated M_r, 5000–6000) is equivalent to 0.7–0.8 nM (for unfractionated heparin, the molar concentration would be lower). At this heparin concentration, the K_d values in Table 1 should be reasonably accurate with one exception: For the binding of bFGF to LMW heparin, the measured K_d of 2.0–3.1 nM should probably be revised to 1.2–2.4 nM.

***(ii)* Mobilities of GAG–Protein Complexes Are Independent of Protein Concentration.** The assertion that the retardation coefficient R is proportional to the fractional saturation of GAG by protein assumes that the GAG–protein complex has a single fixed mobility. In some cases this may not be true, as results obtained with FN illustrate. Because of protein–protein interactions, mobility of the heparin–FN complex is lower at high FN concentrations than at low FN concentrations, giving rise to a nonlinear Scatchard plot (Fig. 5).

***(iii)* GAGs Are Not Multivalent.** The binding of a second (or third, etc.) protein molecule to a GAG is not likely to produce as large a change in mobility as the binding of the first. Accordingly, if GAGs are multivalent, ACE data will tend to emphasize the behavior of the first site to saturate. If multiple sites of equivalent affinity are present, the Scatchard plots obtained may, for statistical reasons, be nonlinear and possess slopes that lead to an underestimation of the intrinsic K_d of the binding sites (by a factor not exceeding the number of binding sites). A more detailed treatment of the effects of multivalency and protein–protein interactions on ACE patterns will be presented elsewhere (unpublished results).

In this study, measurements were made of the affinity of several proteins for heparin. Where prior information on affinity is available, it agrees reasonably well with the results presented here. For example, affinity chromatographic studies of heparin binding to AT indicate that two populations of heparin exist, one with high affinity and one with low affinity, and that the latter species is more abundant in commercial preparations of heparin (8, 33); the data in Fig. 2 *E* and *F* imply both of these statements. The K_d values reported in Table 1 for the binding of heparin to AT are within or close to the range of values that have been published by others, namely, 12.5–100 nM for the high-affinity fraction of heparin and 20–100 μM for the low-affinity fraction (5, 8, 16). Methodological differences or differences in the ionic composition of buffers may account for the ranges of values.

For bFGF, the values in Table 1 agree reasonably well with affinities reported for the binding of this growth factor to cell surface heparan sulfate, namely, 0.5 nM (34) and 2 nM (35), especially if the values in Table 1 are corrected as described above. The affinity of 91 nM obtained with aFGF is consistent with the fact that the binding of this growth factor to heparin-agarose is apparently weaker than that of bFGF (36).

For FN binding to heparin, ACE analysis uncovered evidence of selective binding of FN to subpopulations of heparin molecules. Although classes exhibiting two distinct K_d values were identified, they were derived from the 52% of heparin molecules that were either most strongly or most weakly retarded; therefore, it is possible that molecules with intermediate affinities were also present. When heparin subpopulations binding strongly and weakly to FN were compared, no difference in overall charge density was detected. Strongly binding heparin molecules were, however, slightly larger on average than weakly binding ones. These are precisely the properties expected if high-affinity binding to fibronectin is mediated by one or more specific rare carbohydrate sequences. A slightly larger size for high-affinity molecules is predicted on statistical grounds, as rare sequences are expected to be most common on long chains (15). Indeed, the same phenomenon has been observed with AT: fractionation of heparin populations by their affinity for AT produces a high-affinity fraction with an average size slightly larger than the low-affinity fraction (15, 16) despite the fact that the binding of AT is mediated by a specific short carbohydrate sequence (19).

If, as the data presented here suggest, FN recognizes specific carbohydrate sequences on heparin, it will be important to investigate the binding of FN to heparan sulfates, which bear the same carbohydrate modifications as heparin but which are widely distributed *in vivo*. Interestingly, large differences have been reported in the degree to which heparan sulfates from different sources bind FN (e.g., refs. 3 and 37). These results raise the possibility that cells, by controlling specific steps in GAG modification, could modulate their ability to use heparan sulfate as a cell-surface receptor for FN (27, 28).

We thank Dr. R. Rosenberg (M.I.T.) for many helpful discussions during the development of this method and for the generous gift of AT. This work was supported by National Institutes of Health Grant NS26862. M.K.L. was supported in part by the Undergraduate Research Opportunities Program of M.I.T.

1. Lindahl, U. & Hook, M. (1978) *Annu. Rev. Biochem.* **47**, 385–417.
2. Jackson, R. L., Busch, S. J. & Cardin, A. D. (1991) *Physiol. Rev.* **71**, 481–539.
3. Yamada, K. M., Kennedy, D. W., Kimata, K. & Pratt, R. M. (1980) *J. Biol. Chem.* **255**, 6055–6063.
4. Del Rosso, M., Cappalletti, R., Viti, M., Vannucchi, S. & Chiarugi, V. (1981) *Biochem. J.* **199**, 699–704.
5. Rosenberg, R. D., Oosta, G. M., Jordan, R. E. & Gardner, W. T. (1980) *Biochem. Biophys. Res. Commun.* **96**, 1200–1208.
6. Jordan, R. E., Oosta, G. M., Gardner, W. T. & Rosenberg, R. D. (1980) *J. Biol. Chem.* **255**, 10073–10080.
7. Skubitz, A. P. N., McCarthy, J. B., Charonis, A. S. & Furcht, L. T. (1988) *J. Biol. Chem.* **263**, 4861–4868.
8. Bjork, I. & Lindahl, U. (1982) *Mol. Cell. Biochem.* **48**, 161–182.
9. Horejsi, V. (1981) *Anal. Biochem.* **112**, 1–8.
10. Lee, M. K. & Lander, A. D. (1989) *J. Cell Biol.* **109**, 109 (abstr.).
11. Herndon, M. E., Lee, M. K. & Lander, A. D. (1990) *J. Cell Biol.* **111**, 267 (abstr.).
12. Lobb, R. R. & Fett, J. W. (1984) *Biochemistry* **23**, 6295–6299.
13. Glabe, C. G., Harty, P. K. & Rosen, S. D. (1983) *Anal. Biochem.* **130**, 287–294.
14. Smith, J. W. & Knauer, D. J. (1987) *Anal. Biochem.* **160**, 105–114.
15. Laurent, T. C., Tengblad, A., Thunberg, L., Hook, M. & Lindahl, U. (1978) *Biochem. J.* **175**, 691–701.
16. Jordan, R., Beeler, D. & Rosenberg, R. (1979) *J. Biol. Chem.* **254**, 2902–2913.
17. Rosenberg, R. D., Jordan, R. E., Favreau, L. V. & Lam, L. H. (1979) *Biochem. Biophys. Res. Commun.* **86**, 1319–1324.
18. Danielsson, A. & Bjork, I. (1981) *Biochem. J.* **193**, 427–433.
19. Lindahl, U., Thunbereg, L., Backstrom, G., Riesenfeld, J., Norling, K. & Bjork, I. (1984) *J. Biol. Chem.* **259**, 12368–12376.
20. Hynes, R. O. (1985) *Annu. Rev. Cell Biol.* **25**, 295–305.
21. Ruoslahti, E. (1988) *Annu. Rev. Biochem.* **57**, 375–413.
22. Ruoslahti, E. & Engvall, E. (1980) *Blochlm. Biophys. Acta* **631**, 350–358.
23. Stamatoglou, S. C. & Keller, J. M. (1982) *Biochim. Biophys. Acta* **719**, 90–97.
24. Welsh, E. J., Frangou, S. A., Morris, E. R., Rees, D. A. & Chavin, S. I. (1983) *Biopolymers* **22**, 821–831.
25. Osterlund, E., Eronen, I., Osterlund, K. & Vuento, M. (1985) *Biochemistry* **24**, 2661–2667.
26. Johansson, S. & Hook, M. (1980) *Biochem. J.* **187**, 521–524.
27. Gill, P. J., Silbert, C. K. & Silbert, J. E. (1986) *Biochemistry* **25**, 405–410.
28. Saunders, S. & Bernfield, M. (1988) *J. Cell Biol.* **106**, 423–430.
29. Yamada, K. M. (1983) *Annu. Rev. Biochem.* **52**, 761–799.
30. Homandberg, G. A. (1987) *Biopolymers* **26**, 2087–2098.
31. Hummel, J. P. & Dryer, W. J. (1962) *Biochim. Biophys. Acta* **63**, 530–532.
32. Horwitz, A., Duggan, K., Greggs, R., Decker, C. & Buck, C. (1985) *J. Cell Biol.* **101**, 2134–2144.
33. Lam, L. H., Silbert, J. E. & Rosenberg, R. D. (1976) *Biochem. Biophys. Res. Commun.* **69**, 570–577.
34. Walicke, P. A., Feige, J.-J. & Baird, A. (1989) *J. Biol. Chem.* **264**, 4120–4126.
35. Moscatelli, D. (1987) *J. Cell Physiol.* **131**, 123–130.
36. Lobb, R. R., Harber, J. W. & Fett, J. W. (1986) *Anal. Biochem.* **154**, 1–14.
37. Laterra, J., Ansbacher, R. & Culp, L. A. (1980) *Proc. Natl. Acad. Sci. USA* **77**, 6662–6666.

had the additional scans, there were still significant increases in temporopolar blood during the production of anticipatory anxiety.
20. B. R. Kaada, *Handbook of Physiology*, Section 1, *Neurophysiology*, J. Field and H. W. Magoun, Eds. (American Physiological Society, Washington, DC, 1960), vol. 2, pp. 1345–1372.
21. W. Penfield and H. Jasper, *Epilepsy and the Functional Anatomy of the Human Brain* (Little, Brown, Boston, 1954).
22. A. Kling and H. D. Steklin, *Brain Behav. Evol.* **13**, 216 (1976).
23. E. Halgren and R. Walter, *Brain* **101**, 83 (1978); P. Gloor, A. Olivier, L. F. Quesney, F. Andermann, S. Horowitz, *Ann. Neurol.* **12**, 129 (1982); E. Strauss, A. Risser, M. W. Jones, *Arch. Neurol.* **39**, 626 (1982).
24. M. Wall *et al.*, *J. Clin. Psychiatry* **46**, 143 (1985); M. Wall, D. Mielke, J. S. Luther, *ibid.* **47**, 219 (1986); A. M. Ghadirian *et al.*, *ibid.*, p. 270.
25. M. M. Mesulam and E. J. Mufson, *J. Comp. Neurol.* **212**, 1 (1982); M. A. Moran, E. J. Mufson, M. M. Mesulam, *ibid.*, **256**, 88 (1987).
26. There was no significant difference between the left-to-right ratio of parahippocampal blood in the second and third scans ($P = 0.97$). Thus, the abnormal parahippocampal asymmetry in patients with panic disorder seems to be unrelated to a state of anticipatory anxiety.
27. J. Talairach and G. Szikla, *Atlas d'Anatomie Stereotaxique du Telencephale* (Masson, Paris, 1967).
28. We thank J. Stern and J. Price for helpful suggestions, L. Lich for technical support, and S. Sirkin and J. Woodward for secretarial assistance. Supported by National Institute of Mental Health Physician Scientist Award MH-00615 (E.M.R.); National Institute of Neurological and Communicative Disorders and Stroke (NINCDS) Teacher Investigator Award NS-00904 (P.T.F.); NINCDS grant NS-06833; National Heart, Lung, and Blood Institute grant HL-13851; and a grant from the Upjohn company.

29 August 1988; accepted 11 November 1988

Structure and Function of Human Amphiregulin: A Member of the Epidermal Growth Factor Family

MOHAMMED SHOYAB, GREGORY D. PLOWMAN, VICKI L. MCDONALD, J. GARRETT BRADLEY, GEORGE J. TODARO

The complete amino acid sequence of amphiregulin, a bifunctional cell growth modulator, was determined. The truncated form contains 78 amino acids, whereas a larger form of amphiregulin contains six additional amino acids at the amino-terminal end. The amino-terminal half of amphiregulin is extremely hydrophilic and contains unusually high numbers of lysine, arginine, and asparagine residues. The carboxyl-terminal half of amphiregulin (residues 46 to 84) exhibits striking homology to the epidermal growth factor (EGF) family of proteins. Amphiregulin binds to the EGF receptor but not as well as EGF does. Amphiregulin fully supplants the requirement for EGF or transforming growth factor–α in murine keratinocyte growth, but it is a much weaker growth stimulator in other cell systems.

THE LIST OF PEPTIDE GROWTH REGulators has been expanding rapidly. These factors participate in various physiological and pathological conditions, such as cellular communication, growth and development, embryogenesis, immune response, hematopoiesis, cell survival and differentiation, inflammation, tissue repair and remodeling, atherosclerosis, and cancer (*1*). The isolation, characterization, and mechanism of action of regulatory factors for growth and differentiation are of current interest because of the potential use of such regulatory factors in the diagnosis, prognosis, and therapy of neoplasia and because of what these factors reveal about the basic mechanism of normal cellular proliferation and the unrestrained growth of cancer cells. We have recently reported the isolation of a novel glycoprotein termed amphiregulin (AR), which inhibits growth of A431 human epidermoid carcinoma and other human tumor cells and stimulates proliferation of human fibroblasts and other normal and tumor cells (*2*). AR was isolated from serum-free conditioned medium of MCF-7 human breast carcinoma cells that had been treated with 12-*O*-tetradecanoylphorbol-13-acetate (*2*). We now report the complete amino acid sequence of amphiregulin and compare its biological properties with those of the other members of the epidermal growth factor (EGF) family proteins.

AR was purified to homogeneity as described (*2*). The homogeneous AR was used for all the chemical and biological studies reported here. The amino acid sequence of human AR (Fig. 1) was determined by automated Edman degradation of *N*-glycanase–treated, reduced, and *S*-pyridylethylated AR (NG-SPE-AR) and of peptide fragments obtained by cleavage of NG-SPE-AR with various endopeptidases. The carboxyl-terminal analysis of NG-SPE-AR was performed with carboxypeptidase P (*Penicillium janthinellum*). The amino-terminal analysis of NG-SPE-AR revealed the presence of two sequences, one starting at residue 1, serine, and the other starting at residue 7, valine (Fig. 1). The yield of the larger form of AR was about 20% of that of the truncated form. The larger AR thus contains six additional amino acids at the amino terminal of the truncated form of AR. The larger form of AR and the truncated AR are single chain polypeptides of 84 and 78 residues, with a calculated molecular weight of 9759 and 9060, respectively (Fig. 1). Both forms of AR have a similar carboxyl-terminal sequence as determined by carboxypeptidase P cleavage (Fig. 1), and both are biologically active.

The sequence of AR was compared with all proteins in the National Biomedical Research Foundation database (release 15, containing 6796 protein sequences), Genetic Sequence Data Bank (Bolt Beranek and Newman, Los Alamos National Laboratory; release 54) and the European Molecular Biology Laboratory DNA sequence library (release 13). These computer-aided searches revealed that AR is a novel protein and a member of the EGF family. This family includes EGF (mouse, human, and rat) (*3–5*), transforming growth factor–α (TGF-α) (*6, 7*), and poxvirus growth factors [vaccinia (VGF), myxoma (MGF), and Shope fibroma (SFGF)] (*8–10*). Tissue-type plasminogen activator (*11*), the mammalian clotting factors IX and X (*12*), the low-density lipoprotein receptor (*13*), bovine protein C (*14*), human proteoglycan core protein (*15*), product of *Drosophila notch* gene (*16*), product of *lin 12* gene (*17*), the product of cell lineage–specific gene of sea urchin *Strongylocentrotus purpuratus* (*18*), cytotactin (*19*), and product of *Pfs* gene of *Plasmodium falciparum* (*20*) also contain EGF-like domains. Alignment of AR structure with the structure of EGF-like growth factors and with other members of EGF-like proteins (Fig. 2) reveals that AR, like other members of the family, contains the hallmark six essential cysteine residues, maintains conservation of cysteine residue spacing in the pattern $CX_7CX_4CX_{10}CX_1CX_8C$, and also contains some of the characteristic and conserved amino acids. AR falls between the members of the growth factor family that look like EGF and TGF-α and those that look like the poxvirus-encoded growth factors (MGF and SFGF), especially in the use of asparagine. The amino-terminal sequence of AR has some analogy with the amino-terminal sequences of the TGF-α's (*6, 7*), VGF (*8*), and MGF (*9*) in that it is rich in prolines, serines, and threonines and, like TGF-α and VGF, has potential N-linked glycosylation sites as well as the possibility for O-linked glycosylation in the region rich in serines, threonines, and prolines. Unlike MGF and SFGF, AR does not have any potential glycosylation site within the growth factor domain of the molecule. On the basis of homology with mouse EGF (*3*) and perfect alignment of six cysteine residues, one would expect the pres-

Oncogen, 3005 First Avenue, Seattle, WA 98121.

ence of three intrachain disulfide bonds in AR involving cysteine residues 46 and 59, 54 and 70, and 72 and 81.

AR is an extremely hydrophilic protein, especially the amino-terminal half of the molecule up to residue 45. A 23–amino acid stretch from residue 23 through 45 contains only five different amino acids (ten lysines, four arginines, four asparagines, three prolines, and two glycines). A tetrapeptide Arg-Lys-Lys-Lys is repeated twice (residues 26 to 29 and 40 to 43) in AR. Such sequences have been reported to serve as a nucleus targeting signal (*21*). The hydropathy profile of AR exhibits little similarity with those of the other members of the EGF family.

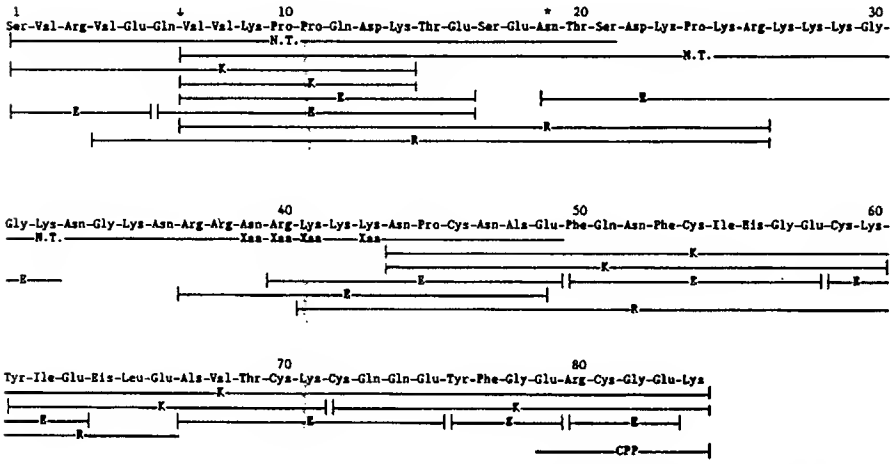

Fig. 1. Amino acid sequence of AR and schematic outline of the data supporting the sequence. The sequence of unfragmented NG-SPE-AR is denoted by N.T. Peptides obtained by cleavage with endopeptidase-Lys-C (K), with endopeptidase-Arg (R), and with endopeptidase-Glu, *Staphylococcus aureus* V8 protease (E) are indicated. CPP denotes the carboxyl-terminal sequence determined by digestion of AR with carboxypeptidase P. Residues identified with Edman degradation or by amino acid analysis are indicated by lines. Vertical bars show beginnings and endings of fragments. Lines without two vertical bars indicate incomplete sequences; ↓ indicates the start of truncated AR; and * indicates potential glycosylation site. AR was reduced with 2-mercaptoethanol and alkylated with 4-vinylpyridine. SPE-AR was purified by reversed phase high-performance liquid chromatography (rp-HPLC). SPE-AR was treated with *N*-glycanase to remove N-linked oligosaccharides, and NG-SPE-AR was purified by rpHPLC. NG-SPE-AR was cleaved with various endopeptidases, and the resulting peptides were separated by an rpHPLC C_8 column. Peptide sequences were determined with an Applied Biosystems model 475A gas-phase sequencer. Identification of phenylthiohydantoin amino acid derivatives was carried out, on line, on a model 120A analyzer (Applied Biosystems). For carboxyl-terminal analysis, NG-SPE-AR was incubated with CPP, portions were withdrawn at various times, and the reaction was terminated. Released amino acids were derivatized with phenyl isothiocynate and phenylthiocarbamyl amino acid derivates were analyzed and quantitated by using micro amino acid derivatizer and analyzer (Applied Biosystem, model number 420-A0-03).

The binding properties of AR were compared with those of mouse EGF in radioreceptor assays (Fig. 3A). AR inhibited the binding of ^{125}I-labeled EGF to A431 cells as well as to A431 plasma membranes. A 50% inhibition of ^{125}I-EGF binding to fixed cells and membranes was seen at about 1.1 and 1.8 n*M* EGF, respectively, whereas a 50% reduction in EGF binding to cells and membranes was seen at approximately 1.8 and 5.7 n*M* AR, respectively. Unlabeled EGF completely inhibited the ^{125}I-EGF–receptor interaction at higher concentrations in both systems (Fig. 3A). However, the maximum competition with AR was 75% and 50% for binding to cells and membranes, respectively (Fig. 3A). The competition curves for AR were not parallel to that seen with EGF. These results suggest that AR has a lower affinity for EGF receptors on A431 cells than does EGF itself. Structural differences between AR and EGF might explain the binding data shown in Fig. 3. It is also possible that AR might have its specific receptor closely related to the EGF receptor.

EGF or TGF-α induce anchorage-independent growth of rat kidney cells NRK-SA6 in the presence of TGF-β (*22*). EGF induced anchorage-independent growth of NRK cells in a dose-dependent manner in the presence of TGF-β, whereas AR was found to be a noninducer of colony formation in soft agar of NRK cells (Fig. 3B). The continued growth of a murine keratinocyte cell line, Balb/MK, is dependent on EGF or TGF-α (*23*). Balb/MK cells did not proliferate in the absence of AR or EGF. However, these cells proliferated equally well in the presence of AR or of EGF (Fig. 3C). Thus,

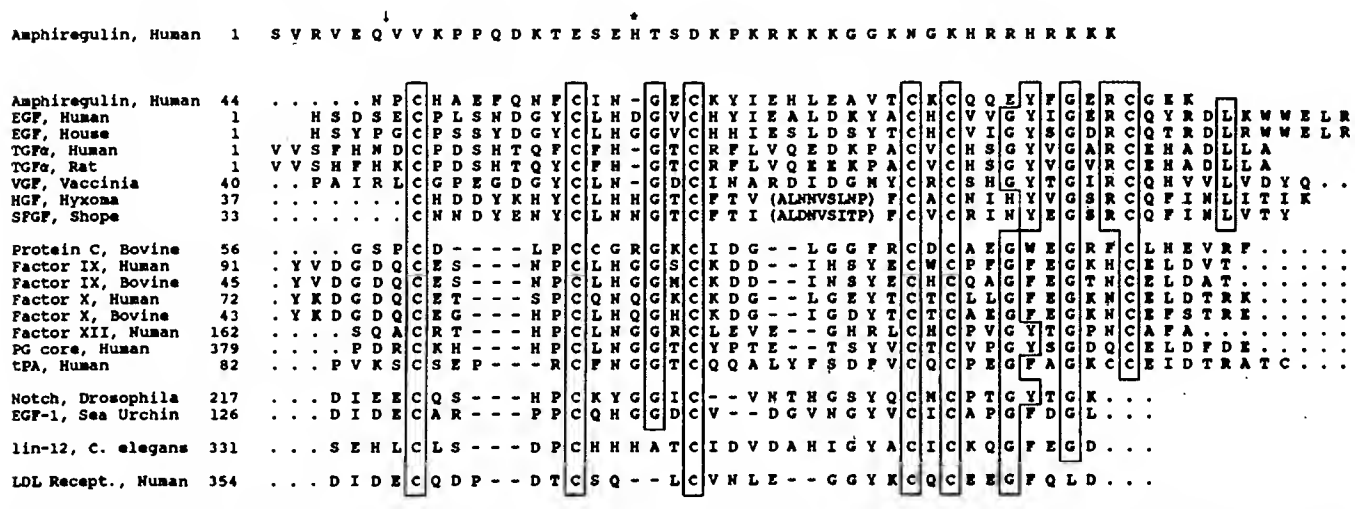

Fig. 2. Alignment of AR sequence with other EGF-like proteins. Amino acids are represented by standard one-letter symbols (*24*). Only residues appearing in eight or more proteins are boxed. Hyphens indicate gap introduced to maximize homology. Dots at the beginning and the end of sequences indicate the use of only partial sequence of a given protein. Numbers at the beginning of every sequence indicate the number of amino acid residues within the total protein sequence; ↓, beginning of the sequence of the truncated form of AR; and *, potential glycosylation site.

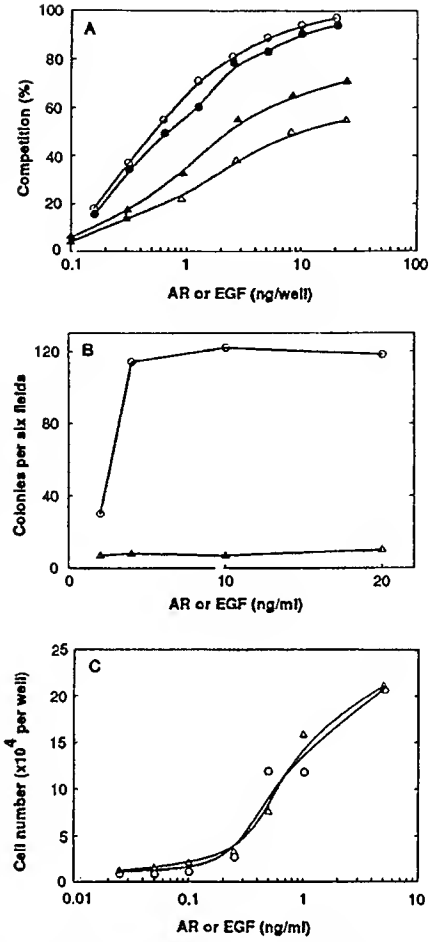

Fig. 3. (**A**) Competition of ^{125}I-EGF binding to the fixed A431 cells (solid symbols) or A431 plasma membranes (open symbols) by murine EGF and AR. EGF was radioiodinated with ^{125}I as described (*25*). The binding assays were performed either in 48-well tissue culture plates when Formalin-fixed A431 cells were used as described (*26*) or by immobilizing plasma membranes onto 96-well poly(vinyl chloride) plates as described (*27*). The binding assays used 4 ng of ^{125}I-labeled mouse EGF per milliliter, containing ~1.9×10^5 dpm. Samples of 100 and 50 μl were used per well for assays with fixed cells and membranes, respectively. Circles indicate EGF, and triangles indicate AR. (**B**) Effect of EGF and AR on NRK-SA6 cell colony formation in soft agar in the presence of TGF-β (1 ng/ml). A 0.38-ml base layer of 0.5% agar (Agar Noble, Difco Laboratories, Detroit) in Dulbecco's minimum essential medium containing 10% heat-inactivated fetal bovine serum (FBS) was added to 24-well Costar tissue culture plates. A 0.3% agar (0.38 ml) containing the same medium-FBS mixture, 6×10^3 to 12×10^3 test cells, and the factors to be tested were overlaid on the basal layer of agar. The plates were incubated at 37°C in the humidified atmosphere of 5% CO_2 in air. Colonies were enumerated unfixed and unstained, and the number of colonies was scored between days 7 and 10. Colonies were defined as a cluster of at least eight cells. Circles, EGF; and triangles, AR. (**C**) Effect of AR and EGF on the growth of murine keratinocytes. Balb/MK cells were plated at 1×10^4 cells per well in 1 ml of low calcium medium (*23*) in 24-well Costar plates (area ~2 cm^2 per well) and incubated overnight at 37°C. Then media were removed and replaced with 1 ml of medium containing various concentrations of AR or EGF in triplicate. The control wells received only medium without any AR or EGF. Plates were incubated at 37°C for 4 days, then medium was removed, wells were rinsed two times with 1 ml of phosphate-buffered saline, and the cells were detached with trypsin-EDTA and counted. Circles, EGF; and triangles, AR.

AR can supplant the EGF requirement in these cells. These results indicate that, like EGF and TGF-α, AR acts as a growth stimulator, but is much weaker on some cells (normal rat kidney) and comparable on others (murine keratinocytes).

Available structural data should allow studies on the cloning, structure, topology, expression, and regulation of amphiregulin gene in both the physiological and pathological conditions. These studies may also provide clues to design agonists and antagonists of this bifunctional growth regulator.

REFERENCES AND NOTES

1. D. Evered, J. Nugent, J. Whelan, Eds., *Ciba Found. Symp.* 116 (1985); G. Carpenter and S. Cohen, *Annu. Rev. Biochem.* 48, 193 (1979); E. Rozengurt, *Science* 234, 161 (1986); A. B. Pardee, *Cancer Res.* 47, 1488 (1987); A. S. Goustin, E. B. Leof, G. D. Shipley, H. L. Moses, *ibid.* 46, 1015 (1986); M. B. Sporn and A. B. Roberts, *J. Clin. Invest.* 78, 329 (1986); L. Sachs, *Sci. Am.* 254, 40 (January 1986); L. J. Old, *ibid.* 258, 59 (May 1988); B. Beutler and A. Cerami, *N. Engl. J. Med.* 316, 379 (1987); J. E. Groopman, *Cell* 50, 5 (1987); M. J. Clemens and M. A. McNurlan, *Biochem. J.* 226, 345 (1985).
2. M. Shoyab, V. L. McDonald, J. G. Bradley, G. J. Todaro, *Proc. Natl. Acad. Sci. U.S.A.* 85, 6528 (1988).
3. C. R. Savage, Jr., T. Inagami, S. Cohen, *J. Biol. Chem.* 247, 7612 (1972); C. R. Savage, Jr., J. H. Hash, S. Cohen, *ibid.* 248, 7669 (1973); R. F. Doolittle, D. F. Feng, M. S. Johnson, *Nature* 307, 558 (1984).
4. H. Gregory, *Nature* 257, 325 (1975).
5. R. J. Simpson *et al.*, *Eur. J. Biochem.* 153, 629 (1985).
6. G. Todaro, C. Fryling, J. DeLarco, *Proc. Natl. Acad. Sci. U.S.A.* 77, 5258 (1980); H. Marquardt, M. W. Hunkapiller, L. E. Hood, G. J. Todaro, *Science* 223, 1079 (1984).
7. R. Derynck *et al.*, *Cell* 38, 287 (1984); D. Lee, T. Rose, N. Webb, G. J. Todaro, *Nature* 313, 489 (1985).
8. M. C. Blomquist, L. C. Hunt, W. C. Barker, *Proc. Natl. Acad. Sci. U.S.A.* 81, 7363 (1984); J. P. Brown, D. R. Twardzik, H. Marquardt, G. J. Todaro, *Nature* 313, 491 (1985).
9. C. D. Porter and L. C. Archard, *J. Gen. Virol.* 68, 673 (1987).
10. W. Chang, C. Upton, S.-L. Hu, A. F. Purchio, G. McFadden, *Mol. Cell. Biol.* 7, 535 (1987).
11. D. Pennica *et al.*, *Nature* 301, 214 (1983).
12. K. Kurachi and E. W. Davie, *Proc. Natl. Acad. Sci. U.S.A.* 79, 6461 (1982); K. Katayama *et al.*, *ibid.* 76, 4990 (1979); B. A. McMullen *et al.*, *Biochemistry* 22, 2875 (1983); D. L. Enfield *et al.*, *ibid.* 19, 659 (1980); K. Titani *et al.*, *Proc. Natl. Acad. Sci. U.S.A.* 72, 3082 (1975).
13. D. W. Russell *et al.*, *Cell* 37, 577 (1984).
14. P. Fernlund and J. Stenflo, *J. Biol. Chem.* 257, 12170 (1982).
15. T. Krusius, K. R. Gehlsen, E. Ruoslahti, *ibid.* 262, 13120 (1987).
16. K. A. Wharton, K. M. Johansen, T. Xu, S. Artavanis-Tsakonas, *Cell* 43, 567 (1985); S. Kidd, M. R. Kelley, M. W. Young, *Mol. Cell Biol.* 6, 3095 (1986).
17. I. Greenwald, *Cell* 43, 583 (1985).
18. D. A. Hursh, M. E. Andrews, R. A. Raff, *Science* 237, 1487 (1987).
19. F. S. Jones *et al.*, *Proc. Natl. Acad. Sci. U.S.A.* 85, 2186 (1988).
20. D. C. Kaslow *et al.*, *Nature* 333, 74 (1988).
21. Y. Yoneda *et al.*, *Science* 242, 275 (1988).
22. A. B. Robert *et al.*, *Proc. Natl. Acad. Sci. U.S.A.* 78, 5339 (1981).
23. B. E. Weissman and S. A. Aaronson, *Cell* 32, 599 (1983); R. J. Coffey *et al.*, *Cancer Res.* 48, 1596 (1988).
24. Abbreviations for the amino acid residues are: A, Ala; C, Cys; D, Asp; E, Glu; F, Phe; G, Gly; H, His; I, Ile; K, Lys; L, Leu; M, Met; N, Asn; P, Pro; Q, Gln; R, Arg; S, Ser; T, Thr; V, Val; W, Trp; and Y, Tyr.
25. K. Barridge, *Methods Enzymol.* 50, 54 (1978).
26. G. Carpenter, L. King, Jr., S. Cohen, *J. Biol. Chem.* 254, 4884 (1979); J. E. DeLarco *et al.*, *ibid.* 255, 3685 (1980).
27. E. S. Kimball and T. C. Warren, *Biochim. Biophys. Acta* 771, 82 (1984).

28. We thank L. Kissinger for help with the binding assays and P. Yoshida for assistance in manuscript preparation.

29 July 1988; accepted 18 November 1988

MOLECULAR AND CELLULAR BIOLOGY, Mar. 1994, p. 1635–1646
0270-7306/94/$04.00+0

Vol. 14, No. 3

The Heparin-Binding Domain of Amphiregulin Necessitates the Precursor Pro-Region for Growth Factor Secretion

BARBARA A. THORNE* AND GREGORY D. PLOWMAN†
Bristol-Myers Squibb Pharmaceutical Research Institute, Seattle, Washington 98121

Received 28 September 1993/Returned for modification 3 November 1993/Accepted 30 November 1993

The five members of the human epidermal growth factor (EGF) family (EGF, transforming growth factor α [TGF-α], heparin-binding EGF-like growth factor [HB-EGF], betacellulin, and amphiregulin [AR]) are synthesized as transmembrane proteins whose extracellular domains are proteolytically processed to release the biologically active mature growth factors. These factors all activate the EGF receptor, but in contrast to EGF and TGF-α, the mature forms of HB-EGF and AR are also glycosylated, heparin-binding proteins. We have constructed a series of mutants to examine the influence of the distinct precursor domains in the biosynthesis of AR. The transmembrane and cytoplasmic domains of the precursor are not required for secretion of bioactive AR from either COS or mammary epithelium-derived cells, although proteolytic removal of the N-terminal pro-region is less efficient in the absence of the membrane anchor. Deletion of the N-terminal pro-region, however, results in rapid intracellular degradation of the molecule with no detectable secretion of active growth factor. AR secretion is preserved by replacing the native pro-region with the corresponding domain of the HB-EGF precursor but not with that of the TGF-α precursor. In the absence of any N-terminal pro-region, secretion of the molecule is restored by deleting the N-terminal heparin-binding domain of mature AR. Both EGF and TGF-α, in contrast, can be secreted without their pro-regions. However, if the protein is fused with the AR heparin-binding domain, TGF-α secretion is inhibited unless the AR pro-region is also present. We propose that the heparin-binding domain of mature AR necessitates the presence of a specific structural motif in an N-terminal pro-region to permit proper folding, and thus secretion, of a bioactive molecule.

Many peptide growth regulators are synthesized as larger precursor proteins which are posttranslationally processed to the mature factor (reviewed in reference 38). Precursors for a number of growth factors, including transforming growth factor β (TGF-β)-, nerve growth factor-, and platelet-derived growth factor-related molecules, are soluble proteins containing the active peptide at the C terminus preceded by an N-terminal pro sequence (4, 15, 54, 71). Various functions have been ascribed to the pro-regions for this class of molecule. For example, both NGF and TGF-β require their pro sequences for secretion, PDGF is rendered inactive unless the pro sequence is removed, and the TGF-β pro-region is involved in latent complex formation (11, 21, 39–41, 61, 65). However, an increasing number of soluble growth factors are found to be cleaved from integral membrane proteins, suggesting the possibility that such precursors participate in cell-cell communication or juxtacrine interactions (18, 37). For example, colony-stimulating factor 1 and tumor necrosis factor alpha/cachexin can signal through their respective receptors as membrane-anchored molecules, and several lines of evidence indicate a biological function specific to the transmembrane form of Steel factor, the ligand for the c-Kit receptor (10, 20, 33, 47, 59, 64). A large family of growth factors initially synthesized as integral membrane precursors is composed of the epidermal growth factor (EGF)- and heregulin-related molecules.

The human genome encodes five known structurally related proteins that bind and activate the EGF receptor: EGF, TGF-α, heparin-binding EGF-like growth factor (HB-EGF), betacellulin, and amphiregulin (AR) (3, 16, 24, 48, 53, 57, 58). These proteins are all synthesized as part of larger precursors consisting of a signal peptide for localization to the secretory pathway, an N-terminal pro-region, and the mature peptide sequences, followed by a short spacer, a single transmembrane domain, and cytoplasmic tail. The bioactive domains are characterized by a six-cysteine consensus motif, $X_nCX_7CX_{4-5}CX_{10}CXCX_5GX_2CX_n$, and several additional conserved residues (12). Mature HB-EGF and AR also have N-terminal extensions, composed of predominantly basic residues, that are thought to confer their heparin-binding abilities. Outside the EGF-like region, these precursors show little sequence homology, and their biological function(s) remains unclear.

The N-terminal pro-regions vary considerably among the EGF family members: the pro-domain of EGF spans 950 residues and contains nine additional EGF-like sequences, whereas the pro-regions of AR (74 residues), HB-EGF (~54 residues), and TGF-α (17 to 18 residues) are considerably smaller (3, 7, 16, 25, 48). The betacellulin precursor has not yet been characterized but is predicted to contain a pro-region of only about seven residues (53, 57). In the case of EGF, the pro-region can be deleted without loss of protein expression or bioactivity, but the other molecules have not been similarly examined (17, 60). The presence of a transmembrane domain does suggest distinct functions for cell-associated and soluble forms of the factors. Although no physiological role has yet been attributed to the membrane-anchored factors, both EGF and TGF-α can bind and stimulate mitogenesis through the EGF receptor as transmembrane proteins, and the HB-EGF precursor has been implicated as the cellular receptor for diphtheria toxin (1, 6, 9, 43, 70).

Among the EGF family members, TGF-α has served as the primary model for studying precursor function and mechanisms of soluble factor production. Mature peptide is released from this precursor by independent processing at two flanking elastase-like cleavage sites (Ala-Val). Chinese hamster ovary

* Corresponding author. Mailing address: Bristol-Myers Squibb Pharmaceutical Research Institute, 3005 First Ave., Seattle, WA 98121. Phone: (206) 727-3463.
† Present address: Sugen, Inc., Redwood City, CA 94063–4720.

(CHO) cells stably transfected with TGF-α efficiently cleave the N-terminal site but accumulate membrane-anchored factor as a result of inefficient cleavage at the C-terminal site (63). In contrast, retrovirally transformed rat embryo fibroblasts and hepatocarcinoma cells apparently process both sites at similar rates, resulting in the secretion of both *meso*-TGF-α (containing N-terminal pro-sequences) and the mature peptide (27, 36, 62). In certain cell types, cleavage at the C-terminal site is dramatically stimulated by activators of protein kinase C or elevated cytosolic calcium levels (44, 45). This regulated response is dependent on the cytoplasmic domain of the precursor (8).

While related to the other EGF family members, AR has several features which distinguish it from the TGF-α model. Precursor sequences flanking mature AR lack homology with the TGF-α cleavage sites, so processing may be mediated by different enzymes and thus subject to different regulating factors. Mature AR is a glycosylated heparin-binding peptide, and soluble heparin sulfate-like molecules inhibit its mitogenic activity. It also has a significantly lower affinity for the EGF receptor on A431 cells than do other family members (58). This reduction may be due to the absence of a leucine at position 42 in AR (as measured from the first cysteine of the EGF-like repeat), a residue critical for the activity of EGF and TGF-α and conserved in HB-EGF (19, 34, 50). However, AR may be a more specific and natural regulator of normal epithelial cells than the other factors, as evidenced by its discovery as an autocrine mitogen for cultured human keratinocytes, mammary epithelial cells (HMEC), and colorectal cells and by its diminished potency on mesenchymal cells (14, 31, 35, 58). Given the differences in the mature factors, the biologic relevance of the AR precursor may also differ from that of TGF-α.

In this study, we address the functions of AR precursor (ARP) domains. Using deletion analysis, our initial experiments examine the roles of the N-terminal pro-region, transmembrane, and cytoplasmic domains in the synthesis and secretion of bioactive peptide. This report demonstrates that both the N-terminal pro-region and the membrane anchor are important for the release of mature AR, with the pro-region being required for protein secretion while the transmembrane domain facilitates posttranslational removal of the pro-region.

MATERIALS AND METHODS

Cell lines. COS-1 (ATCC CRL 1650), 184A1N4-TH (13), and NRHer5 (5) cells were cultured in Dulbecco's modified Eagle medium (DMEM) supplemented with 10% fetal bovine serum (FBS). Normal HMEC (Clonetics Corp.) were cultured in mammary epithelium growth medium (Clonetics Corp.). All cells were maintained at 37°C in 5% CO_2.

Transient transfection assay. One day prior to transfection, COS cells were plated at 10^6 cells per 100-mm-diameter dish, and 184A1N4-TH cells were plated at twice that density. Cells were transfected with 30 μg of plasmid DNA by the DEAE-dextran-chloroquine method (55) and cultured for 2 days in DMEM–10% FBS. Cells were then washed twice and cultured for an additional 24 h in serum-free DMEM (5 ml/100-mm-diameter dish) before harvesting for Western blot (immunoblot) analysis.

For metabolic labeling experiments, cells were trypsinized 24 h after transfection, replated in parallel 35-mm-diameter dishes, and cultured for an additional 24 h. For pulse-chase experiments, cells were preincubated for 30 min in cysteine-free minimal essential medium and then labeled for 15 min in the same medium supplemented with 200 μCi of [^{35}S]cysteine (New England Nuclear) per ml. Plates were washed twice with DMEM and chased in 1 ml of DMEM–2% FBS at 37°C for the indicated lengths of time. For steady-state labeling experiments, cells were cultured for 24 h in cysteine-free minimal essential medium containing 2% dialyzed FBS, 1% complete DMEM, and 50 μCi of [^{35}S]Cys or [^{35}S]methionine-cysteine mix (EXPRE^{35}S^{35}S; New England Nuclear) per ml.

Construction of mutant AR. Human AR cDNA (48) was excised at *Hga*I and *Eco*RV sites and subcloned into pBluescript II SK(+) (Stratagene). Mutations were generated in this template by using one- or two-step PCR protocols and synthetic oligodeoxynucleotide primers (29). Secondary structure predictions of N-terminal pro-regions were based on the original method of Chou and Fasman, using the PeptideStructure program in the Genetics Computer Group sequence analysis software (Genetics Computer, Inc.) (30).

The ARTL construct terminates following arginine 225 in the ARP, which is immediately C terminal to its putative membrane-spanning region (...KIALAAIAAFMSAVILTAV AVITVQLRR^{225}). The PA and NPA constructs were truncated following threonine 188 in the precursor, seven residues C terminal to the final Cys of the EGF-like motif (...GERCGEKSMKT^{188}). Mature AR isolated from tetradecanoyl phorbol acetate-treated MCF7 cells was previously reported to terminate at lysine 184 in the precursor; however, sequence analysis of recombinant AR purified from CHO cells reveals equimolar amounts of peptide terminating at lysine 187 and threonine 188 (unpublished data). Mature 18-kDa AR produced endogenously by both cultured normal HMEC and normal human keratinocytes can be metabolically labeled with [^{35}S]methionine (unpublished data), indicating that the C terminus of native AR extends to at least methionine 186, since no other methionines are found within or immediately N terminal to the mature factor.

Constructs with N-terminal deletions (ARNP and NPA) were generated by fusing the signal sequence from the human TGF-β_1 precursor (MPPSGLRLLPLLLPLLWLLVLTPSRPA AG) (22) in frame with the N terminus of the predominant form of mature AR, beginning with valine 107 in the precursor (^{107}VVKPPQNK...). The domain swap mutants HB-AR and TGF-AR replaced the first 107 residues of the ARP with the first 72 and 38 residues of the human HB-EGF (24) and TGF-α (16) precursors, respectively. The human TGF-α cDNA used for this construct was isolated from A431 cells. Like one of the two forms of rat TGF-α message produced by exon sliding (7), this cDNA encodes a 159-residue primary translation product lacking alanine at position 32. The construct AR-NB contains a 43-residue internal deletion (from serine 101 to lysine 143) that leaves the N-terminal pro-region intact but removes the hydrophilic region of the mature factor just N terminal to the EGF-like motif (which begins at cysteine 146). The construct ARNP-NB contains the TGF-β signal sequence fused in frame to asparagine 144 (^{144}NPCNA EFQNFC...), deleting the first 143 residues of the ARP. Constructs ARNPΔN and ARNPΔC, created by using ARNP as the template for PCR priming, delete residues corresponding to amino acids 107 to 122 and 123 to 143, respectively, in the ARP (see Fig. 9A).

The TGF-α-based constructs (Pα, NPα, PAα, and NPAα) were derived from the human TGF-α cDNA described above (7, 16), and all were truncated at a position corresponding to the C terminus of the mature factor (...CEHADLLA^{88}). The N-terminal deletion mutant (NPα) was created by fusing the TGF-β_1 signal sequence in frame with the N terminus of mature TGF-α (^{39}VVSHFNDCPDSHTQFC...). The N-terminal regions of the AR–TGF-α chimeric constructs were de-

rived from the full-length ARP and pro-less ARNP constructs; PAα contains the first 143 residues of the ARP residues, and NPAα contains the TGF-β_1 signal with ARP residues 107 to 143. For both chimeras, these sequences were fused to the EGF-like domain of TGF-α, beginning at residue 45 in the TGF-α precursor (^{45}DCPDSHTQFC...).

All PCR products were sequence verified, and the final constructs were directionally subcloned into the cDM8 expression vector (Invitrogen Corp.) at *Hin*dIII and *Not*I sites. The vector drives expression from the cytomegalovirus promoter and contains the simian virus 40 (SV40) origin of replication to allow plasmid amplification in cells expressing the SV40 T antigen.

Western blot analysis. Culture supernatants were clarified and dialyzed against 0.1 M acetic acid, dried in a Speed Vac concentrator (Savant), and resuspended directly in sodium dodecyl sulfate (SDS) sample buffer (50 mM Tris-Cl [pH 6.8], 2% SDS, 0.05% bromophenol blue, 10% glycerol, 2.5% 2-mercaptoethanol). Cell extracts were prepared as follows. Monolayers from 100-mm-diameter dishes were washed twice with phosphate-buffered saline (PBS) and scraped on ice in 1 ml of hypotonic buffer (20 mM *N*-2-hydroxyethylpiperazine-*N'*-2-ethanesulfonic acid [HEPES; pH 7.4], 1 mM EDTA, 1 mM $MgCl_2$, 1 mM phenylmethylsulfonyl fluoride [PMSF], 20 μg of aprotinin per ml). Cells were then incubated for 30 min on ice and Dounce homogenized until ~95% appeared broken by visual inspection. Extracts were centrifuged 3 min at 300 × *g* at 4°C to sediment nuclei and unbroken cells, and the supernatants were separated into particulate and soluble fractions by 10 min of centrifugation at 160,000 × *g* (Beckman Optima TLX-120 tabletop ultracentrifuge). Pellets (particulate fraction) were resuspended directly in SDS sample buffer, while supernatants (soluble fraction) were first dried in a Speed Vac concentrator.

Samples were resolved by SDS-polyacrylamide gel electrophoresis (PAGE) on 15% acrylamide–0.5% bisacrylamide gels (52) and electrophoretically transferred to nitrocellulose. Nonspecific binding was blocked by preincubating blots in BLOTTO (PBS containing 5% [wt/vol] nonfat dried milk and 0.2% [vol/vol] Nonidet P-40 [Sigma]), and AR was detected by using rabbit antisera raised against synthetic peptides corresponding to either the N-terminal region of the mature factor (^{108}VKPPQNKTESENTSDKPKRKKKG^{130}; antibody [Ab] 035) or the N-terminal pro-region of the precursor (^{71}SSSEP SSGADYDYSEEYDNE^{90}; Ab 042) followed by ^{125}I-protein A. Bands were visualized with a Molecular Dynamics PhosphorImager.

Immunoprecipitations. Cells were solubilized in radioimmunoprecipitation assay (RIPA) buffer (150 mM NaCl, 1.0% Nonidet P-40, 50 mM Tris-HCl [pH 8.0]) containing 1 mM PMSF and 20 μg of aprotinin per ml for 20 min on ice and clarified by 10 min of centrifugation at 15,000 × *g* at 4°C. To reduce nonspecific background in metabolically labeled cell extracts, RIPA extracts of unlabeled, nontransfected cells were added at fivefold excess. Medium samples were diluted with an equal volume RIPA buffer and used directly. All samples were preincubated 1 h at 4°C with either protein A-Sepharose or protein G-Sepharose and centrifuged for 10 min at 15,000 × *g* at 4°C to preclear prior to immunoprecipitation. AR was immunoprecipitated by overnight incubation at 4°C with constant mixing, using either affinity-purified Ab 035 and protein A-Sepharose or pooled hybridoma supernatants containing murine monoclonal Abs raised against mature AR (Abs 4.14, 12.33, 12.38, 14.3, 16.21, and 19.23) and protein G-Sepharose. Precipitated samples were washed on ice once each with high-salt buffer (0.5 M NaCl, 1.0% Nonidet P-40, 50 mM Tris-HCl [pH 8.0]), low-salt buffer (1.0% Nonidet P-40, 50 mM Tris-HCl [pH 8.0]), and RIPA buffer. Immunoprecipitates were then resuspended in SDS sample buffer and resolved by SDS-PAGE for either Western blotting or direct autoradiography with the PhosphorImager.

To affinity purify Ab 035 for immunoprecipitations, the antiserum was incubated for 3 h at room temperature with immunizing peptide coupled through primary amines to an Affi-Gel 10 support (Bio-Rad). The support beads were then transferred to a small column and washed with PBS, and the bound Abs were eluted with 50 mM glycine (pH 2.0). The eluate was immediately neutralized with 0.06 volume of 1 M Na_2HPO_4 and dialyzed against PBS, and 1% bovine serum albumin (BSA) and 0.02% NaN_3 were added for storage.

Endoglycosidase H digestion. Cell extracts and media were immunoprecipitated with affinity-purified Ab 035. At the final wash, each sample was divided into two tubes, and the immune complexes were resuspended in 10 μl of endoglycosidase H buffer (30 mM sodium acetate [pH 5.4], 0.1 M 2-mercaptoethanol, 0.5% Triton X-100, 1 mM PMSF, 0.2% SDS) and denatured 5 min at 95°C. To one tube, 1 mU of endoglycosidase H (Boehringer Mannheim) was added, and both tubes were incubated 16 h at 37°C. An equal volume of 2× SDS sample buffer was added directly to reactions, and samples were resolved by SDS-PAGE and analyzed by Western blotting.

Heparin binding assay. Heparin acrylic beads (Sigma) in PBS were mixed with medium samples from [^{35}S]cysteine metabolically labeled cells (15 μl of packed resin per 200 μl of medium) for 1 h at 4°C. The heparin beads were collected by centrifugation and washed twice with PBS. Supernatants were diluted with an equal volume of RIPA buffer and used directly for immunoprecipitations. AR was eluted from the heparin beads by incubation for 1 h at 4°C with 75 μl of 1 M NaCl in sodium phosphate buffer (pH 7.2). The eluate was diluted with 200 μl each of low-salt and RIPA buffers and then used for immunoprecipitations.

EGF receptor autophosphorylation assay. NRHer5 cells were seeded in 12-well plates at 5 × 10^4 cells per well and cultured for 24 h (cells achieved ~50% confluence). Culture medium was then replaced (0.5 ml per well sample) with standards diluted in DMEM containing 0.1% BSA and with conditioned media from transfected cells diluted with an equal volume of DMEM containing 0.1% BSA. Following a 10-min incubation at room temperature, medium was removed and cells were solubilized for 10 min on ice in PBS-TDS (10 mM sodium phosphate [pH 7.25], 150 mM NaCl, 1% Triton X-100, 0.5% sodium deoxycholate, 0.1% SDS, 0.2% NaN_3, 1 mM NaF, 1 mM PMSF, 20 μg of aprotinin per ml), with occasional vortexing. Clarified extracts were incubated 1 h at 4°C with an anti-EGF receptor antibody (EGFR1; Amersham). Protein A-Sepharose was then added, and samples were incubated for an additional hour. Immune complexes were washed three times with PBS-TDS, resolved on a 7% polyacrylamide–0.23% bisacrylamide gel, and electrophoretically transferred to nitrocellulose. Phosphorylation of the receptor was assessed by Western blotting with an antiphosphotyrosine primary antibody (PY20; ICN Biochemicals) and ^{125}I-labeled sheep anti-mouse $F(ab')_2$ (Amersham). Bands were detected and quantitated on the PhosphorImager.

TGF-α ELISA. A TGF-α sandwich enzyme-linked immunosorbent assay (ELISA; Oncogene Science, Inc.) was used for quantitating TGF-α immunoreactivity as instructed by the manufacturer. Culture medium was diluted 40-fold with assay buffer and then analyzed directly.

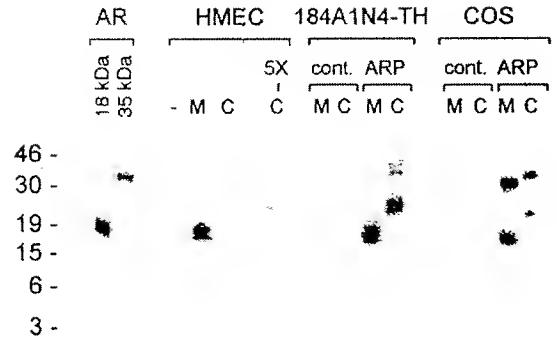

FIG. 1. Western blot analysis of HMEC, 184A1N4-TH, and COS cell AR. Conditioned media (M) and cell extracts (C) from normal HMEC and transfected COS and 184A1N4-TH cells were examined on SDS-polyacrylamide gels by immunoblotting with the AR-specific antiserum Ab 035. Cells were transfected with either control vector (cont.) or a construct containing the cDNA for the full-length ARP. Shown is the particulate fraction of Dounce-homogenized cells. The soluble fraction of cell extracts contained no detectable AR. The 18- and 35-kDa AR standards (50 ng of each) were purified from the conditioned medium of CHO cells transfected with a full-length precursor construct. HMEC samples correspond to 20% of a 100-mm-diameter dish of cells, except for the lane labeled 5×, which was immunoprecipitated from the extract of an entire 100-mm-diameter dish. Samples from 184A1N4-TH and COS cells correspond to 5% of a 100-mm-diameter dish. Sizes are indicated in kilodaltons.

RESULTS

Transient expression system for studying AR synthesis and secretion. To study the effects of precursor mutations on the synthesis and secretion of AR, we wished to have an expression system that lacked high levels of endogenous AR yet represented a cell lineage in which this factor is normally found. Normal proliferating HMEC express and secrete bioactive AR. However, transformed mammary epithelial cells typically lose AR expression, providing a potentially suitable background for studying mutants (14, 35). The HMEC line chosen for these studies, 184A1N4-TH, stably expresses the SV40 T antigen and is thus functionally similar to COS cells (13). Plasmids containing the SV40 origin are replicated to high copy number in such cells, allowing expression of foreign protein to be readily achieved in transient transfection assays.

To assess the validity of the model system, AR produced in COS and 184A1N4-TH cells transiently transfected with the full-length ARP cDNA was compared with that produced by normal HMEC. Two days after transfection, cells were changed to serum-free culture medium for an additional 24 h to collect secreted products. Cells were then harvested and fractionated into soluble and particulate fractions (see Materials and Methods). Secreted and cell-associated proteins were analyzed by Western blotting with a polyclonal antiserum directed against the N-terminal region of the mature peptide (Fig. 1). Normal HMEC secrete predominantly an 18-kDa form comigrating with mature AR, although a 35-kDa form comigrating with gp35 (soluble factor extended by the N-terminal pro-region from the precursor) was also detected. Relatively little AR was cell associated, with the predominant form migrating at 25 kDa, although a 42-kDa species was also detected. Both forms are consistent with the presence of a ~7-kDa transmembrane and cytoplasmic domain.

When transfected with vector alone, neither COS nor 184A1N4-TH cells produced detectable AR. However, cells transfected with the ARP construct secreted both 18- and 35-kDa forms. While COS cells produced similar levels of the two forms, the 184A1N4-TH cells predominantly secreted 18-kDa AR, similar to HMEC. Cell extracts of both lines had high levels of both the 25- and 42-kDa forms.

AR deletion mutants. To assess the role(s) of the membrane anchor and N-terminal pro-regions in the synthesis and secretion of bioactive AR, four deletion mutants were constructed (Fig. 2 and Materials and Methods): (i) ARTL (tail-less, deleting the cytoplasmic domain only leaving the membrane-spanning region intact), (ii) PA (soluble pro-AR, deleting both the transmembrane and cytoplasmic domains), (iii) ARNP (no-pro, deleting the N-terminal pro-region only), and (iv) NPA (soluble no-pro, deleting both N-terminal pro-region and transmembrane domains). Deletions were made in the cDNA for the full-length precursor by using PCR techniques, and all PCR products were confirmed by complete sequence analysis. Both the ARNP and NPA constructs utilized the N-terminal signal sequence from human TGF-β_1 to direct protein to the secretory pathway.

Native ARP and the four deletion mutants were transiently expressed in both COS and 184A1N4-TH cells. Secretion of bioactive material was assessed by testing conditioned media from transfected cells for the ability to stimulate ligand-induced EGF receptor autophosphorylation in intact cells (Fig. 3). Medium from cells transfected with vector alone exhibited no EGF-like activity, whereas cells transfected with the full-length precursor produced significant levels of receptor phosphorylation, corresponding to ~50 to 200 ng of AR activity per ml in the undiluted culture medium, depending on the transfection experiment. Deletion of either the cytoplasmic (ARTL) or transmembrane (PA) domain did not dramatically affect the secretion of bioactive material. However, no stimulation of EGF receptor autophosphorylation was observed with constructs lacking the N-terminal pro-region (ARNP and NPA).

Secreted and cell-associated protein from transfected cells was analyzed by Western blotting with Abs directed against either the mature peptide or the N-terminal pro-region (Fig. 4A and B). Data from 184A1N4-TH cells are shown, although similar results were found with COS cells. In agreement with the bioassay, AR immunoreactive protein was found in the media of cells transfected with the three constructs containing the N-terminal pro-region (ARP, ARTL, and PA) but not those lacking this domain (ARNP and NPA). Both the 18- and 35-kDa forms were secreted from transfected cells, with the 18-kDa peptide predominating for the two transmembrane precursors (ARP and ARTL) and the 35-kDa form predominating for the variant lacking a membrane anchor (PA). As before, the native precursor produced cell-associated forms migrating at 42 and 25 kDa. However two smaller proteins, migrating at 37 and 20 kDa, were found in extracts of ARTL-transfected cells, and the PA construct generated primarily a 35-kDa cell-associated form. These increased mobilities are consistent with precursors lacking either the cytoplasmic domain alone (ARTL) or both the transmembrane and cytoplasmic domains (PA). In comparison with either PA or the native ARP, a higher proportion of the ARTL-derived protein was typically cell associated, although the differences were not always dramatic (ARP and ARTL samples in Fig. 4A and C reflect the range of differences observed). No AR immunoreactivity was found in extracts of ARNP-transfected cells, although a 16-kDa form was found in cells expressing the NPA construct. In all cases where AR protein was detected, the higher-molecular-weight forms in both media and cell extracts also cross-reacted with the N-terminal pro-region-specific antiserum (Fig. 4B). Thus, the three mutant molecules

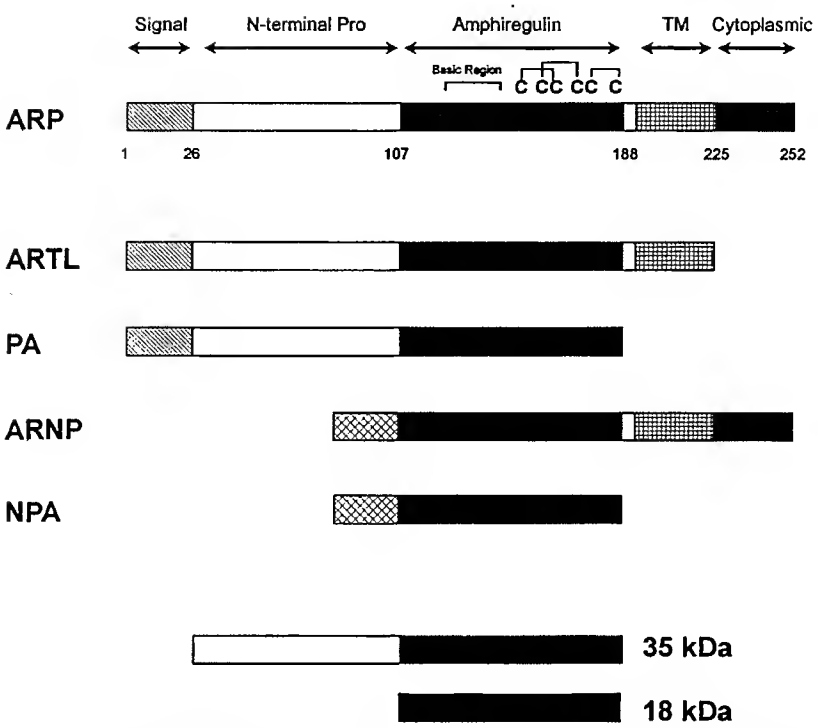

FIG. 2. AR deletion constructs. Functional domains and amino acid positions within the human ARP are indicated on the full-length construct, ARP. The EGF-like motif is represented by the six disulfide-linked cysteines (C). Compositions of the 35- and 18-kDa secreted products are also indicated. Signal, N-terminal signal sequence (, native AR signal; , TGF-β signal); TM, transmembrane domain.

possessing the AR pro-region (ARP, ARTL, and PA) were secreted from transfected cells, while those lacking this domain (ARNP and NPA) were not.

Particulate and soluble fractions of cell extracts were next compared (Fig. 4C). Data from COS cells are shown, although 184A1N4-TH cells demonstrated similar results. Only the PA construct produced AR in the soluble fraction. However, approximately half of the intracellular PA and essentially all of the NPA was found in the particulate fraction, even though neither was predicted to possess a membrane anchor. To resolve this discrepancy, we examined the possibility that these forms were restricted to the endoplasmic reticulum, which would suggest insoluble aggregates of misfolded protein (see references 26, 46, and 51 for reviews).

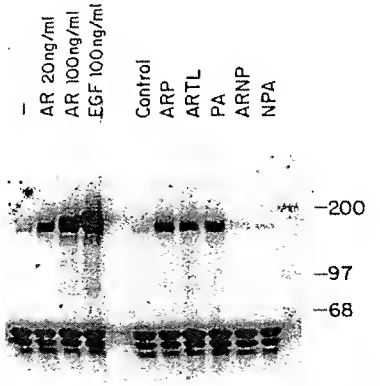

FIG. 3. Bioactivities of AR deletion mutants. NRHer5 cells were stimulated either with purified recombinant AR or EGF or with the conditioned medium from transfected COS cells. The 175-kDa EGF receptor was immunoprecipitated from solubilized NRHer5 cells, and autophosphorylation was assessed by antiphosphotyrosine Western blotting. The immunoprecipitating Ab appears in all lanes as a triplet migrating below the 68-kDa marker. Sizes are indicated in kilodaltons.

Since mature AR is a glycoprotein with N-linked oligosaccharides, the secreted and cell-associated proteins were examined for sensitivity to endoglycosidase H. This enzyme preferentially hydrolyzes high-mannose N-linked carbohydrates, such as intermediates found in the endoplasmic reticulum, and does not hydrolyze the complex carbohydrates produced during maturation in the Golgi complex. As shown in Fig. 5, AR synthesized from the PA construct and found in the particulate fraction of cell extracts was shifted to a single, faster-migrating band following digestion with endoglycosidase H. In contrast, the 25-kDa cell-associated form produced from the full-length precursor was endoglycosidase H insensitive. The secreted forms from both constructs were unaffected by this enzyme. These results suggest that despite high levels of PA released from cells, this membrane anchor-less molecule may have suboptimal folding and secretion efficiency.

AR from the NPA construct found in cell extracts was not affected by endoglycosidase H digestion, even immediately following a 15-min metabolic labeling with [^{35}S]cysteine, when all of the AR produced from the full-length precursor was endoglycosidase H sensitive (Fig. 5B). This observation suggests a lack of N-linked glycosylation in the NPA variant and correlates well with its migration on SDS-PAGE as a protein ~2 kDa smaller than the mature native factor. Protein misfolding and aggregation in the endoplasmic reticulum would be

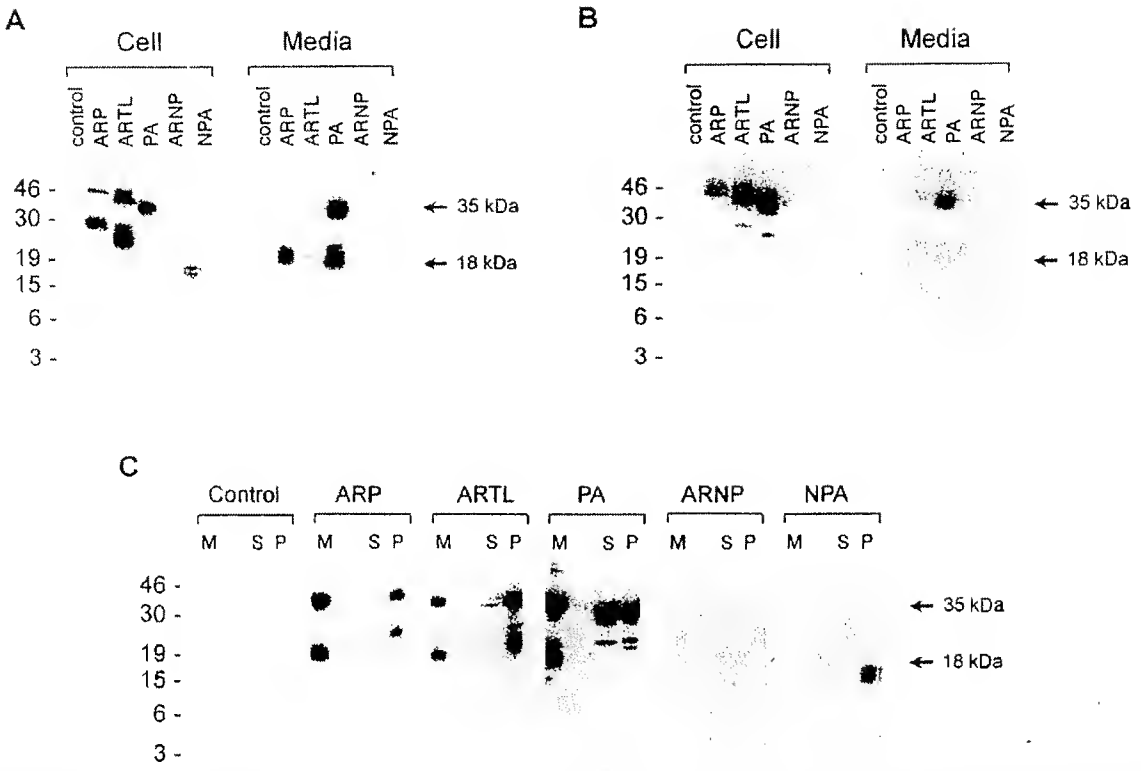

FIG. 4. Expression of AR protein from deletion mutant constructs. Cell extracts and conditioned media from transfected 184A1N4-TH cells (A and B) and COS cells (C) were examined on SDS-polyacrylamide gels by immunoblotting with antisera directed against either the mature peptide (Ab 035 [A and C]) or the N-terminal pro-region (Ab 042 [B]). All lanes correspond to 5% of a confluent 100-mm-diameter dish of cells. COS cell extracts were separated into soluble (S) and particulate (P) fractions. M, medium. Positions of molecular size markers (in kilodaltons) are shown on the left, and positions of migration of the 35- and 18-kDa forms of AR are shown on the right for reference.

consistent with intracellular accumulation and lack of normal glycosylation and secretion of the NPA construct.

Absence of the N-terminal pro-region results in rapid turnover of the AR precursor. The construct lacking the N-terminal pro-region (ARNP) was not detected in either the media or cell extracts, possibly because of either a deficiency in synthesis or rapid degradation of newly made protein. To distinguish between these possibilities, transfected 184A1N4-TH cells were metabolically labeled for 15 min with [^{35}S]cysteine and then chased for 0 min, 30 min, 1 h, or 4 h (Fig. 6). Immunoprecipitation with affinity-purified anti-AR serum revealed that a 22-kDa protein was synthesized but rapidly turned over ($t_{1/2}$, <30 min) in ARNP-transfected cells. In contrast, the native precursor (ARP) persisted in cell extracts for the entire 4 h and was partially converted from the 42-kDa to the 25-kDa cell-associated form, beginning by 1 h. Release into the media was minimal, even by 4 h. Like the more stable NPA product, the transiently observed ARNP migrated as a protein 2 to 3 kDa smaller than expected (~25 kDa) and was also endoglycosidase H insensitive (not shown).

These experiments indicate that the N-terminal pro-region of the ARP is required for AR secretion, presumably by directing proper folding of the molecule. We next addressed the possibility that the pro-regions of structurally related molecules can perform similar functions.

The N-terminal pro-region of HB-EGF can functionally replace the AR pro-region. While AR has a high degree of similarity to HB-EGF and TGF-α in the domain encompassed by the six cysteines (52 and 33%, respectively), minimal primary sequence homology can be found in the N-terminal pro-regions. Secondary structure predictions, however, suggest a similar distribution of hydrophilic stretches, preponderance of β turns, and lack of α-helical structure in the pro-regions of AR and HB-EGF but not TGF-α. If a conserved structural motif were necessary for proper folding, the pro-region of HB-EGF (and not TGF-α) might function within the context of the ARP and allow protein secretion. This hypothesis was tested by replacing the AR pro-region with that of either HB-EGF (HB-AR) or TGF-α (TGF-AR) (see Materials and Methods).

Expression of native AR, ARNP, HB-AR, and TGF-AR was compared in both 184A1N4-TH and COS cells (Fig. 7). Medium from transfected cells was assessed for bioactivity by measuring EGF receptor autophosphorylation, and Western blots were used to detect cell-associated and secreted AR protein. Comparable secretion of both bioactive material (Fig. 7A) and immunoreactive protein (Fig. 7B) was observed for the native precursor and HB-AR, but no protein was detected for either ARNP or TGF-AR. As previously observed with ARNP, pulse-chase experiments in TGF-AR-transfected cells demonstrated synthesis of an ~20-kDa protein that was turned over with a $t_{1/2}$ of <30 min (not shown).

Deletion of the basic domain abrogates the pro-region requirement. One structural feature shared by mature AR and HB-EGF, but not EGF or TGF-α, is a long (39 and ~34 residues, respectively), highly basic domain N terminal to the

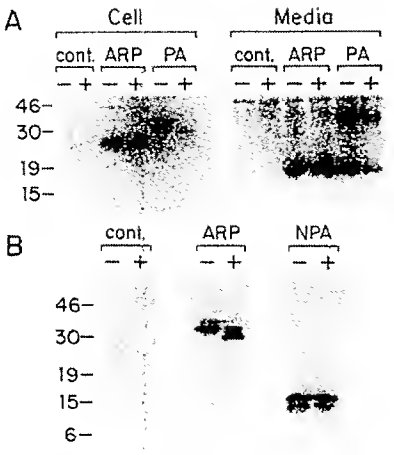

FIG. 5. Endoglycosidase H sensitivity of PA- and NPA-derived proteins. (A) Endoglycosidase H digestion of AR from 184A1N4-TH cells transfected with either control vector (cont.), full-length precursor (ARP), or the PA truncation mutant. Cells were transfected and harvested as for Western blots. Medium samples and the particulate fractions of cell extracts were then detergent solubilized and immunoprecipitated with affinity-purified anti-AR antiserum (Ab 035). Each immunoprecipitate was divided in half for incubation with either buffer alone (−) or endoglycosidase H (+) and then analyzed by Western blotting with the AR-specific antiserum Ab 035. (B) Endoglycosidase H digestion of metabolically labeled 184A1N4-TH cells transfected with either control vector (cont.), full-length precursor (ARP), or the NPA deletion mutant. Transfected cells were metabolically labeled 15 min with [^{35}S]cysteine and immediately detergent solubilized for immunoprecipitation with affinity-purified anti-AR antiserum. Each sample was divided, incubated both without (−) and with (+) endoglycosidase H, and resolved on an SDS-polyacrylamide gel for direct autoradiography. Sizes are indicated in kilodaltons.

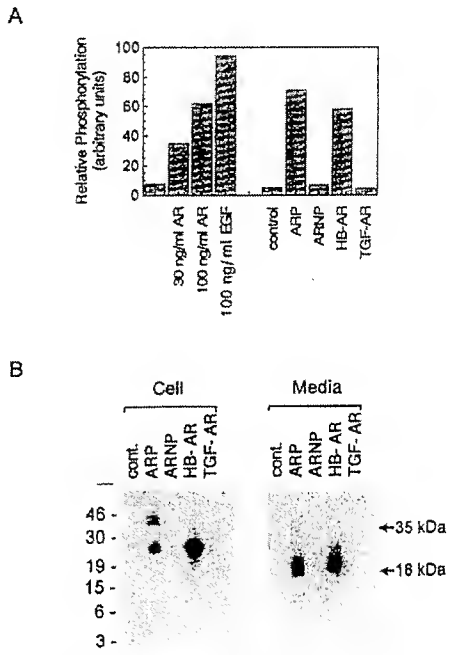

FIG. 7. Bioactivity and Western analysis of HB-AR and TGF-AR expressed in 184A1N4-TH cells. (A) EGF receptor autophosphorylation. NRHer5 cells were stimulated either with purified recombinant AR or EGF or with the conditioned media from transfected cells. EGF receptor was immunoprecipitated from solubilized NRHer5 cells, and autophosphorylation was assessed by antiphosphotyrosine Western blotting. Relative intensities of the 175-kDa phosphorylated receptor bands were determined by using a PhosphorImager and ImageQuant software. Similar results were also reproducibly observed with COS cells. (B) AR Western blot. Cell extracts and media from transfected 184A1N4-TH cells were analyzed by Western blotting with the anti-AR antiserum Ab 035 as described for Fig. 4. Only the particulate fraction of cell extracts is shown; no immunoreactivity was detected in the soluble fraction. Each lane corresponds to 5% of a confluent 100-mm-diameter dish. cont., control. COS cells produced similar results.

first cysteine of the EGF-like motif (24, 48). We hypothesized that the pro-regions of AR and HB-EGF might direct secretion by interacting with this basic domain to allow proper folding of the growth factor. To test this hypothesis, we generated a construct in which the entire N-terminal domain of mature AR was deleted (ARNP-NB [no-pro, no-basic]). A second construct retained the pro region (AR-NB [no-basic only]) to control for alternate mechanisms of pro-region function.

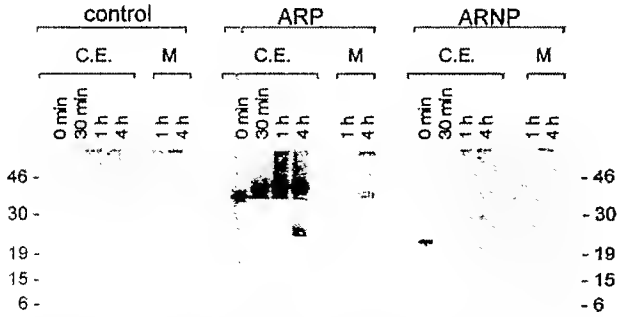

FIG. 6. Pulse-chase of ARNP-transfected 184A1N4-TH cells. Cells transfected with either control vector, full-length precursor (ARP), or the ARNP truncation mutant were metabolically labeled 15 min with [^{35}S]cysteine and then chased for either 0 min, 30 min, 1 h, or 4 h. AR was immunoprecipitated from media (M) and detergent-solubilized cell extracts (C.E.) with affinity-purified anti-AR antiserum Ab 035 and analyzed by direct autoradiography of an SDS-polyacrylamide gel.

Secretion of protein from transfected cells was assessed by immunoprecipitation of AR from the media of cultures metabolically labeled for 24 h with [^{35}S]cysteine. Pooled monoclonal Abs directed against the EGF-like domain were used in these experiments, since the no-basic constructs lack the epitope recognized by the rabbit antiserum previously used. Cells transfected with the ARNP-NB construct secreted a ~6-kDa protein (Fig. 8A), demonstrating that the pro-region is not required for secretion in the absence of the basic domain. Release of a ~30-kDa protein from AR-NB-transfected cells indicates that pro-region does not inhibit AR secretion in the absence of the basic domain. Unlike native AR, neither the 6-kDa ARNP-NB nor the 30-kDa AR-NB peptide was retained on heparin affinity resin (Fig. 8B), consistent with the colocalization of the heparin-binding domain to the basic N terminus of AR.

Closer inspection of the AR N terminus suggests that it may be divided into two subdomains, with most of the basic residues residing in the C-terminal half and the N-linked glycosylation sites residing in the N-terminal half (Fig. 9A). Deleting the C-terminal half (ARNPΔC) allowed secretion in

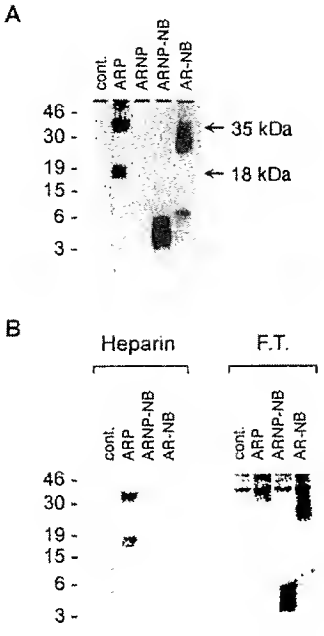

FIG. 8. Secretion of deletion mutants ARNP-NB and AR-NB from transfected 184A1N4-TH cells. (A) Metabolic labeling of 184A1N4-TH cells transfected with AR expression plasmids. Transfected cells were cultured 24 h in the presence of [^{35}S]cysteine, and secreted AR was immunoprecipitated with pooled monoclonal Abs raised against the mature factor. Samples were resolved on an SDS-polyacrylamide gel and visualized by direct autoradiography. cont., control. (B) Binding of metabolically labeled AR to immobilized heparin. Medium samples from metabolically labeled transfected cells were incubated with heparin acrylic beads and separated into bound and free fractions. AR on the heparin beads was eluted with high salt. The eluted samples (heparin) and unbound supernatant (flowthrough [F.T.]) were immunoprecipitated with the pooled anti-AR monoclonal Abs and analyzed by SDS-PAGE. cont., control. Sizes are indicated in kilodaltons.

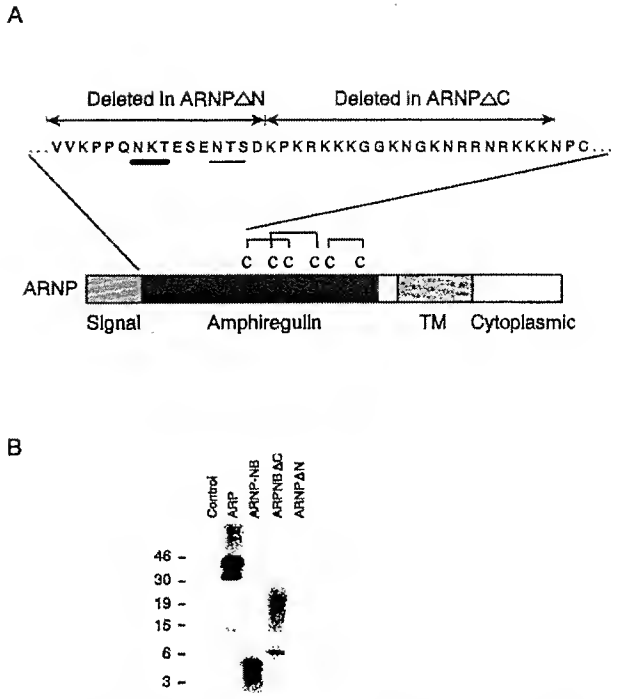

FIG. 9. Secretion of deletion mutants ARNPΔN and ARNPΔC from transfected COS cells. (A) Schematic of N-terminal domain deletions. Functional domains within the parent ARNP precursor are indicated, and the EGF-like motif within the mature factor is represented by the six disulfide-linked cysteines (C). Underlined residues indicate consensus sites for N-linked glycosylation. Thick underline indicates site known to be glycosylated in both MCF7 and CHO cells (unpublished data). Signal, N-terminal signal sequence from TGF-β; TM, transmembrane domain. (B) Metabolic labeling of COS cells transfected with AR expression plasmids. Transfected cells were cultured for 24 h in the presence of [^{35}S]methionine-cysteine, and secreted AR was immunoprecipitated with pooled monoclonal Abs raised against the mature factor. Samples were resolved on an SDS-polyacrylamide gel and visualized by direct autoradiography.

the absence of the pro-region (Fig. 9B). Deleting only the N-terminal half (ARNPΔN) was not effective, indicating that the inhibitory effect is specific to the basic region of mature AR.

The AR N terminus inhibits TGF-α secretion unless the AR pro-region is present. The foregoing results support the hypothesis that an N-terminal basic domain is inhibitory to folding and secretion of EGF-like molecules unless circumvented by a specific structural motif in the pro-region. However, an alternate interpretation is that deletion of the AR pro-region in certain contexts (ARNP and ARNPΔN but not ARNP-NB or ARNPΔC) nonspecifically disrupts the protein folding process. To distinguish between these possibilities, we studied the effect of the AR N terminus on secretion of TGF-α, an EGF-like molecule that lacks an analogous basic domain. Four constructs were designed, and to simplify secretion analysis, none contained the transmembrane or cytoplasmic domain of the TGF-α precursor (Fig. 10 and Materials and Methods): (i) Pα (soluble pro-TGF-α, analogous to the AR-derived PA construct), (ii) NPα (soluble no-pro TGF-α, analogous to NPA), (iii) PAα (chimera fusing the AR basic domain and pro-region to the EGF-like motif of TGF-α), and (iv) NPAα (chimera fusing the AR basic domain only to the EGF-like motif of TGF-α). Secretion of protein was assessed by analyzing the conditioned medium of transfected cells for EGF receptor-stimulating activity and for TGF-α or AR (basic domain) immunoreactivity (Table 1).

Consistent with the model, release of TGF-α bioactivity and immunoreactivity from both Pα- and NPα-transfected cells indicates that the TGF-α pro-region is not required for secretion. Adding the AR basic domain alone (NPAα) prevented detectable secretion, although AR immunoreactive protein in cell extracts confirmed expression (not shown). Finally, secretion of the AR–TGF-α chimera was restored by including the AR pro-region. These results suggest a specific role for the AR pro-region in directing secretion and argue against a simple nonspecific disruption of protein folding for the earlier AR truncation mutants.

DISCUSSION

Like other members of the EGF family of growth regulators, AR is initially synthesized as a transmembrane precursor, consisting of a signal sequence, an N-terminal pro-region, the EGF-like active factor, a small juxtamembrane and single transmembrane domain, and a cytoplasmic domain. Outside the EGF-like repeat, however, the precursors show little sequence homology. While membrane-anchored forms of EGF

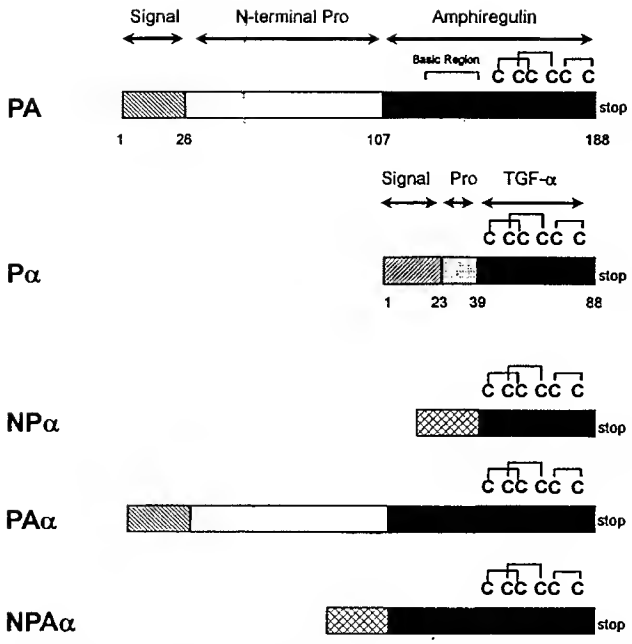

FIG. 10. AR–TGF-α chimeric constructs. Functional domains and amino acid positions within the human AR and TGF-α precursors are indicated in the full-length extracellular domain constructs (PA and Pα). All other deletion and domain swap constructs also truncate at the C terminus of the mature factors. The EGF-like motifs are represented by the six disulfide-linked cysteines (C). Signal sequences used: ▨, native AR signal; ▨, native TGF-α signal; ▨, TGF-β signal.

TABLE 1. Secretion of TGF-α derived chimeric molecules from transfected COS cells

Construct[a]	EGF receptor autophosphorylation[b]	TGF-α immunoreactivity[c]	AR immunoreactivity[d]
Vector	–	–	–
PA	+	–	+
Pα	+	+	–
NPα	+	+	–
NPAα	–	–	–[e]
PAα	+	+	+

[a] COS cells were transfected with each of the expression plasmids as described in Materials and Methods. Two days after transfection, cells were transferred to serum-free medium for an additional 24 h, when samples from the medium were collected for direct analysis.

[b] Ligand-induced EGF receptor autophosphorylation was assessed as in Fig. 3 and 7A. –, phosphorylation indistinguishable from that of unstimulated cells; +, phosphorylation levels >4-fold above background.

[c] Assayed by double-determinant ELISA. –, TGF-α immunoreactivity below detection levels (0.4 ng/ml); +, TGF-α immunoreactivity of ≥10 ng/ml in the conditioned medium.

[d] Determined by Western blotting with an Ab directed against the basic region of the mature factor. Medium samples of constructs with negative activity contained no specific AR bands, and the AR immunoreactive bands in positive samples were comparable in intensity to those observed for secreted forms in Fig. 4 and 7B.

[e] Although no AR immunoreactivity was detected in the conditioned medium, an ~16- to 18-kDa doublet was observed in the particulate fraction of NPAα-transfected cell extracts.

and TGF-α are mitogenic and have been observed in vivo and in cell culture, the biological function of the precursor molecules is still unclear (1, 6, 9, 17, 42, 49, 70). This study examines the role of each of the precursor domains in the secretion of bioactive AR.

AR deletion mutants were transiently expressed in COS and mammary epithelial cells, and conditioned medium was analyzed for secretion of active factor. Protein expression was examined by Western blotting. Active AR was synthesized and secreted by using a construct encoding the native precursor or constructs lacking the transmembrane and/or cytoplasmic domains. In contrast, deletion of the N-terminal pro-region completely abrogated AR release. Secretion was restored with a chimeric protein containing the HB-EGF pro-region but not with a chimera containing the pro-region from the TGF-α precursor. In the absence of a pro-region, secretion was restored by deleting the basic amino acid-rich region near the N terminus of the mature factor. Addition of this basic domain to the EGF-like motif of TGF-α (which itself does not require a pro-region) inhibited secretion of the chimeric molecule unless the AR pro-region was also present. These results demonstrate a role for the N-terminal pro-region in the synthesis and secretion of AR and indicate that a specific structural motif in this region is necessitated by the basic N terminus of the mature factor.

All experiments were performed in both fibroblast-like COS cells and human mammary epithelium-derived 184A1N4-TH cells. Both cell types processed the native precursor to two secreted and two cell-associated isoforms, similar to those produced endogenously by normal HMEC (Fig. 1). The transfected cell lines exhibited proportionately higher levels of the cell-associated AR than the normal cells did, but this may reflect the high rates of synthesis that occur when expression systems that amplify plasmid copy number are used. Importantly, the two expression systems produced similar results for the various mutant precursors. Thus, the observed effects on secretion and processing are probably inherent to the protein domains being examined and not due to tissue-specific factors. Compared with COS cells, however, HMEC did show more efficient removal the N-terminal pro-region from the membrane-anchored AR constructs (ARP and ARTL), which may indicate higher levels of processing enzyme activity in the more appropriate cell type.

The transmembrane and cytoplasmic domains of the precursor are not essential for AR production, since cells expressing just the extracellular sequences (PA construct) secreted bioactive protein at levels comparable to those found for the native precursor (Fig. 3 and 4). This result is consistent with reports that active recombinant EGF can be synthesized in the absence of a membrane anchor (60). However, the transmembrane domain apparently does play a role in the maturation of the ARP. Endoglycosidase H-sensitive PA precursor accumulated in the particulate fraction of cell extracts (Fig. 5), suggesting inefficient folding and transport out of the endoplasmic reticulum. More striking was the less efficient cleavage of the N-terminal pro-region, resulting in proportionately greater secretion of the 35-kDa form, gp35. For example, gp35 accounted for >50% of the AR secreted from PA-transfected 184A1N4-TH cells, compared to 10 to 20% for ARP (Fig. 4A).

Release of soluble TGF-α from its integral membrane precursor is thought to occur at the cell surface (63). Conceivably, similar AR processing by a cell-associated protease could explain the increase in gp35 secretion from PA-transfected cells, since absence of the membrane anchor would diminish the amount of AR in close proximity to the plasma membrane. Indeed, the lack of detectable 18-kDa AR in extracts of these cells indicates that propeptide cleavage must occur either late in the secretory pathway or extracellularly. Also consistent with this hypothesis is the long lag time before initiation of native

ARP processing. In transfected 184A1N4-TH cells, N-terminal cleavage begins approximately 1 h after synthesis, and C-terminal cleavage begins only by 4 h (Fig. 6).

In our experimental systems, deletion of the cytoplasmic domain alone did not prevent AR secretion. However, in comparison with the full-length precursor, this construct (ARTL) consistently produced a greater proportion of cell-associated material, although the relative differences were variable (Fig. 4A and C). The COS cell experiment depicted in Fig. 4C is a conservative example of this phenomenon; ~65% of the mutant protein was found in the cell, compared with ~40% for the native precursor. This observation is interesting in light of recent studies on pro-TGF-α, which demonstrate a role for the cytoplasmic domain in regulating release of mature factor from CHO and Ltk cells (8). Unstimulated cells retained most of the TGF-α on the membrane, but activators of protein kinase C or increases in cytosolic calcium levels lead to rapid and efficient cleavage of the ectodomain (44, 45). Critical for this response was the cytoplasmic carboxyl-terminal valine residue (8). Although it is tempting to speculate that the cytoplasmic domain of the ARP may function similarly, further characterization of the processing mechanism is required. An identical mechanism is unlikely, however, since the ARP terminates in Ala, a residue which was only 10% as effective in regulating TGF-α processing as Val, Leu, or Ile (8).

In contrast to the transmembrane and cytoplasmic domains of AR, the N-terminal pro-region was essential for protein secretion. Two constructs lacking this domain (ARNP and NPA, with and without a membrane anchor, respectively) were synthesized but not released into the media. The transmembrane ARNP was rapidly degraded ($t_{1/2}$, <30 min) (Fig. 6), although the nonanchored NPA accumulated within the cell (Fig. 4). Since a construct with the identical leader sequence in the same context (ARNPΔC [Fig. 9]) was efficiently secreted, the trivial explanation of a nonfunctional signal peptide was eliminated. Lack of secretion is frequently associated with protein misfolding, leading to either rapid turnover or retention in the endoplasmic reticulum, often in associations with proteins such as BiP or as large insoluble aggregates (see references 26, 46, and 51 for reviews). Indeed, the absence of normal N-linked glycosylation for the pro-less mutants suggests they may be structurally aberrant; neither molecule was subject to endoglycosidase H digestion shortly after synthesis, and both migrated as ~2 kDa smaller on SDS-PAGE than the corresponding native forms. The presence of anchor-less NPA in the particulate fraction of cell extracts would also be consistent with formation of insoluble aggregates. However, the reason for different intracellular fates of the anchored and nonanchored mutants is not known.

The requirement of the pro-region for AR secretion is in direct contrast with results for both TGF-α (Table 1) and EGF. Active EGF is readily synthesized and secreted from mammalian cells without its large N-terminal pro-domain, either in the presence or in the absence of a membrane anchor (17, 60). However, there are other examples in which a pro-domain is required for secretion or correct folding. For example, without their pro-sequences, NGF is unstable and is not secreted (61), activin and TGF-β accumulate intracellularly as insoluble aggregates (21), the interchain disulfide bonds necessary for functional von Willebrand factor oligomerization do not form (69), and many enzymes, such as subtilisin and carboxypeptidase Y, do not achieve an active conformation (28, 67). For activin, TGF-β, and von Willebrand factor, the pro-region need not be contiguous with the rest of the precursor to allow secretion or oligomerization but can function when coexpressed as a separate molecule (albeit inefficiently for TGF-β). In vitro, the isolated pro-region of subtilisin can direct proper folding of the denatured enzyme (72). In the case of AR, however, this domain apparently cannot complement the secretion defect when expressed in *trans* (unpublished data).

Substituting the AR pro-region with the comparable region of proHB-EGF, but not that of proTGF-α, restores protein secretion (Fig. 7). Minimal primary sequence homology in this domain suggests a conserved structural motif. Possibilities include (i) secondary structure, such as the preponderance of β turns and lack of α helices predicted for both AR and HB-EGF pro-regions; (ii) a surface patch, consistent with their similar distribution of hydrophilic stretches; or (iii) a posttranslational modification common to pro-AR and pro-HB-EGF but absent in pro-TGF-α. If the pro-region does indeed direct folding and thus exit from the endoplasmic reticulum, modifications occurring late in the secretory pathway (e.g., many types of carbohydrate maturation) are unlikely candidates for such a secretory motif.

AR secretion was also restored by simultaneous removal of both the pro-region and the heparin-binding N-terminal domain of the mature factor. Conversely, TGF-α secretion was inhibited by the AR N terminus and subsequently rescued by the presence of the AR pro-region. These observations suggest that the AR pro-region may function to prevent the heparin-binding sequences from interfering with folding of the EGF-like motif. This hypothesis could explain the different requirements for AR and EGF or TGF-α expression. By removing its basic N terminus, AR becomes structurally more similar to EGF or TGF-α and can then be expressed without additional precursor sequences. A pro-region could fulfill such a function either by directly facilitating correct folding or by masking an inhibitory region in the basic domain. Direct effects on folding have been documented for numerous pro-proteins, including α-lytic protease, in which case pro-sequences accelerate the rate-limiting step in the folding pathway by more than 10^7, and bovine pancreatic trypsin inhibitor, in which case a cysteine in the pro-region acts as a tethered thiol disulfide reagent to assist in native disulfide bond formation (2, 66). Masking inhibitory sequences implies a direct interaction between the pro-region and basic domains, which could also interfere with the heparin-binding function. In support of the second hypothesis, gp35 (containing pro-region sequences) does have a lower affinity for heparin than 18-kDa AR does (unpublished data).

The AR precursor plays a vital role in the production of bioactive factor. The N-terminal pro-region is required for export from the cell, while the transmembrane domain facilitates its subsequent removal. However, additional functions for these domains are still possible. Soluble and integral membrane forms of a growth factor may have distinct biological roles, as in the case of Steel factor. In addition to the phenotypic evidence provided by the steel dicky (Sl^d) mouse, the membrane-anchored factor is more effective at supporting survival of hematopoietic progenitor cells in vitro than is the soluble form (10, 20, 64). A variety of roles for N-terminal pro-regions have also been documented; they include providing sites for signal peptide recognition and cleavage or precursor processing, targeting the protein to specific compartments in the secretory pathway, and directing posttranslational modifications within the mature protein (23, 32, 56, 68). In the case of AR, a direct interaction between the N-terminal pro-region and the heparin-binding domain of the mature factor may modulate its activity. Important considerations for assessing physiological actions of AR should therefore include recognition of its heparin-binding properties and whether high-molecular-weight or transmembrane forms exhibit distinct biological functions.

ACKNOWLEDGMENTS

We thank Martha Stampfer for the 184A1N4-TH cell line and Hsing-Jien Kung for the NRHer5 cell line. We also thank Mike Neubauer and Joe Cook for DNA sequencing, Trent Youngman and Scott Austin for oligodeoxynucleotide synthesis, Jim Blake and Wes Cosand for peptide synthesis, Vicki McDonald, Susan Radka, and Ulrika Stevenson for Ab production, Sharon Buckley and Jan Green for assistance in Ab characterization, and Kelly Bennett for helpful discussions.

REFERENCES

1. **Anklesaria, P., J. Teixidó, M. Laiho, J. H. Pierce, J. S. Greenberger, and J. Massagué.** 1990. Cell-cell adhesion mediated by binding of membrane-anchored transforming growth factor α to epidermal growth factor receptors promotes cell proliferation. Proc. Natl. Acad. Sci. USA **87**:3289–3293.
2. **Baker, D., J. L. Sohl, and D. A. Agard.** 1992. A protein-folding reaction under kinetic control. Nature (London) **356**:263–265.
3. **Bell, G. I., N. M. Fong, M. M. Stempien, M. A. Wormsted, D. Caput, L. Ku, M. S. Urdea, L. B. Rall, and R. Sanchez-Pescador.** 1986. Human epidermal growth factor precursor, cDNA sequence, expression *in vitro* and gene organization. Nucleic Acids Res. **14**:8427–8446.
4. **Betsholtz, C., A. Johnsson, C.-H. Heldin, B. Westermark, P. Lind, M. S. Urdea, R. Eddy, T. B. Shows, K. Philpott, A. L. Mellor, T. J. Knott, and J. Scott.** 1986. cDNA sequence and chromosomal localization of human platelet-derived growth factor A-chain and its expression in tumor cell lines. Nature (London) **320**:695–699.
5. **Bjorge, J. D., T.-O. Chan, M. Antczak, H.-J. Kung, and D. J. Fujita.** 1990. Activated type I phosphatidylinositol kinase is associated with the epidermal growth factor (EGF) receptor following EGF stimulation. Proc. Natl. Acad. Sci. USA **87**:3816–3820.
6. **Blasband, A. J., D. M. Gilligan, L. F. Winchell, S. T. Wong, N. C. Luetteke, K. T. Rogers, and D. C. Lee.** Expression of the TGFα integral membrane precursor induces transformation of NRK cells. Oncogene **5**:1213–1221.
7. **Blasband, A. J., K. T. Rogers, X. Chen, J. C. Azizkhan, and D. C. Lee.** 1990. Characterization of the rat transforming growth factor alpha gene and identification of promoter sequences. Mol. Cell. Biol. **10**:2111–2121.
8. **Bosenberg, M. W., A. Pandiella, and J. Massagué.** 1992. The cytoplasmic carboxy-terminal amino acid specifies cleavage of membrane TGFα into soluble growth factor. Cell **71**:1157–1165.
9. **Brachmann, R., P. B. Lindquist, M. Nagashima, W. Kohr, T. Lipari, M. Napier, and R. Derynck.** 1989. Transmembrane TGF-α precursors activate EGF/TGF-α receptors. Cell **56**:691–700.
10. **Brannan, C. I., S. D. Lyman, D. E. Williams, J. Eisenman, D. M. Anderson, D. Cosman, M. A. Bedell, N. A. Jenkins, and N. G. Copeland.** 1991. Steel-dickie mutation encodes a c-Kit ligand lacking transmembrane and cytoplasmic domains. Proc. Natl. Acad. Sci. USA **88**:4671–4674.
11. **Brunner, A. B., H. Marquardt, A. R. Malacko, M. N. Lioubin, and A. F. Purchio.** 1989. Site-directed mutagenesis of cysteine residues in the pro-region of the transforming growth factor β1 precursor: expression and characterization of mutant proteins. J. Biol. Chem. **264**:13660–13664.
12. **Carpenter, G., and M. I. Wahl.** 1990. The epidermal growth factor family, p. 69–171. *In* M. D. Sporn and A. B. Roberts (ed.), Peptide growth factors and their receptors. Springer, New York.
13. **Clark, R., M. R. Stampfer, R. Milley, E. O'Rourke, K. H. Walen, M. Kriegler, J. Kopplin, and F. McCormick.** Transformation of human mammary epithelial cells by oncogenic retroviruses. Cancer Res. **48**:4689–4694.
14. **Cook, P. W., P. A. Mattox, W. W. Keeble, M. R. Pittelkow, G. D. Plowman, M. Shoyab, J. P. Adelman, and G. D. Shipley.** 1991. A heparin sulfate-regulated human keratinocyte autocrine factor is similar or identical to amphiregulin. Mol. Cell. Biol. **11**:2547–2557.
15. **Derynck, R., J. A. Jarrett, E. Y. Chen, D. H. Eaton, J. R. Bell, R. K. Assoian, A. B. Roberts, M. B. Sporn, and D. V. Goeddel.** 1985. Human transforming growth factor-β complementary DNA sequence and expression in normal and transformed cells. Nature (London) **316**:701–705.
16. **Derynck, R., A. B. Roberts, M. E. Winkler, E. Y. Chen, and D. V. Goeddel.** 1984. Human transforming growth factor-α: precursor structure and expression in E. coli. Cell **38**:287–294.
17. **Dobashi, Y., and D. F. Stern.** 1991. Membrane-anchored forms of EGF stimulate focus formation and intercellular communication. Oncogene **6**:1151–1159.
18. **Ehlers, M. R. W., and J. F. Riordan.** 1991. Membrane proteins with soluble counterparts: role of proteolysis in the release of transmembrane proteins. Biochemistry **30**:10065–10074.
19. **Engler, D. A., R. K. Matsunami, S. R. Campion, C. D. Stringer, A. Stevens, and S. K. Niyogi.** 1988. Cloning of authentic human epidermal growth factor as a bacterial secretory protein and its initial structure-function analysis by site-directed mutagenesis. J. Biol. Chem. **263**:12384–12390.
20. **Flanagan, J. G., D. C. Chan, and P. Leder.** 1991. Transmembrane form of the kit ligand growth factor is determined by alternate splicing and is missing in the Sl^d mutant. Cell **64**:1025–1035.
21. **Gray, A. M., and A. J. Mason.** 1990. Requirement for activin A and transforming growth factor-β1 pro-regions in homodimer assembly. Science **247**:1328–1330.
22. **Gentry, L. E., M. N. Lioubin, A. F. Purchio, and H. Marquardt.** 1988. Molecular events in the processing of recombinant type 1 pre-pro-transforming growth factor beta to the mature polypeptide. Mol. Cell. Biol. **8**:4162–4168.
23. **Gomez, S., G. Boileau, L. Zollinger, C. Nault, M. Rholam, and P. Cohen.** 1989. Site-specific mutagenesis identifies amino acid residues critical in prohormone processing. EMBO J. **8**:2911–2916.
24. **Higashiyama, S., J. A. Abraham, J. Miller, J. C. Fiddes, and M. Klagsbrun.** 1991. A heparin-binding growth factor secreted by macrophage-like cells that is related to EGF. Science **251**:936–939.
25. **Higashiyama, S., K. Lau, G. E. Besner, J. A. Abraham, and M. Klagsbrun.** 1992. Structure of heparin-binding EGF-like growth factor. J. Biol. Chem. **267**:6205–6212.
26. **Hurtley, S. M., and A. Helenius.** 1989. Protein oligomerization in the endoplasmic reticulum. Annu. Rev. Cell Biol. **5**:277–307.
27. **Ignotz, R. A., B. Kelly, R. J. Davis, and J. Massagué.** 1986. Biologically active precursor for transforming growth factor type α, released by retrovirally transformed cells. Proc. Natl. Acad. Sci. USA **83**:6307–6311.
28. **Ikemura, H., H. Takagi, and M. Inouye.** 1987. Requirement of pro-sequence for the production of active subtilisin E in *Escherichia coli*. J. Biol. Chem. **262**:7859–7864.
29. **Innis, M. A., D. H. Gelfand, J. J. Sninsky, and T. J. White (ed.).** 1990. PCR protocols. Academic Press Inc., San Diego, Calif.
30. **Jameson, B. A., and H. Wolf.** 1988. The antigenic index: a novel method for predicting antigenic determinants. Comput. Appl. Biosci. **4**:181–186.
31. **Johnson, G. R., T. Saeki, A. W. Gordon, M. Shoyab, D. S. Salomon, and K. Stromberg.** 1992. Autocrine action of amphiregulin in a colon carcinoma cell line and immunocytochemical localization of amphiregulin in human colon. J. Cell Biol. **118**:741–751.
32. **Jorgensen, M. J., A. B. Cantor, B. C. Furie, C. L. Brown, C. B. Shoemaker, and B. Furie.** 1987. Recognition site directing vitamin K-dependent γ-carboxylation resides on the propeptide of factor IX. Cell **48**:185–191.
33. **Kriegler, M., C. Perez, K. DeFay, I. Albert, and S. D. Lu.** 1988. A novel form of TNF/cachectin is a cell surface cytotoxic transmembrane protein: ramifications for the complex physiology of TNF. Cell **53**:45–53.
34. **Lazar, E., S. Watanabe, S. Dalton, and M. B. Sporn.** 1988. Transforming growth factor α: mutation of aspartic acid 47 and leucine 48 results in different biological activities. Mol. Cell. Biol. **8**:1247–1252.
35. **Li, S., G. D. Plowman, S. D. Buckley, and G. D. Shipley.** 1992. Heparin inhibition of autonomous growth implicates amphiregulin as an autocrine growth factor for normal human mammary epithelial cells. J. Cell Physiol. **153**:103–111.
36. **Luetteke, N. C., G. K. Michalopoulos, J. Teixidó, R. Gilmore, J. Massagué, and D. C. Lee.** 1988. Characterization of high molecular weight transforming growth factor α produced by rat hepatocellular carcinoma cells. Biochemistry **27**:6487–6494.
37. **Massagué, J.** 1990. Transforming growth factor-α: a model for

membrane-anchored growth factors. J. Biol. Chem. **265**:21393–21396.
38. **Massagué, J., and A. Pandiella.** 1993. Membrane-anchored growth factors. Annu. Rev. Biochem. **62**:515–541.
39. **Mercola, M., P. L. Delninger, S. M. Shamah, J. Porter, C. Y. Wang, and C. D. Stiles.** 1990. Dominant-negative mutants of a platelet derived growth factor gene. Genes Dev. **4**:2333–2341.
40. **Miyazono, K., U. Hellman, C. Wernstedt, and C.-H. Heldin.** 1988. Latent high molecular weight complex of transforming growth factor β1. J. Biol. Chem. **263**:6407–6415.
41. **Miyazono, K., A. Olofsson, P. Colosetti, and C.-H. Heldin.** 1991. A role of the latent TGF-β1-binding protein in the assembly and secretion of TGF-β1. EMBO J. **10**:1091–1101.
42. **Mroczkowski, B., M. Relch, K. Chen, G. I. Bell, and S. Cohen.** 1989. Recombinant human epidermal growth factor precursor is a glycosylated membrane protein with biological activity. Mol. Cell. Biol. **9**:2771–2778.
43. **Naglich, J. G., J. E. Metherall, D. W. Russell, and L. Eldels.** 1992. Expression cloning of a diphtheria toxin receptor: identity with a heparin-binding EGF-like growth factor precursor. Cell **69**:1051–1061.
44. **Pandiella, A., and J. Massagué.** 1991. Cleavage of the membrane precursor for transforming growth factor α is a regulated process. Proc. Natl. Acad. Sci. USA **88**:1726–1730.
45. **Pandiella, A., and J. Massagué.** 1991. Multiple signals activate cleavage of the membrane transforming growth factor α precursor. J. Biol. Chem. **266**:5769–5773.
46. **Pelham, H. R. B.** 1989. Control of protein exit from the endoplasmic reticulum. Annu. Rev. Cell Biol. **5**:1–23.
47. **Perez, C., I. Albert, K. DeFay, N. Zachariades, L. Gooding, and M. Kriegler.** 1990. A nonsecretable cell surface mutant of tumor necrosis factor (TNF) kills by cell-to-cell contact. Cell **63**:251–258.
48. **Plowman, G. D., J. M. Green, V. L. McDonald, M. G. Neubauer, C. M. Disteche, G. J. Todaro, and M. Shoyab.** 1990. The amphiregulin gene encodes a novel epidermal growth factor-related protein with tumor-inhibitory activity. Mol. Cell. Biol. **10**:1969–1981.
49. **Rall, L. B., J. Scott, G. I. Bell, R. J. Crawford, J. D. Penschow, H. D. Niall, and J. P. Coghlan.** 1985. Mouse prepro-epidermal growth factor synthesis by the kidney and other tissues. Nature (London) **313**:228–231.
50. **Ray, P., F. J. Moy, G. T. Montelione, J.-F. Liu, S. A. Narang, H. A. Scheraga, and R. Wu.** 1988. Structure-function studies of murine epidermal growth factor: expression and site directed mutagenesis of epidermal growth factor gene. Biochemistry **27**:7289–7295.
51. **Rose, J. K., and R. W. Doms.** 1988. Regulation of protein export from the endoplasmic reticulum. Annu. Rev. Cell Biol. **4**:257–288.
52. **Sambrook, J., E. F. Fritsch, and T. Maniatis.** 1989. Molecular cloning: a laboratory manual, 2nd ed. Cold Spring Harbor Laboratory Press, Cold Spring Harbor, N.Y.
53. **Sasada, R., Y. Ono, Y. Taniyama, Y. Shing, J. Folkman, and K. Igarashi.** 1993. Cloning and expression of cDNA encoding human betacellulin, a new member of the EGF family. Biochem. Biophys. Res. Commun. **190**:1173–1179.
54. **Scott, J., M. Selby, M. Urdea, M. Qiroga, G. I. Bell, and W. J. Rutter.** 1983. Isolation and nucleotide sequence of a cDNA encoding the precursor of mouse nerve growth factor. Nature (London) **302**:538–540.
55. **Seed, B., and A. Aruffo.** 1987. Molecular cloning of the CD2 antigen, the T-cell erythrocyte receptor, by a rapid immunoselection method. Proc. Natl. Acad. Sci. USA **84**:3365–3369.
56. **Sevarino, K. A., P. Stork, R. Ventimiglia, G. Mandel, and R. H. Goodman.** 1989. Amino-terminal sequences of prosomatostatin direct intracellular targeting but not processing specificity. Cell **57**:11–19.
57. **Shing, Y., G. Christofori, D. Hanahan, Y. Ono, R. Sasada, K. Igarashi, and J. Folkman.** 1993. Betacellulin: a mitogen from pancreatic β cell tumors. Science **259**:1604–1607.
58. **Shoyab, M., G. D. Plowman, V. L. McDonald, J. G. Bradley, and G. J. Todaro.** 1989. Structure and function of human amphiregulin: a member of the epidermal growth factor family. Science **243**:1074–1076.
59. **Stein, J., G. V. Borzillo, and C. W. Rettenmier.** 1990. Direct stimulation of cells expressing receptors for macrophage colony-stimulating factor (CSF-1) by a plasma membrane-bound precursor of human CSF-1. Blood **76**:1308–1314.
60. **Stern, D. F., D. L. Hare, M. A. Cecchini, and R. A. Weinberg.** 1987. Construction of a novel oncogene based on synthetic sequences encoding epidermal growth factor. Science **235**:321–324.
61. **Suter, U., J. V. Heymach, and E. M. Shooter.** 1991. Two conserved domains in the NGF propeptide are necessary and sufficient for the biosynthesis of correctly processed and biologically active NGF. EMBO J. **10**:2395–2400.
62. **Teixidó, J., and J. Massagué.** 1988. Structural properties of a soluble bioactive precursor for transforming growth factor-α. J. Biol. Chem. **263**:3924–3929.
63. **Teixidó, J., S. T. Wong, D. C. Lee, and J. Massagué.** 1990. Generation of transforming growth factor-α from the cell surface by an O-glycosylation-independent multistep process. J. Biol. Chem. **265**:6410–6415.
64. **Toksoz, D., K. M. Zsebo, K. A. Smith, S. Hu, D. Brankow, S. V. Suggs, F. H. Martin, and D. A. Williams.** 1992. Support of human hematopoiesis in long-term bone marrow cultures by murine stromal cells selectively expressing the membrane-bound and secreted forms of the human homolog of the steel gene product, stem cell factor. Proc. Natl. Acad. Sci. USA **89**:7350–7354.
65. **Wakefield, L. M., D. M. Smith, K. C. Flanders, and M. B. Sporn.** 1988. Latent transforming growth factor-β from human platelets: a high molecular weight complex containing precursor sequences. J. Biol. Chem. **263**:7646–7654.
66. **Weissman, J. S., and P. S. Kim.** 1992. The pro region of BPTI facilitates folding. Cell **71**:841–851.
67. **Winther, J. R., and P. Sørensen.** 1991. Propeptide of carboxypeptidase Y provides a chaperone-like function as well as inhibition of the enzymatic activity. Proc. Natl. Acad. Sci. USA **88**:9330–9334.
68. **Wiren, K. M., J. T. Potts, and H. M. Kronenberg.** 1988. Importance of the propeptide sequence in human preproparathyroid hormone for signal sequence function. J. Biol. Chem. **263**:19771–19777.
69. **Wise, R. J., D. D. Pittman, R. I. Handin, R. J. Kaufman, and S. H. Orkin.** 1988. The propeptide of vonWillebrand factor independently mediates the assembly of vonWillebrand multimers. Cell **52**:229–236.
70. **Wong, S. T., L. F. Winchell, B. K. McCune, H. S. Earp, J. Teixidó, J. Massagué, B. Herman, and D. C. Lee.** 1989. The TGF-α precursor expressed on the cell surface binds to the EGF receptor on adjacent cells, leading to signal transduction. Cell **56**:495–506.
71. **Young, R. M., A. E. Mendoza, T. Collins, and S. H. Orkin.** 1990. Alternatively spliced platelet-derived growth factor A-chain transcripts are not tumor specific but encode normal cellular proteins. Mol. Cell. Biol. **10**:6051–6054.
72. **Zhu, X., Y. Ohta, F. Jordan, and M. Inouye.** 1989. Pro-sequence of subtilisin can guide the refolding of denatured subtilisin in an intermolecular process. Nature (London) **339**:483–484.

THE JOURNAL OF BIOLOGICAL CHEMISTRY

Vol. 269, No. 43, Issue of October 28, pp. 27149–27154, 1994
Printed in U.S.A.

Heparan Sulfate Is Essential to Amphiregulin-induced Mitogenic Signaling by the Epidermal Growth Factor Receptor*

(Received for publication, June 20, 1994, and in revised form, July 18, 1994)

Gibbes R. Johnson‡ and Lily Wong

From the Division of Cytokine Biology, Center for Biologics Evaluation and Research, Food and Drug Administration, Bethesda, Maryland 20892

Human amphiregulin (AR) is a heparin-binding growth factor which functions by binding to and activating the epidermal growth factor (EGF) receptor tyrosine kinase. AR contains an EGF-like domain (residues 44–84) and a Lys/Arg-rich NH_2-terminal extension (residues 1–43). Synthetic peptides corresponding to residues 8–26, 26–44, and 68–84 of AR were tested for their ability to compete for the binding of AR to immobilized heparin. AR^{8-26} and AR^{68-84} had no significant effect on the binding of AR to heparin, whereas AR^{26-44} bound to heparin and blocked the binding of AR to heparin. Both soluble heparin and heparan sulfate inhibited AR-induced mitogenesis in MCF-10A human mammary epithelial cells with an IC_{50} of 5 and 2 μg/ml, respectively, whereas soluble chondroitin sulfate had only a slight inhibitory effect. When MCF-10A cells were grown in the presence of chlorate, an inhibitor of sulfation, or exposed to the glycosaminoglycan-degrading enzymes heparitinase or heparinase, the ability of AR to evoke mitogenesis in these cells was lost. Chlorate, heparitinase, or heparinase treatment inhibited AR-induced autophosphorylation of tyrosine residues in the EGF receptor. None of these treatments had any significant effect on EGF-triggered mitogenic signaling by the EGF receptor. These results indicate that extracellular heparan sulfate glycosaminoglycan is essential to AR-induced mitogenic signaling by the EGF receptor tyrosine kinase.

Human amphiregulin (AR)[1] is a heparin-binding polypeptide growth regulator which consists of an epidermal growth factor (EGF)-like domain and a very basic NH_2-terminal extension which contains glycosylation sites and putative nuclear localization signals (1–3). AR influences the proliferation of cells by binding to the extracellular domain of the EGF receptor (EGFR) which results in autophosphorylation of the EGFR, activation of the EGFR tyrosine kinase, and rapid tyrosine phosphorylation of a number of cellular substrates including $p185^{erbB2}$ (4). AR stimulates the proliferation of normal and malignant epithelial cells, fibroblasts, and keratinocytes (1–7). *In vivo*, AR is expressed by a large number of normal tissues (8) but appears to be localized exclusively to the epithelium of the human colon (7, 9), stomach (10, 11), breast (12), and pancreas (13). AR has been shown to drive the proliferation of human colon carcinoma cells via an autocrine mechanism (7) and is commonly overexpressed in human cancers of the colon (7, 9, 14, 15), breast (12, 16), stomach (10, 11, 15), and pancreas (13).

Heparin affinity chromatography has been utilized to purify AR from the conditioned medium of human keratinocytes (2) as well as phorbol ester-treated human breast carcinoma cells (3), and 30 μg/ml of soluble heparin has been shown to inhibit the ability of AR to stimulate the growth of keratinocytes (2). In addition to AR, a number of heparin-binding growth factors have been discovered within the last several years which contain an EGF-like domain such as schwannoma-derived growth factor (SDGF) (17), heparin-binding EGF-like growth factor (HB-EGF) (18), betacellulin (19), heregulin (20), and *neu* differentiation factor (21). The bioactivity of AR appears to be mediated exclusively through the EGFR (4, 7), as may be the case for SDGF, HB-EGF, and betacellulin, whereas the action of heregulin and *neu* differentiation factor appears to involve the *erb*B2, *erb*B3, and/or *erb*B4 EGFR-like tyrosine kinases (22–25). Since it is very unlikely that these growth factors would ever encounter heparin *in vivo* (26), the physiological significance of their ability to bind heparin is not clear. Proteoglycans are proteins which contain covalently attached sulfated glycosaminoglycan (GAG), exist on the surface of cells and in the extracellular matrix and are believed to play important roles in a wide range of biological processes which include cell division, morphogenesis and cancer (26–29). One important subset of these molecules is the heparan sulfate (HS) proteoglycan (30–32) whose HS chain is structurally related to heparin, but in general, is sulfated to a lesser degree. HS proteoglycan has been shown to be obligatory for the mitogenic activity of basic and acidic fibroblast growth factor (FGF) (33–37) and vascular endothelial growth factor (38). HS also appears to play an important role in the HB-EGF stimulation of smooth muscle cell migration (39).

Recently, we isolated multiple, structurally distinct forms of AR (3). The predominant ~16.5-kDa forms contained sialic acid-rich complex *N*-linked oligosaccharide, in addition to *O*-linked carbohydrate. However, a non-glycosylated ~9.5-kDa species was also isolated which contained an intact EGF-like core, but had a truncated NH_2-terminal extension. All of these forms bound strongly to heparin and were biologically active, demonstrating that the oligosaccharide moieties and the extreme NH_2-terminal region of AR are not essential to heparin-binding nor bioactivity (3). This previous work also suggested that the ability of AR to bind heparin may be related to its ability to activate the EGFR tyrosine kinase. In this report, we provide strong evidence that extracellular HS GAG is essential to AR-triggered mitogenic signaling by the EGFR.

EXPERIMENTAL PROCEDURES

Purification of AR—Human AR was purified to homogeneity from the conditioned medium of phorbol 12-myristate 13-acetate-treated MCF-7

* The costs of publication of this article were defrayed in part by the payment of page charges. This article must therefore be hereby marked "*advertisement*" in accordance with 18 U.S.C. Section 1734 solely to indicate this fact.

‡ To whom correspondence should be addressed: Division of Cytokine Biology, CBER, FDA, HFM-511, Bldg. 29A, 8800 Rockville Pike, Bethesda, MD 20892. Tel.: 301-496-9012; Fax: 301-402-1659.

[1] The abbreviations used are: AR, human amphiregulin; EGF, human epidermal growth factor; EGFR, epidermal growth factor receptor; FGF, fibroblast growth factor; HB-EGF, heparin-binding EGF-like growth factor; GAG, glycosaminoglycan; HS, heparan sulfate; TGF-α, transforming growth factor-α; PAGE, polyacrylamide gel electrophoresis; SDGF, schwannoma-derived growth factor.

human breast carcinoma cells by sequential heparin affinity, immunoaffinity, and reverse phase-high performance chromatography as described in Johnson *et al.* (3).

Preparation of AR Peptides—Peptides corresponding to residues 8–26 and 26–44 of AR were synthesized and purified as described previously (7). The peptide corresponding to residues 68–84 of AR was prepared as described in Johnson *et al.* (3).

Binding of AR to Immobilized Heparin—Twenty-five ng of AR and 5 µl of heparin cross-linked to agarose (~1 µg heparin/µl resin; Sigma) were added to 300 µl of 20 mM Hepes, 50 mM NaCl, pH 7.4 (buffer) in the absence or presence of 20 µg of AR peptide. The mixture was rotated end over end for 4 h at 4 °C and centrifuged, and the pellet was washed three times with 1 ml of buffer. The pellet was boiled for 5 min in 20 µl of SDS-polyacrylamide gel electrophoresis (PAGE) sample buffer. SDS-PAGE and Western blotting were performed as described in Johnson *et al.* (3).

Digestion of AR with N-Glycosidase F—One unit of *N*-glycosidase F (Boehringer Mannheim) was added to 100 ng of AR in 300 µl of 20 mM Hepes, 50 mM NaCl, pH 7.4, and incubated for 4 h at 37 °C.

Cell Culture and Mitogenesis Assay—MCF-10A human mammary epithelial cells were cultured and the mitogenesis assay was performed as described previously (3, 4). Briefly, 64 h after the addition of 250 pM AR or EGF (Life Technologies, Inc.), cells in 96-well plates were pulsed for 6 h with [^{3}H]thymidine (2 µCi/well; Amersham Corp.), DNA was harvested, and the incorporation of [^{3}H]thymidine into DNA was quantitated.

EGFR Autophosphorylation Assay—Ligand-induced autophosphorylation of tyrosine residues in the EGFR was measured as described in Johnson *et al.* (4). MCF-10A cells were plated into 100-mm dishes at a density of 785,000 cells per dish and after 2 days of growth were stimulated with 250 pM AR or EGF for 9 min at 37 °C. The EGFR was immunoprecipitated using E7 antiserum directed against the cytoplasmic domain of the human EGFR (40), fractionated in an 8% SDS-PAGE gel, and transferred to a polyvinyl difluoride membrane, and tyrosine-phosphorylated EGFR was detected using biotinylated PY-20 antibody (ICN Biomedicals), streptavidin-horseradish peroxidase conjugate, and enhanced chemiluminescence (Amersham).

Western Blotting Analysis of EGFR—Prior to immunoprecipitation of the EGFR in the autophosphorylation assay, aliquots of total cell crude lysates were taken to evaluate cellular EGFR levels. Proteins were fractionated in an 8% polyacrylamide SDS-PAGE gel and transferred to a polyvinyl difluoride membrane, and EGFR was detected using E7 antiserum (40), the Vectastain ABC Elite kit (Vector Laboratories), and enhanced chemiluminescence.

RESULTS

Residues 26–44 of AR Interact with Heparin—The binding of AR to immobilized heparin has greatly facilitated the purification of AR derived from the conditioned medium of human keratinocytes (2) and human breast carcinoma cells (3). To study the interaction of AR and heparin, a micro-assay was developed in which AR can be bound to a small quantity of heparin that has been cross-linked to agarose (5 µl). After washing the resin, bound AR can be released by boiling the resin in SDS-PAGE sample buffer. The AR is then fractionated in an SDS-PAGE gel and detected by Western blot analysis (Fig. 1). To identify heparin-binding regions in the AR molecule, various synthetic peptides which correspond to distinct regions of AR were tested for the ability to block the binding of AR to immobilized heparin. Peptides which correspond to residues 8–26 and 68–84 had no significant effect on the binding of AR to immobilized heparin (Fig. 1*A*). However, the peptide corresponding to residues 26–44 bound to heparin, as evidenced by the fact that when the Western blot was performed using antibodies directed against residues 26–44 it resulted in a very strong immunopositive streak running down that lane of the gel (Fig. 1*A*). To confirm that AR$^{26-44}$ bound to the same site on the heparin molecule as did AR and thus, could compete for the binding of AR to heparin, the experiment was repeated and AR was detected in the Western blot using an antibody directed against residues 8–26 of AR (AR-Ab3). Since there are two potential *N*-linked glycosylation sites within residues 8–26 of AR, it was necessary to first digest AR with *N*-glycosidase F so

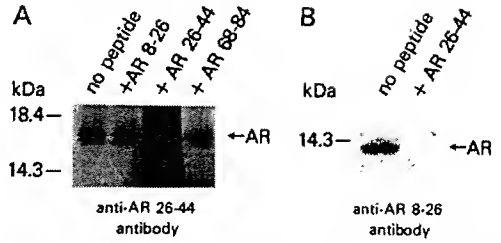

FIG. 1. **Effect of AR peptides on the binding of AR to immobilized heparin.** Twenty-five ng of AR were added to 5 µl of heparin-agarose (~5 µg of immobilized heparin) in 300 µl of 20 mM Hepes, 50 mM NaCl, pH 7.4 (buffer), in the absence or presence of 20 µg of peptide corresponding to residues 8–26 of AR (*AR 8–26*), 26–44 (*AR 26–44*), or 68–84 (*AR 68–84*). After incubation for 4 h at 4 °C, the resin was washed three times with 1 ml of buffer and boiled in SDS-PAGE sample buffer. The sample was fractionated by SDS-PAGE under reducing conditions in a 16% acrylamide gel and transferred to a nitrocellulose membrane. The positions and molecular mass of marker proteins are shown to the left in kilodaltons. In *A*, the nitrocellulose membrane was probed with AR-Ab2 antibodies directed against residues 26–44 of AR (3, 7). In *B*, AR was digested with *N*-glycosidase F prior to performing the heparin-binding assay and the Western blot was probed with AR-Ab3 antibodies directed against residues 8–26 of AR (3). The specificity of the antibodies used was confirmed by performing Western blot analyses using purified control preimmune antibodies (data not shown).

that these antipeptide antibodies could recognize the molecule in Western blot analysis (3). As shown in Fig. 1*B*, the AR$^{26-44}$ peptide completely blocked the binding of AR to heparin. These results demonstrate that residues 26–44 constitute a heparin-binding region in the AR molecule.

Effect of Soluble GAGs on AR-Induced Mitogenesis in Human Mammary Epithelial Cells—Various soluble GAGs were then tested for the ability to affect mitogenesis evoked by AR and EGF in MCF-10A human mammary epithelial cells. MCF-10A is an immortalized nontransformed cell line in which the action of AR is mediated solely by the EGFR tyrosine kinase (4). Previous work from our laboratory has demonstrated that in MCF-10A cells there is an excellent correlation between AR- and EGF-driven increases in cell number and increases in the incorporation of [^{3}H]thymidine into DNA (DNA synthesis) (3, 4). As shown in Fig. 2, both soluble heparin (*Panel A*) and HS (*Panel B*) inhibited mitogenesis induced by 250 pM AR with an IC_{50} of 5 and 2 µg/ml, respectively. However, even at very high concentrations of soluble heparin or HS (100 µg/ml) complete inhibition of AR action was not observed in MCF-10A cells (Fig. 2). Soluble chondroitin sulfate was found to have only a slight inhibitory effect on AR-induced DNA synthesis (Fig. 2*C*) and none of the three GAGs had any significant effect on mitogenesis triggered by EGF (Fig. 2, *A–C*). These results suggested that soluble HS/heparin compete with an extracellular HS-like GAG molecule for binding of AR and that the interaction between this extracellular HS-like molecule and AR is important to the eventual activation of the EGFR.

Chlorate Inhibits AR-triggered Mitogenesis and EGFR Autophosphorylation in MCF-10A Cells—To determine if HS GAG produced by MCF-10A cells is critical to AR-induced mitogenic signaling by the EGFR, two distinct approaches were used. First, cells were grown in the presence of chlorate to specifically interfere with the proper biosynthesis of the sulfated GAG chains. Chlorate is a competitive inhibitor of ATP sulfurylase action because it competes with the recognition of sulfate by the enzyme (41). Growth of cells in the presence of chlorate results in reduced sulfation of GAGs (33). MCF-10A cells which were cultured in 10 mM sodium chlorate lost the ability to respond to exogenous 250 pM AR (Fig. 3*A*). However, chlorate also had a slight inhibitory effect on mitogenesis induced by 250 pM EGF (Fig. 3*B*). To confirm that the inhibition of cell growth caused by chlorate is via the competitive inhibition of sulfation, 5 mM

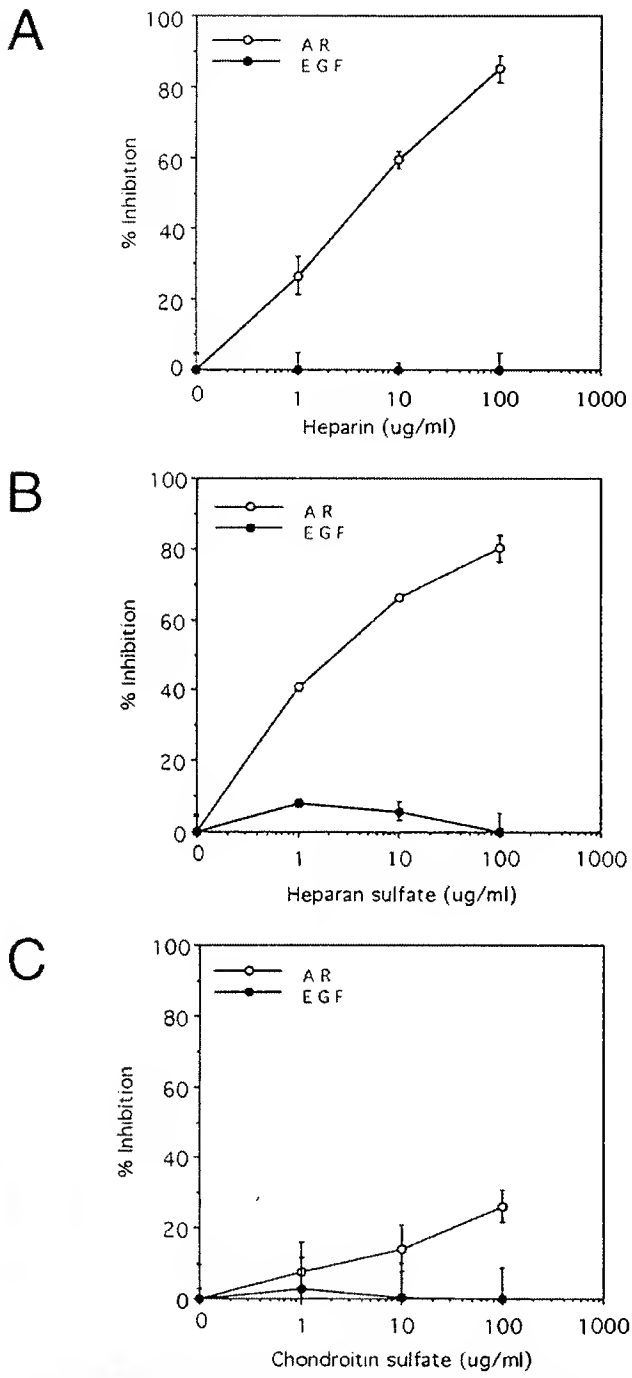

FIG. 2. **Effect of sulfated glycosaminoglycans on AR-induced mitogenesis in human mammary epithelial cells.** MCF-10A cells were cultured as described previously (4), plated into 96-well plates at a density of 2000 cells/well and a mitogenesis assay was performed (3) by adding 250 pM AR or EGF in the absence or presence of various concentrations of soluble heparin (*A*), heparan sulfate (*B*), or chondroitin sulfate (*C*) (Sigma). DNA synthesis was determined by quantifying the incorporation of [^{3}H]thymidine into DNA. Percent inhibition of DNA synthesis for each concentration of glycosaminoglycan was calculated relative to the level of DNA synthesis achieved in the presence of growth factor and the absence of the glycosaminoglycan. Data points represent the mean ± S.E. of experiments performed in triplicate. Values for incorporation of [^{3}H]thymidine into DNA in the absence of glycosaminoglycan for the control (no growth factor), AR and EGF treatment were 8,512, 49,975, and 56,840 cpm/well, respectively. Chondroitin sulfate is a mixture of chondroitin sulfate A and C (Sigma).

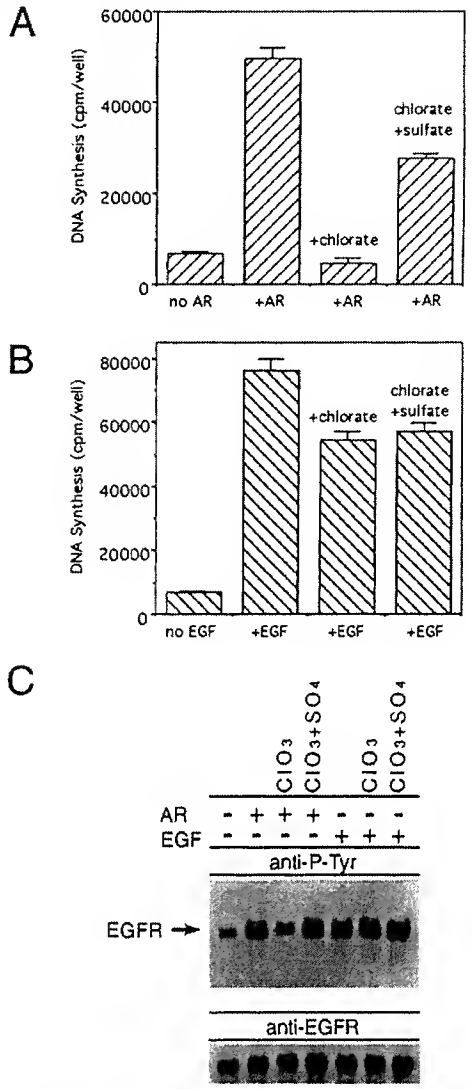

FIG. 3. **Inhibition by chlorate of AR-triggered mitogenic signaling by the EGFR.** MCF-10A cells were cultured for 3 days in medium (4) which lacked or contained 10 mM sodium chlorate (ClO_3^-) with or without an additional 5 mM sodium sulfate (SO_4^{2-}). The cells were trypsinized and plated in the appropriate medium into 96-well plates (2,000 cells/well) for the mitogenesis assay (*A* and *B*) (3) or plated into 100-mm dishes (785,000 cells/dish) for the EGFR autophosphorylation assay (*C*). Mitogenesis induced by 250 pM AR (*A*) or EGF (*B*) was measured by quantifying the incorporation of [^{3}H]thymidine into newly synthesized DNA (cpm/well) after a 64-h exposure to growth factor. Data points represent the mean ± S.E. of experiments performed in triplicate. The EGFR autophosphorylation assay (*C*) was performed as described previously (4). The cells were exposed to 250 pM AR or EGF for 9 min and lysed, and the EGFR was immunoprecipitated using E7 antiserum (40). The EGFR was fractionated in an 8% polyacrylamide SDS-PAGE gel, transferred to a polyvinyl difluoride membrane, and tyrosine-phosphorylated EGFR was detected using biotinylated PY-20 antibody, streptavidin-horseradish peroxidase conjugate, and enhanced chemiluminescence. The bottom of *Panel C* represents a Western blot analysis of an aliquot of total cell crude lysate from each experimental dish which was probed with the anti-EGFR E7 antiserum.

sodium sulfate was added to the medium in the presence of 10 mM chlorate. Sulfate partially rescued the response of the cells to AR (Fig. 3*A*), whereas sulfate had no significant effect on the minor inhibition that chlorate had on EGF-evoked mitogenesis (Fig. 3*B*). These results indicate that the response of the cells to AR is dependent upon normal cellular ATP sulfurylase function whereas, the response of the cells to EGF, as expected, is independent of ATP sulfurylase activity.

The Journal of Biological Chemistry

Mitogenic signaling by the EGFR is believed to occur by ligand-triggered dimerization and autophosphorylation of the EGFR by an intermolecular *trans*-mechanism (42). This activation of the EGFR via autophosphorylation on tyrosine residues results in access of the EGFR tyrosine kinase domain to cytosolic substrates and recruits signaling molecules with Src homology domains (SH2) which can specifically interact with tyrosine-phosphorylated regions of the EGFR. Activation of the EGFR via autophosphorylation appears to be a necessary phenomenon for AR-induced mitogenesis (4). Thus, we investigated the effect that chlorate had on the ability of AR to trigger autophosphorylation of the EGFR. Growth of the cells in 10 mM sodium chlorate significantly reduced the ability of 250 pM AR to drive autophosphorylation of tyrosine residues on the EGFR and the response of the EGFR to AR was completely rescued by 5 mM sodium sulfate (Fig. 3*C*). Neither chlorate nor chlorate plus sulfate had any significant effect on EGF-induced autophosphorylation of the EGFR (Fig. 3*C*). Western blot analysis of cell lysates with anti-EGFR antibodies demonstrated that the treatment of the cells with chlorate had no significant effect on EGFR levels in the MCF-10A cells (bottom of Fig. 3*C*). Therefore, in the case of AR, autophosphorylation of the EGFR and the resultant mitogenic signaling by the EGFR is dependent upon the proper biosyntheis of a sulfated molecule.

Treatment of Cells with Heparitinase or Heparinase Inhibits AR-induced Mitogenic Signaling by the EGFR—The second approach used to study the role that GAGs play in mitogenesis elicited by AR involved the utilization of enzymes which cleave GAG chains at specific sites. Chondroitinase ABC (EC 4.2.2.4) catalyzes the removal of dermatan sulfate and chondroitin sulfate side chains of proteoglycans (43) whereas heparitinase (EC 4.2.2.8) and heparinase (EC 4.2.2.7) cleave distinct sites within HS GAG chains (44). Exposure of MCF-10A cells to either heparitinase or heparinase almost completely blocked the ability of AR to drive mitogenesis, whereas chondroitinase ABC had no effect on this phenomenon (Fig. 4*A*). Heparitinase and heparinase inhibited the AR-stimulated growth of the cells by approximately 93 and 81%, respectively. Conversely, the stimulation of cell division elicited by EGF was not significantly affected by these GAG-degrading enzymes (Fig. 4*B*). Treatment of the cells with heparitinase or heparinase prior to the addition of exogenous AR dramatically inhibited activation of the EGFR as evidenced by the lack of AR-triggered autophosphorylation of tyrosine residues in the EGFR (Fig. 4*C*). In contrast, exposure of the cells to chondroitinase ABC had little or no effect on the response of the EGFR to AR (Fig. 4*C*). These enzymes did not significantly alter the ability of EGF to activate the EGFR nor did they affect EGFR levels in the MCF-10A cells (Fig. 4*C*, *bottom panel*). These results demonstrate that the sulfated GAG which is critical to AR-induced mitogenic signaling by the EGFR is structurally very similar to HS but does not appear to be related to dermatan or chondroitin sulfate.

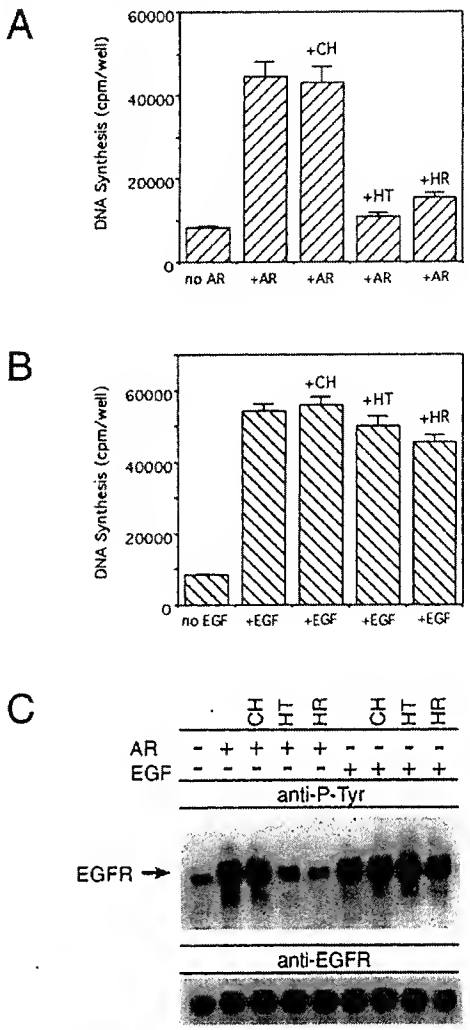

FIG. 4. **Inhibition of AR-induced EGFR mitogenic signaling by heparitinase and heparinase.** MCF-10A cells were plated into 96-well plates at a density of 2,000 cells/well and a mitogenesis assay was performed (3) by adding 250 pM AR (*A*) or EGF (*B*) in the absence or presence of 0.017 unit/ml of chondroitinase ABC (*CH*), heparitinase (*HT*), or heparinase (*HR*) (ICN Biomedicals). Every 12 h, 5 ml of medium with or without 0.0017 unit of the appropriate enzyme were added to each well. Mitogenesis was measured by quantifying the incorporation of [^{3}H]thymidine into newly synthesized DNA (counts/min/well) after a 64-h exposure to growth factor. Data points represent the mean ± S.E. of experiments performed in triplicate. The EGFR autophosphorylation assay (*C*) was performed exactly as described under "Experimental Procedures" except that, prior to exposure to 250 pM AR or EGF, glycosaminoglycan chains were digested by treating the cells for 1 h at 37 °C with 0.02 unit/ml of chondroitinase ABC (*CH*), heparitinase (*HT*), or heparinase (*HR*). The *bottom* of *Panel C* represents a Western blot analysis of an aliquot of total cell crude lysate from each experimental dish which was probed with the anti-EGFR E7 antiserum.

DISCUSSION

AR is a potent stimulator of proliferation in a number of different cell types including normal and malignant epithelial cells, fibroblasts and keratinocytes (1–7). Overexpression of AR has often been observed in human malignancies of the breast, colon, stomach and pancreas (7, 9–16) and in human colon carcinoma cells AR can function as an autocrine growth stimulator (7). However, AR is also expressed by epithelial cells in a number of normal human tissues including the mammary gland (7, 9–13). AR has been shown to act as an autocrine growth factor for normal human mammary epithelial cells (45, 46) and to function as an autocrine growth stimulator in MCF-10A cells when they are transformed by overexpression of activated *ras* or the EGFR-like tyrosine kinase *erb*B2 (47). The work which we have reported here demonstrates that extracellular HS GAG chains play a very important role in AR action in human mammary epithelial cells and are essential to the mitogenic activation of the EGFR which is evoked by AR.

It seems most probable that these HS chains exist on the surface of the cell where they can be covalently linked to an integral membrane protein as in the case of the syndecans (30, 31) or linked to cell surface lipid via glycosyl phosphatidylinositol (PI) as in the case of glypican (32, 48). Treatment of MCF-10A cells with phosphatidylinositol-specific phospholipase C had no effect on AR-induced mitogenesis suggesting that the

HS chains essential to AR functioning are not phosphatidylinositol-anchored.[2] It has been shown that a high affinity receptor for acidic FGF contains covalently attached HS (37). However, even though there are 4 potential GAG attachment sites in the extracellular domain of the EGFR (49) treatment of the cells with the GAG-degrading enzymes had no apparent effect on the migration of the EGFR under conditions of reducing SDS-PAGE (Fig. 4*C*, *bottom panel*). Thus, the HS chains which are critical to AR-triggered mitogenic signaling by the EGFR do not appear to be covalently linked to the EGFR itself, but may be attached to one or more syndecan-like proteoglycans.

On formalin-fixed A431 cells and immobilized plasma membrane preparations, AR is significantly less effective than EGF, at competing for the binding of ^{125}I-EGF to the EGFR (1). Conversely, AR is as potent as EGF in stimulating mitogenesis in MCF-10A cells (4, 47). One interpretation of these findings is that on living cells, HS chains stabilize a mitogenic signaling complex between AR and the EGFR. In the case of basic FGF, soluble heparin can substitute for the presence of the HS proteoglycan and can reconstitute the biological action of basic FGF in cells which lack the requisite HS proteoglycan (33–36). The addition of soluble heparin or heparan sulfate at concentrations ranging from 0.1 ng/ml to 10 μg/ml into the culture medium did not reconstitute the mitogenic response in chlorate-treated MCF-10A cells exposed to AR.[2] This strongly suggests that the HS chain(s) that are essential to AR-triggered activation of the EGFR need to be tethered to the cell surface.

Unlike EGF and transforming growth factor-α (TGF-α), but similar to HB-EGF, AR contains a very basic NH_2-terminal extension, relative to its EGF-like domain (1). The finding that a synthetic peptide corresponding to this region of AR (residues 26–44) binds to heparin-agarose and can compete for the binding of AR to heparin-agarose strongly suggests that this region of AR is at least partially involved in the interaction with HS which is required for AR-induced mitogenic signaling by the EGFR. Consistent with this observation is the fact that a homologous region in HB-EGF appears to be directly involved in the interaction between HB-EGF and heparin (50) and HS appears to be necessary for HB-EGF stimulation of smooth muscle migration (39). Therefore, it is plausible that mechanistically, HB-EGF may function in a manner similar to AR. Whether HS GAG is required for all the biological responses elicited by AR and HB-EGF remains to be seen.

Also contained within residues 26–44 of AR are two putative nuclear localization signals (1) and indeed, immunoreactive AR has been detected in the nucleus of cells *in vitro* and *in vivo* (6, 7, 9–13). The addition of exogenous ^{125}I-AR to several human carcinoma cell lines results in a preferential association of radiolabeled AR with nuclei, relative to radiolabeled EGF (51). Further, expression of SDGF (rat AR) lacking the secretory signal peptide results in nuclear accumulation of SDGF (52). It is possible that this very basic NH_2-terminal region of AR performs distinct functions depending upon whether AR is intracellular or extracellular. Lastly, the finding that an accessory molecule containing HS is needed for efficient AR action provides a mechanism by which AR may act in a more specific manner, relative to EGF and TGF-α. Since the EGFR is expressed on numerous different cell types *in vivo*, AR action, in contrast to that of EGF and TGF-α, may be specifically targeted to cells which co-express EGFR and the proper HS proteoglycan(s).

Acknowledgments—We thank Drs. William Gullick and Sally Prigent for generously supplying us with the AR$^{58-84}$ peptide and Dr. Pier Paolo Di Fiore for generously providing us with the E7 antiserum.

[2] G. R. Johnson, unpublished observations.

REFERENCES

1. Shoyab, M., Plowman, G. D., McDonald, V. L., Bradley, J. G., and Todaro, G J. (1989) *Science* **243**, 1074–1076
2. Cook, P. W., Mattox, P. A., Keeble, W. W., Pittelkow, M. R., Plowman, G. D., Shoyab, M., Adelman, J. P., and Shipley, G. D. (1991) *Mol. Cell. Biol.* **11**, 2547–2557
3. Johnson, G. R., Prigent, S. A., Gullick, W. J., and Stromberg, K. (1993) *J. Biol. Chem.* **268**, 18835–18843
4. Johnson, G. R., Kannan, B., Shoyab, M., and Stromberg, K. (1993) *J. Biol. Chem.* **268**, 2924–2931
5. Shoyab, M., McDonald, V. L., Bradley, J. G., and Todaro, G. J. (1988) *Proc. Natl. Acad. Sci. U. S. A.* **85**, 6528–6532
6. Johnson, G. R., Saeki, T., Auersperg, N., Gordon, A. W., Shoyab, M., Salomon, D. S., and Stromberg, K. (1991) *Biochem. Biophys. Res. Commun.* **180**, 481–488
7. Johnson, G. R., Saeki, T., Gordon, A. W., Shoyab, M., Salomon, D. S., and Stromberg, K. (1992) *J. Cell Biol.* **118**, 741–751
8. Plowman, G. D., Green, J. M., McDonald, V. L., Neubauer, M. G., Disteche, C. M., Todaro, G. J., and Shoyab, M. (1990) *Mol. Cell. Biol.* **10**, 1969–1981
9. Saeki, T., Stromberg, K., Qi, C.-F., Gullick, W. J., Tahara, E., Normanno, N., Ciardiello, F., Kenney, N., Johnson, G. R., and Salomon, D. S. (1992) *Cancer Res.* **52**, 3467–3473
10. Kitadai, Y., Yasui, W., Yokozaki, H., Kuniyasu, H., Ayhan, A., Haruma, K., Kajiyama, G., Johnson, G. R., and Tahara, E. (1993) *Jpn. J. Cancer Res.* **84**, 879–884
11. Saeki, T., Salomon, D. S., Normanno, N., Johnson, G. R., Gullick, W. J., Mandai, K., Moriwaki, S., Takashima, S., Kuniyasu, M., Tahara, E., Kawami, H., Niehiyama, M., and Toge, T. (1994) *Int. J. Oncol.* **5**, 215–223
12. Qi, C.-F., Liscia, D. S., Normanno, N., Merlo, G., Johnson, G. R., Gullick, W. J., Ciardiello, F., Saeki, T., Brandt, R., Kim, N., Kenney, N., and Salomon, D. S. (1994) *Br. J. Cancer* **69**, 903–910
13. Ebert, M., Yokoyama, M., Kobrin, M. S., Friese, H., Lopez, M. E., Buchler, M. W., Johnson, G. R., and Korc, M. (1994) *Cancer Res.* **54**, 3959–3962
14. Ciardiello, F., Kim, N., Saeki, T., Dono, R., Persico, M. G., Plowman, G. D., Garriques, J., Radke, S., Todaro, G. J., and Salomon, D. S. (1991) *Proc. Natl. Acad. Sci. U. S. A.* **88**, 7792–7796
15. Cook, P. W., Pittelkow, M. R., Keeble, W. W., Graves-Deal, R., Coffey, R. J., Jr., and Shipley, G. D. (1992) *Cancer Res.* **52**, 3224–3227
16. LeJeune, S., Leek, R., Horak, E., Plowman, G., Greenall, M., and Harrie, A. L. (1993) *Cancer Res.* **53**, 3597–3602
17. Kimura, H., Fischer, W. H., and Schubert, D. (1990) *Nature* **348**, 257–260
18. Higashiyama, S., Abraham, J. A., Miller, J., Fiddlee, J. C., and Klagebrun, M. (1991) *Science* **251**, 936–939
19. Shing, Y., Chrietofori, G., Hanahan, D., Ono, Y., Sasada, R., Igaraehi, K., and Folkman, J. (1993) *Science* **259**, 1604–1607
20. Holmes, W. E., Sliwkoweki, M. X., Akita, R. W., Henzel, W. J., Lee, J., Park, J. W., Yansura, D., Abadi, N., Raab, H., Lewie, G. D., Shepard, H. M., Kuang, W.-J., Wood, W. I., Goeddel, D. V., and Vandlen, R. L. (1992) *Science* **256**, 1205–1211
21. Wen, D., Peles, E., Cupples, R., Suggs, S. V., Bacus, S. S., Luo, Y., Trail, G., Hu, S., Silbiger, S. M., Levy, R. B., Koski, R. A., Lu, H. S., and Yarden, Y. (1992) *Cell* **69**, 559–572
22. Peles, E., Ben-Levy, R., Tzahar, E., Liu, N., Wen, D., and Yarden, Y. (1993) *EMBO J.* **12**, 961–971
23. Carraway, K. L., III, Sliwkoweki, M. X., Akita, R., Platko, J. V., Guy, P. M., Nuijens, A., Diamonti, A. J., Vandlen, R. L., Cantley, L. C., and Cerione, R. A. (1994) *J. Biol. Chem.* **269**, 14303–14306
24. Sliwkoweki, M. X., Schaefer, G., Akita, R. W., Lofgren, J. A., Fitzpatrick, V. D., Nuijens, A., Fendly, B. M., Cerione, R. A., Vandlen, R. L., and Carraway, K. L., III (1994) *J. Biol. Chem.* **269**, 14661–14665
25. Plowman, G. D., Green, J. M., Culouscou, J.-M., Carlton, G. W., Rothwell, V. M., and Buckley, S. (1993) *Nature* **366**, 473–475
26. Ruoslahti, E. (1989) *J. Biol. Chem.* **264**, 13369–13372
27. Ruoelahti, E., and Yamaguchi, Y. (1991) *Cell* **64**, 867–869
28. Jackson, R. L., Busch, S. J., and Cardin, A. D. (1991) *Physiol. Rev.* **71**, 481–539
29. Esko, J., Rostand, K. S., and Weinke, J. L. (1988) *Science* **241**, 1092–1096
30. Bernfield, M., Kokenyesi, R., Kato, M., Hinkee, M. T., Spring, J., Gallo, R. L., and Lose, E. J. (1992) *Annu. Rev. Cell Biol.* **8**, 365–393
31. Yanagishita, M., and Hascall, V. C. (1992) *J. Biol. Chem.* **267**, 9451–9454
32. David, G. (1993) *FASEB J.* **7**, 1023–1030
33. Rapraeger, A. C., Krufka, A., and Olwin, B. B. (1991) *Science* **252**, 1705–1708
34. Yayon, A., Klagsbrun, M., Eeko, J. D., Leder, P., and Ornitz, D. M. (1991) *Cell* **64**, 841–848
35. Klagebrun, M., and Baird, A. (1991) *Cell* **67**, 229–231
36. Kan, M., Wang, F., Xu, J., Crabb, J. W., Hou, J., McKeehan, W. L. (1993) *Science* **259**, 1918–1921
37. Sakaguchi, K., Yanagiehita, M., Takeuchi, Y., and Aurbach, G. D. (1991) *J. Biol. Chem.* **266**, 7270–7278
38. Gitay-Goren, H., Soker, S., Vlodaveky, I., and Neufeld, G. (1992) *J. Biol. Chem.* **267**, 6093–6098
39. Higashiyama, S., Abraham, J. A., and Klagsbrun, M. (1993) *J. Cell Biol.* **122**, 933–940
40. Di Fiore, P. P., Segatto, O., Lonardo, F., Faziola, F., Pierce, J. H., and Aaroneon, S. A. (1990) *Mol. Cell. Biol.* **10**, 2749–2756
41. Farley, J. R., Nakayama, G., Cryns, D., and Segel, I. H. (1978) *Arch. Biochem. Biophys.* **185**, 376–390
42. Ullrich, A., and Schlessinger, J. (1990) *Cell* **61**, 203–212
43. Oike, Y., Kimata, K., Shinomura, T., Nakazawa, K., and Suzuki, S. (1980) *Biochem. J.* **191**, 193–207
44. Ototani, N., Kikuchi, M., and Yoshizawa, Z. (1981) *Carbohydr. Res.* **88**, 291–303

45. Li, S., Plowman, G. D., Buckley, S. D., and Shipley, G. D. (1992) *J. Cell. Physiol.* **153**, 103–111
46. Kenney, N., Johnson, G., Selvam, M. P., Kim, N., Qi, C.-F., Saeki, T., Brandt, R., Wallace-Jones, B., Ciardiello, F., Shoyab, M., Plowman, G., Day, A., Selomon, D. S., and Normanno, N. (1993) *Mol. Cell Differ.* **1**, 163–184
47. Normanno, N., Selvam, M. P., Qi, C.-F., Saeki, T., Johnson, G., Kim, N., Ciardiello, F., Shoyab, M., Plowman, G., Brandt, R., Todaro, G., and Salomon, D. S. (1994) *Proc. Natl. Acad. Sci. U. S. A.* **91**, 2790–2794
48. Carey, D. J., and Stahl, R. C. (1990) *J. Cell Biol.* **111**, 2053–2062
49. Ullrich, A., Coussens, L., Hayflick, J. S., Dull, T. J., Gray, A., Tam, A. W., Lee, J., Yarden, Y., Libermann, T. A., Schlessinger, J., Downward, J., Mayes, E. L. V., Whittle, N., Waterfield, M. D., and Seeburg, P. H. (1984) *Nature* **309**, 418–425
50. Thompson, S. A., Higashiyama, S., Wood, K., Pollitt, N. S., Damm, D., McEnroe, G., Garrick, B., Ashton, N., Lau, K., Hancock, N., Klagsbrun, M., and Abraham, J. A. (1994) *J. Biol. Chem.* **269**, 2541–2549
51. Modrell, B., McDonald, V. L., and Shoyab, M. (1992) *Growth Factors* **7**, 305–314
52. Kimura, H. (1993) *Proc. Natl. Acad. Sci. U. S. A.* **90**, 2165–2169

DAS181, A Novel Sialidase Fusion Protein, Protects Mice from Lethal Avian Influenza H5N1 Virus Infection

Jessica A. Belser,[1,2,a] Xiuhua Lu,[1,a] Kristy J. Szretter,[1,2] Xiaoping Jin,[1] Laura M. Aschenbrenner,[3] Alice Lee,[3] Stephen Hawley,[3] Do Hyong Kim,[3] Michael P. Malakhov,[3] Mang Yu,[3] Fang Fang,[3] and Jacqueline M. Katz[1]

[1]Influenza Division, National Center for Immunization and Respiratory Diseases, Centers for Disease Control and Prevention, and [2]Emory University, Atlanta, Georgia; [3]NexBio, Inc., San Diego, California

Increasing resistance to currently available influenza antivirals highlights the need to develop alternate approaches for the prevention and/or treatment of influenza. DAS181 (Fludase), a novel sialidase fusion protein that enzymatically removes sialic acids on respiratory epithelium, exhibits potent antiviral activity against influenza A and B viruses. Here, we use a mouse model to evaluate the efficacy of DAS181 treatment against a highly pathogenic avian influenza H5N1 virus. When used to treat mice daily beginning 1 day before infection with A/Vietnam/1203/2004(H5N1) virus, DAS181 treatment at 1 mg/kg/day protected 100% of mice from fatal disease, prevented viral dissemination to the brain, and effectively blocked infection in 70% of mice. DAS181 at 1 mg/kg/day was also effective therapeutically, conferring enhanced survival of H5N1 virus–challenged mice when treatment was begun 72 h after infection. This notable antiviral activity underscores the potential utility of DAS181 as a new class of drug that is effective against influenza viruses with pandemic potential.

Since late 2003, highly pathogenic avian influenza (HPAI) H5N1 viruses have devastated poultry populations across Asia, Europe, and Africa and have caused >300 laboratory-confirmed human infections, with a fatality rate of ~60% [1]. These events highlight the potential for a pandemic strain, such as H5N1, to arise from avian species. In such an event, effective antiviral drugs will be an essential control measure, particularly in the first stages of a pandemic when antigenically well-matched vaccines are not yet available [2]. Currently licensed anti-influenza drugs consist of the adamantine M2 ion-channel blockers and the neuraminidase inhibitors, oseltamivir and zanamivir [3, 4]. Unfortunately, a majority of clade 1 and some clade 2 H5N1 viruses circulating in southeast Asia are resistant to the M2 blockers [5–8]. Isolation of quasispecies that include oseltamivir-resistant variants from H5N1 virus–infected patients has raised further concerns that existing antiviral modalities for H5N1 viruses are inadequate [9, 10] and emphasize the need to develop novel therapeutic agents that are effective against avian influenza viruses with pandemic potential [11].

Influenza viruses initiate infection by binding to terminal sialic acid receptors on glycoconjugates on the surface of susceptible host cells. Therefore, a drug with sialidase activity that can remove available receptors on human airway epithelium has the potential to prevent or reduce the infectivity of multiple influenza subtypes. DAS181 (Fludase) is a recombinant fusion protein consisting of a sialidase catalytic domain derived from *Acti-*

Received 24 April 2007; accepted 29 May 2007; electronically published 31 October 2007.

Potential conflicts of interest: L.M.A., A.L., S.H., D.H.K., M.P.M., M.Y., and F.F. declare that they have competing financial interests. J.M.K. received funding from NexBio, Inc., to cover the cost of this research. J.A.B., X.L., K.J.S., and X.J. declare that they have no potential conflicts.

Present in part: IX International Symposium on Respiratory Viral Infections, Hong Kong, March 2007 (abstract VII-3); Options for the Control of Influenza VI, Toronto, June 2007 (abstract 071).

Financial support: Oak Ridge Institute for Science and Education (support to J.A.B. and K.J.S.); National Institute of Allergy and Infectious Diseases, National Institutes of Health (grant RAI056786-03, grant U01AI070281-01, and contract HHSN266200600015C); Centers for Disease Control and Prevention.

The findings and conclusions in this report are those of the author(s) and do not necessarily represent the views of the Centers for Disease Control and Prevention.

[a] J.A.B. and X.L. contributed equally to this work.

Reprints or correspondence: Dr. Jacqueline M. Katz, Influenza Division MS G-16, 1600 Clifton Rd. NE, Atlanta, GA 30333 (JKatz@cdc.gov); or, Fang Fang, NexBio, Inc., 10665 Sorrento Valley Rd., San Diego, CA 92121 (ffang@nexbio.com).

The Journal of Infectious Diseases 2007; 196:1493–9

0022-1899/2007/19610-0012$15.00
DOI: 10.1086/522609

nomyces viscosus fused with a respiratory epithelium–anchoring domain that tethers the drug to the site of influenza virus infection in humans and cleaves both $\alpha(2,6)$-linked and $\alpha(2,3)$-linked sialic acid receptors, which are preferentially recognized by human and avian/equine influenza viruses, respectively [12]. DAS181 has exhibited potent antiviral activity against both influenza A and B viruses in vitro and has reduced replication of H1N1 viruses in mice and ferrets [12]. However, the in vivo activity of the drug against avian influenza viruses with pandemic potential is not known. Here, we demonstrate that DAS181 can effectively protect mice from lethal disease, significantly reduce virus replication, and even prevent infection with an HPAI H5N1 virus.

MATERIALS AND METHODS

Virus. The HPAI A/Vietnam/1203/2004(H5N1) virus (hereafter, VN/1203) was grown in the allantoic cavity of 10-day-old enbryonated hens' eggs at 37°C. Allantoic fluid was collected 26 h after inoculation and stored in aliquots at −70°C. The EID_{50} titer was determined by serial titration of virus in eggs and was calculated by the method of Reed and Muench [13]. All experiments with highly pathogenic viruses were conducted under biosafety level 3 containment, including enhancements required by the US Department of Agriculture and the Select Agent Program [14]. Laboratory workers wore appropriate respiratory equipment at all times (RACAL Health and Safety). Animal research was approved by the Centers for Disease Control and Prevention's Institutional Animal Care and Use Committee and was conducted in an Association for Assessment and Accreditation of Laboratory Animal Care International–accredited animal facility.

Infection of mice and challenge experiments. Six-to-eight-week-old female BALB/c mice (Charles River Laboratories) were lightly anesthetized with CO_2, and 50 μL of infectious virus diluted in PBS was inoculated intranasally (inl). The MLD_{50} of VN/1203 was determined as described elsewhere [15]. To evaluate the degree of drug efficacy, mice were challenged inl with 3 MLD_{50} ($1 \times 10^{2.3}$ EID_{50}) or 1.5 MLD_{50} ($1 \times 10^{2.0}$ EID_{50}) of VN/1203. Three to five mice per group were killed 6 or 9 days after infection. Lung and brain tissues were collected and titrated for virus as described elsewhere [15]. Briefly, whole lungs and brains were collected and homogenized in 1 mL of PBS, clarified by centrifugation, and serially titrated in eggs. Virus titers were expressed as the mean ± SE $\log_{10}$ EID_{50}/mL. The remaining 12–20 mice in each group were observed daily for weight loss and survival for 21 days.

Treatment of mice with DAS181. BALB/c mice were anesthetized by intraperitoneal injection with 100 mg/kg ketamine before treatment with DAS181 or placebo (sterile PBS); 10 U (8 μg) or 30 U (23 μg) of DAS181 or PBS was delivered inl to respiratory mucosa in a 50-μL volume once or twice daily for a total of 7 or 8 days. One unit of DAS181 is equivalent to 0.77 μg of protein. To evaluate the prophylactic and therapeutic efficacy of DAS181 against an HPAI H5N1 virus, mice were treated with DAS181 starting 24 h before or 24, 48, or 72 h after inl infection with VN/1203.

Serum collection and antibody assays. Serum samples were isolated from blood collected from the orbital plexus of mice and treated with receptor-destroying enzyme from *Vibrio cholerae* (Denka-Seiken) before testing for the presence of H5 hemagglutinin (HA)–specific antibodies [16]. The hemagglutination-inhibition (HI) assay was performed using 4 hemagglutinating units of VN/1203 and 1% horse red blood cells, as described elsewhere [17]. Serum samples with titers ≥40 (≥$\log_2$ 5.32), indicating a ≥4-fold increase in antibody compared with preinfection titers, were considered to be positive for H5 antibody. H5 HA–specific IgG antibody was detected by ELISA. The ELISA was performed as described elsewhere [18], except that 1 μg/mL of purified baculovirus-expressed H5 recombinant VN/1203 HA protein was used to coat plates (Protein Sciences). The ELISA end-point titers were expressed as the highest dilution that yielded an optical density >2 times the mean plus SD of similarly diluted negative control samples. A titer >100 was considered to be positive. Because the ELISA is generally more sensitive than the HI in the detection of influenza virus–sensitive antibody, a positive result by ELISA was considered to be evidence of productive H5N1 virus infection in mice; untreated and uninfected (naive) mice have HI antibody titers ≤10 and IgG titers <100.

Statistical analysis. Mean time-to-death values were calculated by the SAS life test; mice that survived the observation period were assigned a value 21 days for this life test. The survival function was calculated by the Kaplan-Meier method, and hazard ratios were established by the Cox proportional hazards regression model. The significance of survival in test groups versus the placebo group was determined by Fisher's exact test. The significance of weight loss in mice was determined by analysis of variance. The significance of viral titers was determined by a 2-tailed Student's *t* test; $P < .05$ was considered to indicate significance. All statistical analyses were performed with SAS for Windows software (version 9.1; SAS Institute).

RESULTS

Prophylactic efficacy of DAS181 against a highly virulent H5N1 virus in mice. A previous study determined that DAS181 at a dose range of 0.3 to 1 mg/kg/day was effective in inhibiting replication of a neurotropic H1N1 influenza virus in BALB/c mice [12]. To evaluate the prophylactic efficacy of DAS181 against a highly virulent H5N1 virus, BALB/c mice were treated inl with 1 mg/kg DAS181 once daily or 0.33 mg/kg DAS181 once or twice (0.66 mg/kg/day, or ~0.7 mg/kg/day) daily for 7 days beginning 1 day before challenge with 3 or 1.5

Table 1. Survival in mice prophylactically administered DAS181 and lethally challenged with A/Vietnam/1203/2004(H5N1) virus (VN/1203).

Total dose per day[a]	Mean weight loss on day 5 after infection, %	No. infected/total no. (%)[b]	No. of survivors/total no. (%)[c]	Time to death, mean ± SE, days[d]	Hazard ratio for death
3 MLD_{50} challenge					
1 mg/kg	0.0[e]	4/12 (33)	12/12 (100)[e]	>21.0 ± 0.0[e]	0.000[e]
0.7 mg/kg[f]	2.5[e]	14/16 (88)	11/16 (69)	9.4 ± 0.3[e]	0.096[e]
0.3 mg/kg	3.7[g]	13/15 (87)	6/15 (40)	10.7 ± 0.7[e]	0.203[e]
PBS	16.0	14/14 (100)	0/14 (0)	6.7 ± 0.3	1.000
1.5 MLD_{50} challenge					
1 mg/kg	0.0[e]	4/14 (29)	14/14 (100)[e]	>21.0 ± 0.0[e]	0.000[e]
0.7 mg/kg[f]	6.2[e]	13/16 (81)	15/16 (94)[g]	20.2 ± 1.1[e]	0.013[e]
0.3 mg/kg	2.3[e]	12/17 (71)	8/17 (47)	12.3 ± 0.6[e]	0.137[e]
PBS	16.2	16/16 (100)	0/16 (0)	7.3 ± 0.4	1.000

[a] Once- or twice-daily dosing of DAS181 or vehicle only (PBS) for 8 days commencing 24 h before virus challenge. Challenge was with 3 or 1.5 MLD_{50} of VN/1203; mice were challenged intranasally with VN/1203 after 2 or 3 treatments.

[b] No. of mice that became infected or that were positive for antibody to VN/1203 as detected by hemagglutination-inhibition assay or ELISA per the total no. of mice.

[c] No. of survivors per the total no. of mice; mice were monitored daily for survival and weight loss for 21 days after challenge.

[d] Mean day of death for all mice in each group; mice that survived the observation period (21 days) were given a value of 21.

[e] $P < .0001$, compared with the PBS control group.

[f] Mice received 0.3 mg/kg DAS181 twice daily.

[g] $P < .05$, compared with the PBS control group.

MLD_{50} of VN/1203. Mice were monitored daily for 21 days for weight loss and survival. Mice treated with DAS181 at 1 mg/kg/day and challenged with either virus dose were completely protected from death and effectively lost no weight ($P < .0005$), whereas 100% of mock–treated mice (PBS) died of infection, with a mean weight loss of 16% on day 5 after infection and a mean time to death of ~7 days (table 1 and figure 1*A* and 1*B*). Mice that received DAS181 at 0.3 or 0.7 mg/kg/day also exhibited a significant reduction in weight loss ($P < .05$) and enhanced survival, compared with mock-treated mice. In particular, at 0.7 mg/kg/day, DAS181 reduced mortality by 70% and 94% ($P < .05$) in mice challenged with 3 or 1.5 MLD_{50}, respectively.

To assess the effect of DAS181 treatment on H5N1 virus replication and systemic spread, we next determined viral titers in

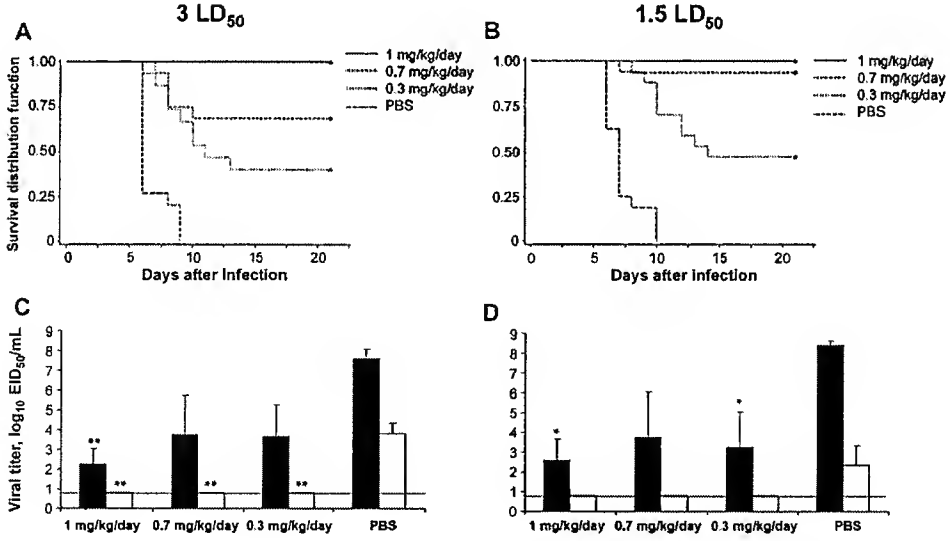

Figure 1. Prophylactic efficacy of DAS181 against a highly virulent H5N1 virus in mice. Mice were administered 1 mg/kg DAS181 once daily, 0.3 mg/kg DAS181 once or twice (0.7 mg/kg/day) daily, or PBS from 1 day before challenge to 6 days after infection. Mice were challenged with 3 or 1.5 MLD_{50} of A/Vietnam/1203/2004(H5N1) virus and monitored daily for survival (*A* and *B*). Mean ± SE virus titers in the lungs *(black bars)* and brains *(white bars)* of mice are shown on day 6 after infection (*C* and *D*). The limit of detection is $1 \times 10^{1.5}$ EID_{50}/mL for lungs and $1 \times 10^{0.8}$ EID_{50}/mL for brains *(horizontal line)*. $^*P < .05$ and $^{**}P < .005$, compared with PBS-treated mice (Student's *t* test).

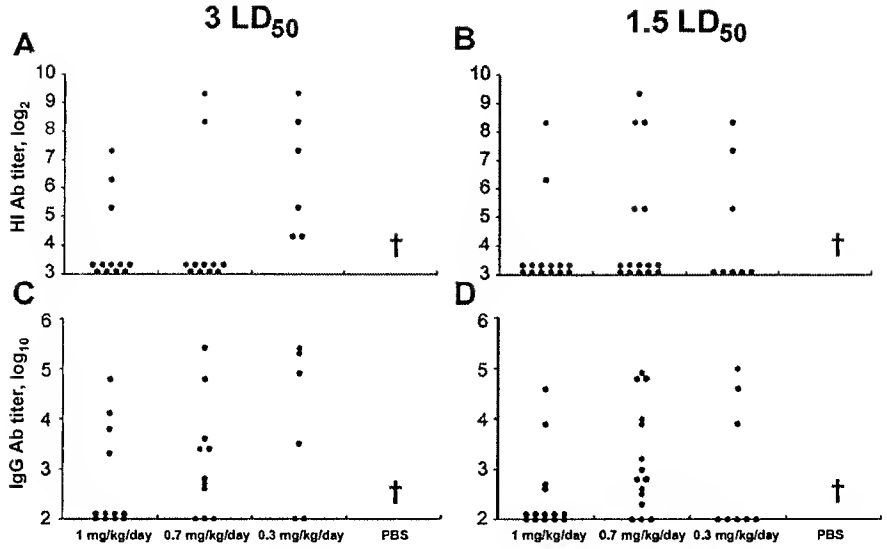

Figure 2. Hemagglutinin (HA)–specific hemagglutination-inhibition (HI) and IgG antibody (Ab) titers in serum from mice surviving challenge with a highly virulent H5N1 virus. Serum samples were collected from mice that were treated with DAS181 as indicated and that survived challenge with 3 or 1.5 MLD_{50} of A/Vietnam/1203/2004(H5N1) virus; samples were tested for the presence of HI Ab (*A* and *B*) and IgG Ab by ELISA (*C* and *D*). A positive result by ELISA was considered to be evidence for productive H5N1 infection in mice. The limit of detection for IgG Ab titer is 100. HI Ab titers ≥40 (log_2 5.32) reflect a 4-fold rise above that in preinfection serum and are considered to be positive. †Control mice treated with PBS did not survive to 4 weeks after infection.

the lungs and brains of mice 6 days after infection, when virus replication in these organs peaks in untreated mice [15, 19]. Treatment of mice with any dose of DAS181 reduced virus titers in the lungs by at least 10,000-fold, compared with those in mock-treated mice (figure 1*C* and 1*D*); similar results were observed with either challenge dose of VN/1203. Strikingly, virus was not detected in the brains of mice receiving DAS181 at any dose.

Blocking of influenza virus infection in mice after prophylactic administration of DAS181. To assess the extent to which mice administered DAS181 were actually infected with the H5N1 virus, we determined the levels of H5-specific HI or IgG antibody in serum samples collected from surviving mice (table 1 and figure 2). H5-specific antibody was detected in a majority of survivors that received DAS181 at 0.3 or 0.7 mg/kg/day but in only one-third of survivors that received DAS181 at 1 mg/kg/day, indicating that a majority of mice receiving this dose were not productively infected with VN/1203. This effect was seen at either challenge dose of VN/1203. These results demonstrate that daily inl delivery of DAS181 significantly reduced

Table 2. Survival in mice therapeutically administered DAS181 after lethal challenge with A/Vietnam/1203/2004(H5N1) virus (VN/1203).

Dose per treatment[a]	Dosing schedule[b]	Mean weight loss on day 5 after infection, %	No. of survivors/total no. (%)[c]	Time to death, mean ± SE, days[d]	Hazard ratio for death
1 mg/kg	24 h before	5.6[e]	19/20 (95)[e]	20.7 ± 0.4[e]	0.007[e]
1 mg/kg	24 h after	18.2	14/20 (70)[e]	11.4 ± 0.4[e]	0.046[e]
1 mg/kg	48 h after	17.1	7/20 (35)[f]	10.2 ± 0.4[e]	0.133[e]
1 mg/kg	72 h after	13.3	3/20 (15)	9.5 ± 0.3[e]	0.209[e]
PBS	24 h after	22.0	0/20 (0)	6.9 ± 0.3	1.000

[a] Once-daily dosing of DAS181 or vehicle only (PBS) for 8 days (24 h before) or 7 days. Challenge was with 3 MLD_{50} VN/1203.

[b] Dosing commenced 24 h before or 24, 48, or 72 h after virus challenge.

[c] No. of survivors per the total no. of mice; mice were monitored daily for survival and weight loss for 21 days after challenge.

[d] Mean day of death for all mice in each group; mice that survived the observation period (21 days) were given a value of 21.

[e] $P < .0001$, compared with the PBS control group.

[f] $P < .05$, compared with the PBS control group.

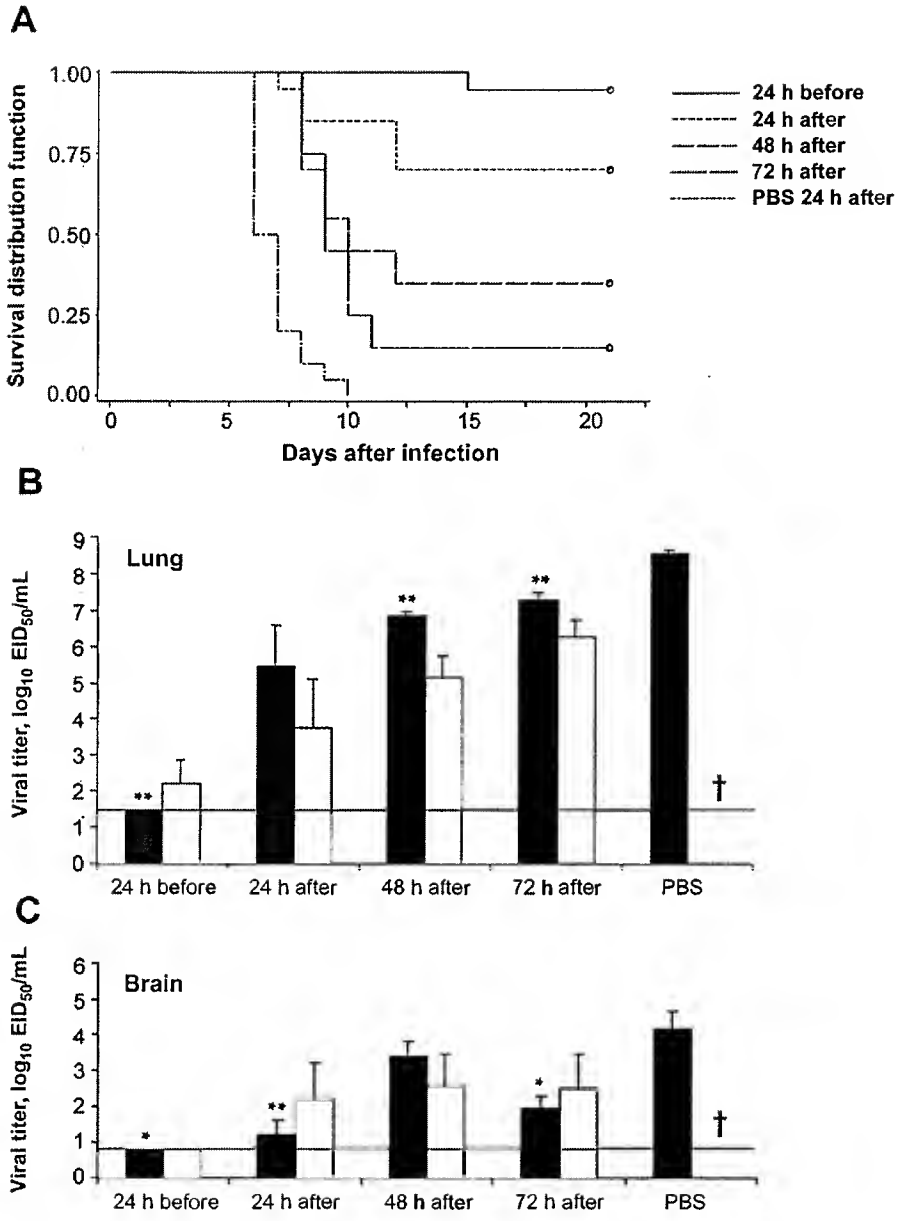

Figure 3. Therapeutic efficacy of DAS181 against a highly virulent H5N1 virus in mice. Mice were administered DAS181 at 1 mg/kg/day or PBS daily for 7–8 days as indicated. Mice were challenged with 3 MLD_{50} of A/Vietnam/1203/2004(H5N1) virus and monitored daily for survival *(A)*. Mean ± SE virus titers in lungs *(B)* or brains *(C)* of mice on day 6 *(black bars)* or day 9 *(white bars)* after infection are shown. The limit of detection *(horizontal line)* is $1 \times 10^{1.5}$ EID_{50}/mL for lungs and $1 \times 10^{0.8}$ EID_{50}/mL for brains. †Control mice treated with PBS did not survive to day 9. $^{*}P < .05$ and $^{**}P < .005$, compared with PBS-treated mice (Student's *t* test).

H5N1 virus replication and spread and, at a dose of 1 mg/kg/day, protected 100% of mice from death and a majority of mice from infection with a highly virulent H5N1 virus.

Therapeutic efficacy of DAS181 against a highly virulent H5N1 virus in mice. We next evaluated the therapeutic activity of inl DAS181 at 1 mg/kg/day when treatment was initiated 24, 48, or 72 h after challenge with 3 MLD_{50} of VN/1203. As a control for antiviral efficacy, one group of mice received drug at 1 mg/kg/day starting 24 h before challenge; this group exhibited a 95% survival rate, similar to that observed in the previous experiment. Therapeutic administration of DAS181 was unable to protect mice from infection with VN/1203, as demonstrated by substantial weight loss between groups that was not statistically significant regardless of the day treatment was initiated. When treatment was delayed until 24 h after infection, mice exhibited substantial weight loss but had a significantly delayed mean time to death compared with the mock-treated group ($P < .0001$), and, remarkably, 70% of treated mice survived the lethal chal-

lenge ($P < .0001$). Delaying treatment until 48 or 72 h after infection reduced overall survival to 35% and 15%, respectively (table 2 and figure 3*A*).

We next determined the effect of postchallenge treatment on viral titers on days 6 and 9 after infection, to establish whether viral load increased after cessation of treatment. When treatment was begun 1 day before challenge and completed on day 6 after infection, day 6 and 9 lung viral titers remained at least 5 logs lower than those detected in mock-treated mice; day 9 titers were not significantly higher than those detected on day 6 after infection (figure 3*B*). As expected, delaying treatment until after challenge resulted in substantially more virus replication in mouse lungs, but, nevertheless, titers were lower than those in mock-treated mice in all groups. Furthermore, in mice that began treatment 1 day after challenge and that ceased treatment on day 8 after infection, day 9 lung virus titers were dropping and not rebounding. Postchallenge treatment with DAS181 was unable to prevent virus spread to the brain (figure 3*C*); however, treatment started as late as 72 h after infection significantly reduced viral titers in the brain on day 6 after infection These results suggest that DAS181 treatment, even when initiated early after infection, was able to control virus replication until late in infection, providing time for adaptive immune responses to come into play.

DISCUSSION

High viral burden has been implicated as a critical feature of H5N1 virus pathogenesis in humans [20], suggesting that clinical management of human H5N1 disease should focus on suppression of virus replication through the use of effective antivirals. In the present study, we have demonstrated that the novel sialidase fusion protein DAS181 has dose-dependent antiviral activity in mice against a highly virulent H5N1 virus isolated from a human with a fatal case of influenza. When delivered before challenge at a dose of 1 mg/kg/day, DAS181 not only protected mice from lethal disease but completely blocked infection in ~70% of mice. DAS181 was also effective when administered after challenge. Most importantly, after a 7-day treatment regimen, there was no significant increase in viral titers after cessation of treatment.

The mouse model has been widely used to evaluate the efficacy of neuraminidase inhibitors against both human and avian influenza viruses [21–24]. The efficient replication and systemic spread of VN/1203 in the mouse without the need for prior adaptation made this an appropriate choice to evaluate the antiviral efficacy of DAS181 here. Yen et al. [25] demonstrated that an 8-day prophylactic oseltamivir regimen delivered twice daily was required for optimal survival of mice after infection with VN/1203, whereas a previous study found that a 5-day oseltamivir regimen was effective against a less virulent 1997 H5N1 strain [24]. At doses of 1 or 10 mg/kg oseltamivir, the 8-day regimen protected 60% and 80% of mice from death, respectively, with the higher dose required to prevent viral replication in the brain [25]. The present study, using a challenge dose of VN/1203 that elicited similar if not higher levels of virus replication than in the study by Yen et al. [25], found that 1 mg/kg DAS181 conferred complete survival by significantly reducing lung viral titers and preventing dissemination of H5N1 virus to the brain. Further assessment of these 2 antiviral strategies awaits a side-by-side comparison. Even so, the prophylactic prevention of infection and significant therapeutic antiviral activity demonstrated by DAS181 in the present study against a highly virulent H5N1 virus is unprecedented.

Whereas currently available influenza antiviral treatments target viral gene products, DAS181 targets host cellular receptors, which may offer a decreased opportunity for the emergence of resistance. Nevertheless, it will be important to evaluate carefully the potential for selection of receptor-binding variants after DAS181 treatment. The remarkable in vivo efficacy against a highly virulent avian H5N1 virus highlights the potential of DAS181 as an effective antiviral agent for both seasonal and pandemic influenza. A phase 1 clinical trial of DAS181 will begin in late 2007.

Acknowledgments

We thank Larisa Gubareva for critical review of the manuscript.

References

1. Cumulative number of confirmed human cases of avian influenza A/(H5N1) reported to WHO. Geneva: World Health Organization, 2007.
2. Stephenson I, Nicholson KG, Wood JM, Zambon MC, Katz JM. Confronting the avian influenza threat: vaccine development for a potential pandemic. Lancet Infect Dis 2004; 4:499–509.
3. Gubareva LV, Kaiser L, Hayden FG. Influenza virus neuraminidase inhibitors. Lancet 2000; 355:827–35.
4. Tominack RL, Hayden FG. Rimantadine hydrochloride and amantadine hydrochloride use in influenza A virus infections. Infect Dis Clin North Am 1987; 1:459–78.
5. Kandun IN, Wibisono H, Sedyaningsih ER, et al. Three Indonesian clusters of H5N1 virus infection in 2005. N Engl J Med 2006; 355:2186–94.
6. WHO. Avian influenza A (H5N1) infection in humans. N Engl J Med 2005; 353:1374–85.
7. Cheung CL, Rayner JM, Smith GJ, et al. Distribution of amantadine-resistant H5N1 avian influenza variants in Asia. J Infect Dis 2006; 193: 1626–9.
8. Evolution of H5N1 avian influenza viruses in Asia. Emerg Infect Dis 2005; 11:1515–21.
9. de Jong MD, Tran TT, Truong HK, et al. Oseltamivir resistance during treatment of influenza A (H5N1) infection. N Engl J Med 2005; 353: 2667–72.
10. Le QM, Kiso M, Someya K, et al. Avian flu: isolation of drug-resistant H5N1 virus. Nature 2005; 437:1108.
11. Moscona A. Oseltamivir resistance—disabling our influenza defenses. N Engl J Med 2005; 353:2633–6.
12. Malakhov MP, Aschenbrenner LM, Smee DF, et al. Sialidase fusion protein as a novel broad-spectrum inhibitor of influenza virus infection. Antimicrob Agents Chemother 2006; 50:1470–9.

13. Reed LJ, Muench HA. A simple method of estimating fifty per cent endpoints. Am J Hyg 1938; 27:493–7.
14. Richmond JY, McKinney RWM. Laboratory biosafety level criteria. In: Richmond JY, McKinney RW, eds. Biosafety in microbiological and biomedical laboratories. 4th ed. Atlanta: Centers for Disease Control and Prevention, 1999:17–52.
15. Lu X, Tumpey TM, Morken T, Zaki SR, Cox NJ, Katz JM. A mouse model for the evaluation of pathogenesis and immunity to influenza A (H5N1) viruses isolated from humans. J Virol 1999; 73:5903–11.
16. Kendal AP, Skehel JJ, Pereira MS. In: Smithwick RW, ed. Concepts and procedures for laboratory-based influenza surveillance. Atlanta: Centers for Disease Control, 1982:B17–35.
17. Stephenson I, Wood JM, Nicholson KG, Zambon MC. Sialic acid receptor specificity on erythrocytes affects detection of antibody to avian influenza haemagglutinin. J Med Virol 2003; 70:391–8.
18. Katz JM, Lu X, Young SA, Galphin JC. Adjuvant activity of the heat-labile enterotoxin from enterotoxigenic *Escherichia coli* for oral administration of inactivated influenza virus vaccine. J Infect Dis 1997; 175:352–63.
19. Maines TR, Lu XH, Erb SM, et al. Avian influenza (H5N1) viruses isolated from humans in Asia in 2004 exhibit increased virulence in mammals. J Virol 2005; 79:11788–800.
20. de Jong MD, Simmons CP, Thanh TT, et al. Fatal outcome of human influenza A (H5N1) is associated with high viral load and hypercytokinemia. Nat Med 2006; 12:1203–7.
21. Gubareva LV, McCullers JA, Bethell RC, Webster RG. Characterization of influenza A/HongKong/156/97 (H5N1) virus in a mouse model and protective effect of zanamivir on H5N1 infection in mice. J Infect Dis 1998; 178:1592–6.
22. Sidwell RW, Huffman JH, Barnard DL, et al. Inhibition of influenza virus infections in mice by GS4104, an orally effective influenza virus neuraminidase inhibitor. Antiviral Res 1998; 37:107–20.
23. Leneva IA, Roberts N, Govorkova EA, Goloubeva OG, Webster RG. The neuraminidase inhibitor GS4104 (oseltamivir phosphate) is efficacious against A/Hong Kong/156/97 (H5N1) and A/Hong Kong/1074/99 (H9N2) influenza viruses. Antiviral Res 2000; 48:101–15.
24. Govorkova EA, Leneva IA, Goloubeva OG, Bush K, Webster RG. Comparison of efficacies of RWJ-270201, zanamivir, and oseltamivir against H5N1, H9N2, and other avian influenza viruses. Antimicrob Agents Chemother 2001; 45:2723–32.
25. Yen HL, Monto AS, Webster RG, Govorkova EA. Virulence may determine the necessary duration and dosage of oseltamivir treatment for highly pathogenic A/Vietnam/1203/04 influenza virus in mice. J Infect Dis 2005; 192:665–72.

ANTIMICROBIAL AGENTS AND CHEMOTHERAPY, Apr. 2006, p. 1470–1479 Vol. 50, No. 4
0066-4804/06/$08.00+0 doi:10.1128/AAC.50.4.1470–1479.2006

Sialidase Fusion Protein as a Novel Broad-Spectrum Inhibitor of Influenza Virus Infection

Michael P. Malakhov,[1] Laura M. Aschenbrenner,[1] Donald F. Smee,[2] Miles K. Wandersee,[2] Robert W. Sidwell,[2] Larisa V. Gubareva,[3] Vasiliy P. Mishin,[3] Frederick G. Hayden,[3] Do Hyong Kim,[1] Alice Ing,[1] Erin R. Campbell,[1] Mang Yu,[1] and Fang Fang[1]*

NexBio, Inc., 6330 Nancy Ridge Dr., Suite 105, San Diego, California 92121[1]; Institute for Antiviral Research, Utah State University, Logan, Utah 84322[2]; and Division of Infectious Diseases and International Health, Department of Internal Medicine, University of Virginia, Charlottesville, Virginia 22908[3]

Received 9 November 2005/Returned for modification 13 January 2006/Accepted 1 February 2006

Influenza is a highly infectious disease characterized by recurrent annual epidemics and unpredictable major worldwide pandemics. Rapid spread of tbe bighly pathogenic avian H5N1 strain and escalating buman infections by the virus have set off the alarm for a global pandemic. To provide an urgently needed alternative treatment modality for influenza, we have generated a recombinant fusion protein composed of a sialidase catalytic domain derived from *Actinomyces viscosus* fused witb a cell surface-ancboring sequence. The sialidase fusion protein is to be applied topically as an inbalant to remove the influenza viral receptors, sialic acids, from the airway epithelium. We demonstrate that a sialidase fusion construct, DAS181, effectively cleaves sialic acid receptors used by both human and avian influenza viruses. Tbe treatment provides long-lasting effect and is nontoxic to the cells. DAS181 demonstrated potent antiviral and cell protective efficacies against a panel of laboratory strains and clinical isolates of IFV A and IFV B, with virus replication inhibition 50% effective concentrations in the range of 0.04 to 0.9 nM. Mouse and ferret studies confirmed significant in vivo efficacy of the sialidase fusion in both prophylactic and treatment modes.

Influenza, caused by infection with influenza virus A (IFV A) and IFV B, carries enormous direct and indirect socioeconomic impacts. Since 1997, a new avian IFV A virus of the H5N1 type has been causing epidemics in wild birds, as well as in domestic poultry. Alarmingly, human infections by this virus are also on the rise. Thus far, >100 people have been confirmed to be infected by the virus and >50 of them have died (5). Evidence has also shown that since 1999, the H5N1 virus has been evolving rapidly in ducks and has become increasingly pathogenic in both chicken and mice (7). All of these are serious warning signs that a pandemic may be imminent. No vaccine is currently available against the future pandemic virus. The neuraminidase inhibitor (NAI), oseltamivir, was linked to a surprisingly high frequency of drug-resistant viruses in children (26). Oseltamivir-resistant H5N1 virus has also been isolated from a patient who had been taking the drug as a prophylactic measure (27). For these reasons, it is imperative to develop alternative approaches to prevent and treat influenza.

The host cell receptors for influenza A and B viruses are cell surface sialic acids (20). The predominant type of sialic acids is *N*-acetylneuraminic acid (Neu5Ac), which is the biosynthetic precursor for most of the other types. In nature, Neu5Ac is mostly linked to the penultimate galactose residues of carbohydrate side chains via α(2,3)- or α(2,6)-linkages. Both Neu5Ac α(2,3)-Gal and Neu5Ac α(2,6)-Gal molecules can be recognized as a receptor by influenza viruses (44), but human viruses prefer α(2,6)-linked sialic acid, whereas avian and equine viruses predominantly recognize α(2,3)-linked sialic acid (20). The human respiratory epithelium expresses both forms of sialic acids, but α(2,6)-linked sialic acid is more abundant than α(2,3)-linked sialic acid (15, 29). This explains the fact that avian influenza viruses can infect humans, although the infection is very inefficient. The relatively low abundance of α(2,3)-linked sialic acid in human airway epithelium in large part causes the species barrier for avian viruses. This demonstrates that merely reducing the sialic acid level on the airway surface would have significant impact on IFV infectivity to humans.

To render the target cells inaccessible to influenza viruses, we generated a novel recombinant fusion protein consisting of a sialidase fused with a respiratory epithelium-anchoring domain. Sialidases, also referred to as neuraminidases, are a family of exoglycosidases that catalyze the removal of terminal sialic acid residues from various glycoconjugates, such as glycoproteins and glycolipids. Sialidases were previously demonstrated to be effective inhibitors of influenza virus infection in vitro. Even before sialic acid was proven to be the receptor for influenza viruses, it was observed that when sialic acid was enzymatically removed from the cell surface, the cells were less susceptible to infection by influenza viruses (12). In several experiments performed much later, MDCK (Madin-Darby canine kidney) or EAC (Ehrlich ascites carcinoma) cells were briefly treated with *Vibrio cholerae* sialidase and then infected with influenza virus. Influenza virus infections were decreased by 90 to 100% as a result of the sialidase treatment (6, 13, 52). *Micromonospora viridifaciens* sialidase was also used to destroy cellular influenza virus receptors in cell culture assays (2). In another case, influenza virus NA, which is also a sialidase, was expressed in CV-1 cells by vaccinia virus. The cells expressing

* Corresponding author. Mailing address: NexBio, Inc., 6330 Nancy Ridge Dr., Suite 105, San Diego, CA 92121. Phone: (858) 452-2631. Fax: (858) 452 0133. E-mail: ffang@nexbio.com.

the flu NA were resistant to subsequent influenza virus infections (9).

More than 15 sialidase proteins have been purified from microbes and higher eukaryotes. They vary greatly from one another in substrate specificity and enzyme kinetics. Among them, the large bacterial sialidases tend to be the more robust enzymes (1, 8, 11). Among the large bacterial sialidases, such as the ones from *Arthrobacter ureafaciens*, *Clostridium perfringens*, *V. cholerae*, and *Actinomyces viscosus*, the catalytic domain of *A. viscosus* sialidase was selected as the sialidase component of the novel therapeutic candidate for influenza based on three criteria: (i) *A. viscosus* sialidase has broad substrate specificity (54); (ii) it has one of the highest specific activities reported (54); and (iii) it should be well tolerated by the human immune system because *A. viscosus* is a part of the normal oral and gastrointestinal flora in humans (53) which normally exposes the human mucosal surface to the sialidase.

Because influenza viruses primarily infect the upper and central respiratory tract, the sialidase fusion protein will be delivered as an inhalant in humans. However, retention of drug molecules delivered to the respiratory mucosa is generally short due to the mucociliary clearance mechanisms. We reasoned that an epithelium-anchoring domain would tether the sialidase to the respiratory epithelium and increase its retention time and potency. We use the heparin-binding sequence derived from the human protein amphiregulin (AR) (46) as the epithelium-anchoring domain because of its high affinity to heparin and its ability to bind to the glycosaminoglycans (GAGs) present on the respiratory epithelial surface. Here we present data demonstrating potent protective effect of the novel sialidase fusion protein against a spectrum of influenza viruses both in vitro and in vivo.

MATERIALS AND METHODS

Cloning of the sialidase catalytic domain/amphiregulin GAG binding sequence fusion proteins. AvCD-AR (DAS181) consists of a heparin-binding domain derived from amphiregulin (amino acid residues 125 to 145 in GenBank entry AAH09799) fused via its N terminus to the catalytic domain of *A. viscosus* sialidase (AvCD, amino acid residues 274 to 667 in GenBank entry X62276) (59). The boundaries of catalytic domain were determined based on structural homology to enzymes of *M. viridifaciens* and *Salmonella enterica* serovar Typhimurium (PDB accession numbers 1EUR and 2SIM [www.rcsb.org/pdb]). A three-dimensional homology model was built by using the Swiss-Model software (www.expasy.org/swissmod). The DNA fragment coding for AvCD-AR was cloned into pTrc99a vector (Pharmacia) under the control of IPTG (isopropyl-β-D-thiogalactopyranoside)-inducible promoter. In another construct AR-AvCD (DAS178), the AR sequence was fused via its C terminus of the AvCD domain. Two control constructs, DAS180 and DAS185, were also made. To make DAS180, the AR sequence in DAS178 was deleted and a N-terminal His_6 tag was added. DAS185 differs from DAS181 in amino acid alteration (Y348F) at the sialidase reactive center that resulted in a >400 times reduction in sialidase activity (data not shown).

Protein expression, purification, and activity assay. The DAS181, DAS178, or DAS185 constructs were expressed in the BL21 strain of *Escherichia coli*. Cells were lysed by sonication in 50 mM phosphate buffer (pH 8.0), 0.3 M NaCl, and 10% glycerol. Clarified lysate was passed through an SP-Sepharose column. Proteins were eluted from the column with lysis buffer that contained 0.8 M NaCl. The fraction eluted from SP-Sepharose was adjusted to 1.9 M $(NH_4)_2SO_4$, clarified by centrifugation, and loaded onto a butyl-Sepharose column. The column was washed with 2 volumes of 1.3 M $(NH_4)_2SO_4$, and the fusion protein was eluted with 0.65 M $(NH_4)_2SO_4$. For the final step, size exclusion chromatography was performed on Sephacryl S-200 equilibrated with phosphate-buffered saline (PBS). Protein purity was assessed by sodium dodecyl sulfate-polyacrylamide gel electrophoresis, reversed-phase high-pressure liquid chromatography, and enzyme-linked immunosorbent assay with the antibodies generated against *E. coli* cell proteins and estimated to be >98% (not shown). For the purification of DAS180 (His_6-AvCD), cation exchange on SP-Sepharose was replaced with metal chelate affinity chromatography on nickel-charged chelating Sepharose (Amersham). All buffers remained the same, except that elution was performed with 0.25 M imidazole in lysis buffer.

Neu2 was expressed and purified as previously described (34). *C. perfringens* and *A. ureafaciens* sialidases were purchased from Sigma (St. Louis, MO) and Prozyme (San Leandro, CA), respectively.

The sialidase activity was measured by using the fluorogenic substrate 4-MU-NANA (4-methylumbelliferyl-*N*-acetyl-α-D-neuraminic acid; Sigma). One unit of sialidase is defined as the amount of enzyme that releases 10 nmol of MU from 4-MU-NANA in 10 min at 37°C (50 mM CH_3COOH-NaOH buffer [pH 5.5]) in a reaction that contains 20 nmol of MU-NANA in a 0.2-ml volume (38). The protein concentration was determined by using Bio-Rad's Bradford kit. The specific activity of AvCD-AR was 1,300 U/mg of protein (0.77 μg of DAS181 protein per unit of activity).

Cell surface sialic acid detection. Confluent monolayers of MDCK cells in 96-well plates were treated with 100 mU (0.1 ml total volume) of DAS181 or DAS180/well for 1 or 2 h at 37°C. The cells were then washed three times with PBS and either fixed immediately with 0.05% glutaraldehyde in PBS or chased for various times with growth media and then fixed. Levels of α(2,6)-linked sialic acid, α(2,3)-linked sialic acid, or total sialic acid were detected by using a cell-based enzyme-linked lectin assay (23) with minor modifications. The fixed cells were blocked with 3% bovine serum albumin (BSA) in PBS and streptavidin-biotin blocking reagent (Vector Laboratories, Burlingame, CA) to block endogenous streptavidin- and biotin-binding sites. Cells were rinsed once with PBS–0.1% Tween 20 (PBST) and incubated with either 2 μg of biotinylated SNA lectin (Vector Laboratories)/ml, 20 μg of biotinylated MAA lectin (Vector Laboratories)/ml, or 20 μg of biotinylated LFA lectin (EY Laboratories, San Mateo, CA)/ml for 2 h at 37°C. SNA (*Sambucus nigra*) is specific for Neu5Ac α(2,6)-Gal, MAA (*Maackia amurensis*) is specific for Neu5Ac α(2,3)-Gal, and LFA (*Limax flavus*) is specific for sialic acids. The cells were washed four times in PBST. Secondary detection of the bound lectin was accomplished by incubating the cells with 5 μg of streptavidin-HRP (streptavidin conjugated with horseradish peroxidase; Vector Laboratories)/ml for 1 h at 37°C. Cells were washed five times in PBST, developed in tetramethyl benzidine (TMB; Sigma), and stopped in 1 M H_2SO_4. The absorbance was measured at 450 nm, and the percentage of sialic acid remaining was calculated by using the following calculation: 100% × [(absorbance of treated cells − background)/(absorbance of vehicle-treated cells − background)]. Wells treated with streptavidin-HRP alone without the lectins were the background controls.

IFV binding to MDCK and fetuin-coated plates. A/PR/8/34 was biotinylated with EZ-link Sulfo-NHS-SS-Biotin (Pierce). 100 μl of fetuin (10 mg/ml) was adsorbed to a 96-well plate overnight and blocked with 3% BSA for 30 min at 37°C. Confluent MDCK monolayers in 96-well plates (5.75×10^5 cells per well) and the fetuin-coated plates were treated with either binding medium (Dulbecco modified Eagle medium–F-12 [DMEM:F12] plus 0.2% BSA) alone or 5 U of DAS181/ml in binding medium for 2 h at 37°C. After the incubation, the plates were washed two times with ice-cold PBS, and the plates were chilled further for 30 min at 4°C. The input virus was diluted in binding medium on ice, added to the appropriate wells, and incubated for 90 min at 4°C. Cells were washed three times with chilled PBS to remove unbound virus, fixed with 0.05% glutaraldehyde, incubated with streptavidin-HRP, and developed by using TMB. Wells without the virus were included for background streptavidin-HRP binding.

Cell protection assay. All laboratory IFV A and B strains were obtained from the American Type Culture Collection (Manassas, VA) with the exception of A/turkey/Wisconsin/66, A/PR/8/34, A/Japan/305/57, and A/Victoria/504/2000, which were from Charles River Laboratories. The low-passage 2004 IFV clinical virus isolates (A/New Caledonia/20/99, A/Panama/2007/99, and B/Hong Kong/330/01) were generously provided by Alexander Klimov, Centers for Disease Control and Prevention. The A/gull virus was obtained from Robert Webster, St. Jude Children's Research Hospital (Memphis, TN). For cell protection assays, quadruplicate MDCK cell monolayers in microplate wells were treated with various dilutions of DAS181 in EDB-BSA (10 mM sodium acetate [pH 6.0], 0.1 M NaCl, 10 mM $CaCl_2$, 0.5 mM $MgCl_2$, and 0.5% BSA) at 37°C for 2 h. Influenza viruses (multiplicity of infection [MOI] of 0.01) were added to both the sialidase-treated cells and the control cells treated with the enzyme dilution buffer only. After 1 h, the cells were washed with PBS three times and incubated at either 37 or 35°C in DMEM:F12 supplemented with 0.2% ITS (insulin-transferrin-selenium; Invitrogen, Carlsbad, CA) and 0.3 μg of acetylated trypsin (Sigma)/ml. After 72 h, the cells were stained with 0.5% crystal violet in 20% methanol for 5 min, rinsed with tap water, and dried. The level of viable cells in each well was quantitated by extracting crystal violet with 70% ethanol and reading the absor-

bance at 570 nm. The percentage of cell protection was calculated by using the following formula: 100 × [(sialidase-treated sample − virus only)/(uninfected sample − virus only)].

Viral replication inhibition assay. Quadruplicate MDCK monolayers in 96-well plates were treated with various dilutions of DAS181 in EDB-BSA buffer for 2 h at 37°C. Both the sialidase-treated cells and the untreated control cells (treated with only EDB-BSA buffer) were infected with a virus MOI of 0.01. After 30 min, the cells were washed two times with PBS and incubated at either 37 or 35°C in DMEM:F12 supplemented with 0.2% ITS and 0.3 μg of acetylated trypsin (Sigma, St. Louis, MO)/ml. At 40 to 48 h postinfection, the cells were fixed in 0.05% glutaraldehyde in PBS. They were then blocked in 3% BSA in PBS for 30 min at 37°C (or 4°C overnight). Cells were washed once with PBST. Each well was incubated with 50 μl of either 6.8 μg of anti-IFV A NP monoclonal antibody or 7.2 μg of anti-IFV B NP antibody (Fitzgerald Industries, Concord, MA)/ml for 2 h at 37°C. The excess primary antibody was washed away with four washes of PBST. Each well was then incubated with 50 μl of a 1:5,000 dilution of protein G conjugated to HRP (Sigma). Excess secondary reagent was removed by washing the plates five times with PBST. Plates were developed by incubating each well with 50 μl of TMB substrate (Sigma) and were stopped by the addition of 50 μl of 1 M H_2SO_4. The absorbance was measured at 450 nm. Wells containing uninfected cells were used as the background control.

Mouse studies. The experiments were conducted according to the protocol approved by the Animal Care and Use Committee and conducted at the Laboratory of Animal Research Center at Utah State University, which is accredited by the Association for the Assessment and Accreditation of Laboratory Animal Care, International (AAALAC). Female BALB/c mice (18 to 21 g) were obtained from Charles River Laboratories (Wilmington, MA) and were maintained on Wayne Lab Blox and tap water ad libitum. The animals were quarantined for 24 h prior to use. Influenza virus A/NWS/33 (H1N1) was originally obtained from Kenneth Cochran of the University of Michigan (Ann Arbor, MI). It was passaged in MDCK cells and pretitrated in mice prior to use in the experiments. Arterial oxygen saturation (SaO_2) was determined by using the Ohmeda Biox 3800 pulse oximeter (Ohmeda, Louisville, OH). The ear probe attachment was used, and the probe was placed on the thigh of the animal. Readings were made after a 30-s stabilization time for each animal. Use of an earlier Ohmeda model (model 3740) for measuring effects of influenza virus on SaO_2 in mice has been previously described (48). To determine lung virus titer, each mouse lung was homogenized, and various dilutions were assayed in triplicate for infectious virus in MDCK cells as described previously (47). Each lung homogenate was centrifuged at 2,000 × g for 5 min, and the supernatants were used in these assays. Increases in the numbers of total survivors were evaluated by chi-square analysis with Yates' correction. Increases in the mean day to death, differences in mean SaO_2 values, the mean lung weight, and mean virus titers were analyzed by using a two-tailed *t* test.

In all three studies, mice were anesthetized by intraperitoneal injection of ketamine (100 mg/kg) prior to treatment with DAS181 or placebo and prior to virus inoculation. DAS181 or placebo was given intranasally in a 50-μl volume at each treatment using various regimens as described above. Infection was induced by intranasal inoculation of A/NWS/33 at a 100% lethal dose (LD_{100}) (i.e., 200 PFU per mouse). The infectious dose was based on previous titration results. Apparently, the virus used in the second study was less virulent than expected. The virus was then retitrated, and the newly determined LD_{100} was used in the third study. Generally, 22 mice were used in each treatment group, and 40 were used in the placebo group. Ten mice in each infected, treated group (20 mice in the placebo group) were observed for 21 days for survival; 3 additional mice from each group were sacrificed on days 1, 3, 6, and 9 for assignment of lung score and for the determination of lung weight and lung virus titer. At each time point, three normal control mice were also sacrificed to provide background data.

Ferret study design and methods. The experiment was conducted according to the protocol approved by the Animal Care and Use Committee and conducted at the Center for Comparative Medicine at the University of Virginia, which is accredited by the AAALAC.

Young female ferrets (0.5 to 0.8 kg) (Marshall Farms, North Rose, NY) were allowed to acclimate for 3 days before the experiment. A preparation of DAS178 dissolved in PBS that contains 500 U/ml in sialidase activity was used in the study. Animals in the AR-AvCD treatment groups received 1 ml of AR-AvCD solution at each dose. Ferrets were anesthetized (20 mg of ketamine/1 mg of xylazine per kg, given intramuscularly) and inoculated intranasally (0.5 ml into each nostril) with DAS178 or PBS twice daily (8 a.m. and 6 p.m.) for a total of 7 days (2 days prior to the viral challenge and 5 days after virus inoculation). The ferrets were observed after the drug application for signs of intolerance. Viral inoculation was carried out on day 3 between 10 and 11 a.m. The viral challenge was carried out using human A/Bayern/7/95(H1N1)-like virus at a 50% tissue culture infective dose of 10^5 (50% inhibitory concentration of $\geq 10^4$ in ferrets). The nasal washes were collected from all animals starting day 2 after DAS178 treatment and continued until day 7.

To collect nasal washes, 1 ml of sterile PBS was administered intranasally, the sneezed liquid was harvested, and its volume was recorded. The nasal washes were centrifuged. The pelleted cells were resuspended and counted in a hemacytometer under a microscope. The supernatants were collected, divided into aliquots, and stored at −80°C. The protein concentration in cell-free nasal washes was determined with a protein reagent from Bio-Rad (Hercules, CA). For virus titration of the nasal washes, inoculated MDCK cells were incubated for 3 days at 36°C in a CO_2 incubator. The monolayers were inspected visually for cytopathic effect, and aliquots of the cell culture supernatants from each well were tested for the presence of virus by a standard hemagglutination assay using guinea pig red blood cells. The virus titer was determined by the Spearman-Karber method (18).

FIG. 1. Molecular model of DAS181. The catalytic domain of the sialidase (AvCD) is colored in green and the protruding anchoring domain (AR) on C terminus in blue. The model was built using the SWISS-MODEL software.

RESULTS

Construction, purification, and characterization of DAS181. After many experiments, we chose the *A. viscosus* sialidase catalytic domain and the GAG-binding sequence in human AR as the two basic components of the therapeutic candidates. Most of the data presented here were obtained with the AvCD-AR construct, referred to as DAS181, in which the AR sequence is fused with AvCD at the C terminus (Fig. 1). DAS181 is expressed in *E. coli* and purified to homogeneity. The purified DAS181 protein has an approximate molecular mass of 44,800 Da. The specific activity of DAS181 (1300 U/mg) is more than 100 times higher than that of the human sialidase Neu2 fusion protein (8 U/mg) (34) and more than two times higher than that of *C. perfringens* (333 U/mg) or *A. ureafaciens* (82 U/ml). DAS181 is soluble at concentrations of >50 mg/ml and in 2 M ammonium sulfate. It remains stable at pH 4.5 to 10. No loss of activity for DAS181 was detected after 8 months at 25 or 4°C. DAS181 was incubated with human respiratory mucus at 37°C for 7 days and maintained full activity (data not shown).

DAS181 effectively removes both α(2,3)- and α(2,6)-linked

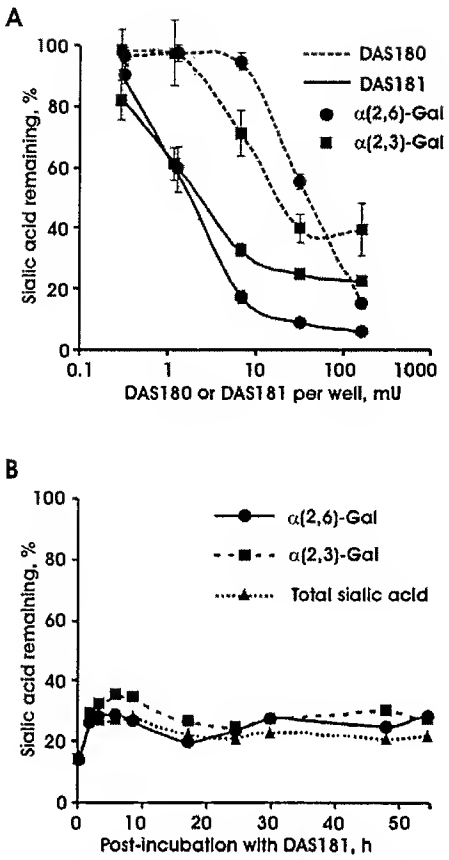

FIG. 2. Sialic acid removal and turnover on MDCK cells. (A) Levels of α(2,6)- and α(2,3)-linked sialic acids and sialic acids in total on the surface of MDCK cells that were pretreated with vehicle (EDB-BSA) or various dilutions of DAS180 (His_6-AvCD) or DAS181 (AvCD-AR) in the vehicle for 1 h. (B) Level of cell surface sialic acid after a single treatment by DAS181. MDCK cells in confluent monolayers were treated with 100 mU of DAS181 for 2 h, washed, and chased for various times with fetal bovine serum-containing medium. The levels of sialic acids were detected with biotinylated lectins. The error bars indicate one standard deviation above or below the mean of three samples.

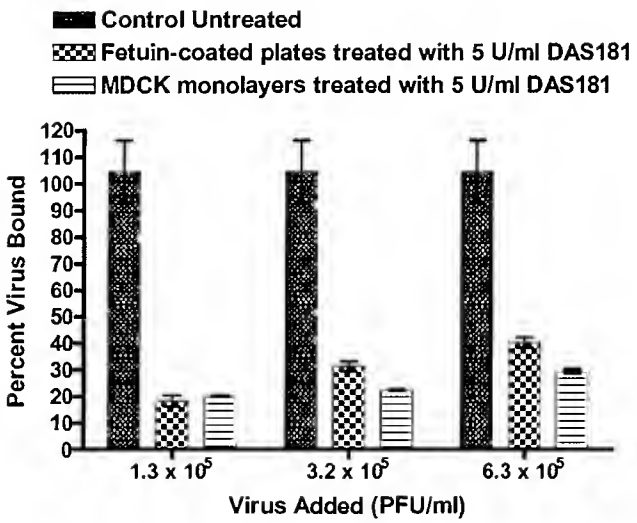

FIG. 3. IFV binding to MDCK and fetuin-coated plates. Biotinylated A/PR/8/34 was allowed to bind to the DAS181-treated fetuin or MDCK monolayers for 30 min at 4°C. The bound virus was detected by using streptavidin-HRP and developed by using TMB. Virus binding to the untreated MDCK cells represented 100%. Wells without the virus were included for background streptavidin-HRP binding. The error bars indicate one standard deviation above or below the mean of three samples.

sialic acid from the cell surface (Fig. 2). As measured by the 50% effective concentration (EC_{50}) for sialic acid removal, DAS181 was more than 10 times more effective than its counterpart (DAS180, His_6-AvCD) that lacks the AR tag (Fig. 2A), demonstrating that the AR tag increases the potency of the sialidase. In MDCK cells, the cell surface sialic acid level remains low and essentially unchanged for at least 2 days after a single treatment by DAS181 (Fig. 2B); the surface sialic acid level in the DAS181 treated MDCK cells rebounded to more than 80% of the normal level after 80 h (data not shown).

Antiviral activity of DAS181 in vitro. Consistent with the proposed mechanism of action for the sialidase fusion protein, the binding of A/PR/8 (H1N1) to DAS181-treated MDCK cells and fetuin (a sialylated protein isolated from fetal bovine serum)-coated wells was greatly diminished (Fig. 3). The extent of binding inhibition correlates very well with the degree of sialic acid removal (data not shown).

DAS181 anti-IFV activity was evaluated in vitro by viral inhibition and cell protection assays in MDCK cells. DAS181 demonstrated potent efficacy against a panel of laboratory strains and recent clinical isolates of influenza A and B viruses in cell protection and/or virus inhibition assays (Tables 1 and 2). These data were further confirmed, with similar EC_{50} values between 1.7 and 13.7 nM, by an experiment performed at a separate facility with four additional IFV strains (A/New Caledonia/20/99 [H1N1], A/Panama/2007/99 [H3N2], A/gull/PA/4175/83 [H5N1], and B/Hong Kong/330/01). DAS181 maintained similar levels of potency even when the IFV infectious dose was increased by 100 times or higher (Table 3). In support of the slow turnover rate of cell surface sialic acid, treatment of cells 24 h prior to the viral challenge protected the cells to the same degree as treating the cells immediately before the challenge (not shown). The anti-IFV activity of DAS181 was also compared to both DAS180 and DAS185, an inactive mutant of DAS181. Based on the cell protection EC_{50}, DAS181 was 5- to 30-fold more potent than DAS180 (data not shown), which again demonstrated that the AR sequence increases treatment potency of the sialidase. As expected, DAS185 provided no protection against IFV (not shown).

The cell protection by DAS181 was further evaluated under various experimental protocols that differed in the following aspects: incubation time with DAS181, washing steps, order of addition of the virus, and whether DAS181 was incubated with cells during the entire course of the infection (Table 4). Variation of the infection protocols altered the EC_{50} values to various degrees. Protocol P1 represents our standard cell protection and inhibition of viral replication assay condition. The three protocols that yielded the lowest EC_{50} values—P3, P4, and P6—represent conventional assay conditions for testing antiviral chemical compounds in which the drug candidate was available throughout the infection. Noticeably, in situations

TABLE 1. Inhibition of IFV replication and cell protection by DAS181[a]

Virus	Mean inhibition of viral replication ± SD		Mean cell protection ± SD	
	EC_{50} (nM)	EC_{90} (nM)	EC_{50} (nM)	EC_{90} (nM)
A/PR/8/34 (H1N1)	0.8 ± 0.9‡	3.2 ± 4.7‡	1.1 ± 0.6*	12.9 ± 9.7†
A/WS/33 (H1N1)	0.4 ± 0.6*	1.1 ± 1.4*	0.2 ± 0.1*	32.7 ± 11.1*
A/NWS/33 (H1N1)	ND	ND	0.4 ± 0.3‡	11.5 ± 19.6*
A/Weiss/43 (H1N1)	0.9 ± 1.6‡	1.7 ± 1.8‡	15.6 ± 16.9§	37.0 ± 40.0*
A/Denver/1/57 (H1N1)	0.5 ± 0.6‡	7.0 ± 12.3*	3.2 ± 4.3§	14.5 ± 14.9*
A/Japan/305/57 (H2N2)	0.3 ± 0.3*	4.7 ± 0.4*	0.1 ± 0.1*	0.2 ± 0.2‡
A/Victoria/504/2000 (H3N2)	0.4 ± 0.6*	4.7 ± 1.9*	1.9 ± 1.9‡	6.5 ± 86.8†
A/Hong Kong/8/68 (H3N2)	0.1 ± 0.1‡	4.4 ± 1.9¶	14.3 ± 23.1§	50.4 ± 37.6†
A/Port Chalmers/1/73 (H3N2)	0.05 ± 0.02†	0.4 ± 0.2‡	2.4 ± 3.2‡	17.7 ± 14.0†
A/Victoria/3/75 (H3N2)	0.1 ± 0.1‡	2.2 ± 4.3¶	2.6 ± 4.2‖	5.1 ± 5.2‡
B/Lee/40	0.3 ± 0.2¶	0.8 ± 0.4§	0.4 ± 0.5*	3.1 ± 4.0*
B/Maryland/1/59	0.04 ± 0.01†	0.7 ± 0.3*	0.5 ± 0.2†	9.8 ± 13.6¶
A/turkey/Wis/66 (H9N2)	0.4 ± 0.1‡	0.8 ± 0.4*	0.1 ± 0.1¶	3.7 ± 4.0*
A/equine/Prague/1/56 (H7N7)	ND	ND	0.2 ± 0.2†	2.8 ± 3.2*

[a] The EC_{50} (or EC_{90}) is the concentration of DAS181 that inhibited viral replication by 50% (or 90%) or that gave rise to 50% (or 90%) cell protection. A value of 1 nM DAS181 equals 45 ng/ml of the protein. Experiments were repeated at least three times, and the actual number of repetitions is indicated as follows: †, 3; *, 4; ‡, 5; ¶, 6; §, 7; and ‖, 8). The error is the standard deviation of these measurements. ND, not determined.

where DAS181 was removed during the remainder of the infection time (P1, P2, and P5), cells were still protected from IFV infection despite higher EC_{50} values. Interestingly, under the similar experimental conditions, oseltamivir was inactive (50).

At the maximum feasible concentration (1,000 U/ml), DAS181 did not affect cell growth curves over a period of 10 days for A549, CACO-2, and MDCK cells (data not shown). In the HAE (human airway epithelium) cultures (49, 60), which closely mimic the native human airway epithelium, DAS181 treatment did not cause cell death, nor did it result in significant changes in the production of gamma interferon, interleukin-1α (IL-1α), IL-1β, IL-2, IL-6, IL-8, IL-10, IL-12p70, and tumor necrosis factor alpha over a 7-day incubation period during which fresh DAS181 was added daily (data not shown). These data indicated that DAS181 treatment would not be cytotoxic to the human airway epithelium.

Prevention and treatment of influenza in vivo. We used a murine model of influenza virus infection (47) to assess the antiviral activity of DAS181 in vivo. Study 1 (see Table 5) demonstrated striking efficacy of DAS181 on the survival of the infected animals when given as a prophylaxis over a very broad dose range. The DAS181 treatment also significantly improved lung function and lung pathology, as measured by lung weight, and markedly inhibited the virus titer in the lungs of infected animals (Fig. 4). Arterial blood oxygen saturation levels were also significantly improved in DAS181-treated mice (not shown). Ribavirin, included as a positive control, also inhibited this virus infection, although not to the extent evoked by DAS181.

To evaluate therapeutic potential of DAS181 as a treatment for influenza, the fusion protein was applied at different time points relative to infection in the second mouse study. Treatments up to 48 h after virus exposure significantly prevented the death of the mice; all treatment regimens significantly reduced lung disease parameters (Table 5). A more stringent test of efficacy was conducted in the following study. Mice infected with IFV were treated by DAS181 once every other day beginning 48 h after virus exposure at dosages of 25 and 5 U/treatment. Significant protection by AvCD-AR was seen at 25 U/treatment.

We also tested the in vivo anti-IFV effect of the sialidase fusion protein in a ferret model which is thought to closely mimic human influenza (31, 42, 51). This experiment was performed with an earlier version of the fusion (DAS178, AR-AvCD). DAS178 differs from DAS181 in the location of AR tag (which caused lower yields in *E. coli*) but was otherwise indistinguishable in cell protection assays. In the vehicle-treated ferrets, virus shedding reached peak values on day 1 or 2 postchallenge, diminished over time, and became negative by

TABLE 2. Cell protection by DAS181 against recent clinical IFV isolates

Virus	Mean cell protection ± SD[a]	
	EC_{50} (nM)	EC_{90} (nM)
A/Singapore/35/2004 (H3N2)	0.6 ± 1.0*	4.5 ± 5.5†
A/Canada/600/2004 (H3N2)	0.1 ± 0.1‡	0.9 ± 0.7‡
A/Texas/05/2004 (H3N2)	0.2 ± 0.2‡	1.9 ± 2.3§
A/Hong Kong/2637/2004 (H1N1)	0.2 ± 0.7‖	26.5 ± 32.4‡
A/Hong Kong/2765/2004 (H1N1)	1.2 ± 1.3*	51.6 ± 69.5¶
B/Peru/1960/2004	0.2 ± 0.1†	0.5 ± 0.2†

[a] *, Six determinations; †, three determinations; ‡, five determinations; §, eight determinations; ‖, four determinations.

TABLE 3. Cell protection by DAS181 against IFV at various MOIs

Virus	EC_{50} (nM)[a] at MOI:			
	0.001	0.01	0.1	1
A/PR/8/34 (H1N1)	0.4	1.5	1.5	2.4*
A/Japan/305/57 (H2N2)	<0.1	<0.1	<0.1	5.9
A/Port Chalmers/1/73 (H3N2)	0.1	0.2	0.3	1.6
B/Maryland/1/59	<0.1	0.6	1.4*	ND
A/turkey/Wis/66 (H9N2)	<0.1	0.3	1.9	39.6
A/equine/1/56 (H7N7)	<0.1	0.3	0.4	5

[a] EC_{50} values were extrapolated from the cell protection assay dose-response curves as described in Materials and Methods, except that the MOI varied from 0.001 to 1. Each EC_{50} was measured in two independent experiments unless otherwise indicated. ND, not determined. *, Single experiment.

TABLE 4. Cell protection efficacy of DAS181 against A/PR/8/34 using various experimental protocols

EC_{50} (nM)[a]	Protocol	Description
1.7	P1	DAS181 for 2 h, add virus for 1 h, wash twice with PBS, add fresh medium, and incubate
2.7	P2	DAS181 for 2 h, add virus for 1 h, aspirate, add fresh medium, and incubate
0.1	P3	DAS181 for 2 h, add virus, and incubate
0.2	P4	DAS181 and immediately add virus and incubate
8.6	P5	Add virus for 1 h, add DAS181 for 2 h, aspirate, add fresh medium, and incubate
0.1	P6	Add virus for 1 h, add DAS181, and incubate

[a] EC_{50} values were extrapolated from cell protection assay dose response curves as described in Materials and Methods.

day 5 (Table 6). In contrast, in the group treated with the sialidase fusion protein, only 3 of 12 ferrets shed virus on day 1 postchallenge, and their nasal virus titers were about 100 times lower than those in the vehicle-treated animals. Three animals were completely protected against infection, signs of illness, and inflammatory response, as confirmed by a lack of seroconversion on day 14 postchallenge. The shedding in the remaining eight ferrets varied during the course of infection. However, in these animals, signs of inflammation in the nasal washes was reduced by about 40% (Fig. 5). It was also noticed that the 7-day treatment of DAS178 at 1,000 U/day (>1 mg/kg/day) did not cause any signs of toxicity or inflammation in ferrets that were not infected by the virus (Fig. 5).

DISCUSSION

The results of in vitro and in vivo studies have demonstrated the ability of a sialidase catalytic domain/AR GAG-binding sequence fusion protein to significantly inhibit the replication of IFVs, prevent influenza, or significantly reduce severity of the disease. By targeting the host cells rather than the virus, the sialidase fusion protein demonstrated distinct anti-IFV properties from the virus-targeting NAIs. In the MDCK cells, the state of cell surface desialylation sustained for at least 2 days after a single DAS181 treatment. Consistent with its long-lasting treatment effect, the subnanomolar EC_{50} of DAS181 was observed under an experimental condition in which the drug candidate was removed from the culture medium after the initial virus challenge (Table 1). In addition, DAS181 potency remained undiminished even when the cell treatment was performed 24 h prior to the virus challenge (not shown). This is in contrast to the NAIs: the EC_{50} of oseltamivir in-

TABLE 5. Intranasally administered DAS181 protected mice a from lethal dose of influenza A/NWS/33 (H1N1) virus

Study and compound, dosage/treatment[a]	Dosing time start[b]	Surv/total[c]	Mean day to death ± SD[d]	Mean day 11 % SaO_2 ± SD	Mean lung virus titer (log_{10}/g)	Mean day 6 lung wt (mg)
Study 1						
AvCD-AR, 60 U/treat	48 h pre	10/10***[g]	>21.0 ± 0.0***	87.2 ± 6.6***	1.7***[d]	130***
AvCD-AR, 30 U/treat	48 h pre	10/10***	>21.0 ± 0.0***	89.2 ± 4.3***	1.5***[d]	–[e]
AvCD-AR, 3 U/treat	48 h pre	6/6***	>21.0 ± 0.0***	85.2 ± 6.3***	3.0**[d]	205
AvCD-AR, 0.3 U/treat	48 h pre	7/7***	>21.0 ± 0.0***	84.6 ± 6.2***	2.6***[d]	120***
AvCD-AR, 0.03 U/treat	48 h pre	3/5**	13.0 ± 2.8**	82.6 ± 5.6***	5.4**[d]	190**
Ribavirin, 75 mg/kg	4 h pre	4/10**	9.8 ± 3.0	77.2 ± 3.2**	5.45**[d]	155***
Vehicle	48 h pre	0/19	8.9 ± 1.4	75.0 ± 0.0	6.75[d]	325
Normal control	48 h pre	–	–	91.0 ± 3.6	0.0[d]	115
Study 2						
AvCD-AR, 30 U/treat	48 h pre	11/11*	>21.0 ± 0.0***	89.2 ± 6.0**	1.8***[A]	126***
AvCD-AR, 30 U/treat	24 h pre	11/11*	>21.0 ± 0.0***	85.1 ± 4.9	2.0***[B]	154**
AvCD-AR, 30 U/treat	4 h post	11/11*	>21.0 ± 0.0***	91.0 ± 5.1***	1.8***[C]	158**
AvCD-AR, 30 U/treat	12 h post	11/11*	>21.0 ± 0.0***	87.7 ± 4.3**	1.45***[C]	174**
AvCD-AR, 30 U/treat	24 h post	11/11*	>21.0 ± 0.0***	85.7 ± 6.7	1.2***[C]	158**
AvCD-AR, 30 U/treat	48 h post	11/11*	>21.0 ± 0.0***	85.1 ± 6.1	1.0***[C]	198*
AvCD-AR, 30 U/treat	72 h post	9/11	9.0 ± 1.4	79.4 ± 3.1	2.0**[C]	210*
Ribavirin, 75 mg/kg	4 h pre	8/10	15.0 ± 0.8*	86.7 ± 7.1*	4.4[C]	164**
Vehicle	48 h post	12/21	9.6 ± 3.0	80.5 ± 6.3	4.4[C]	295
Normal control	–	–	–	90.0 ± 6.1	0.0[C]	118
Study 3						
AvCD-AR, 25 U/treat	48 h post	6/10**	8.8 ± 1.0***	81.3 ± 7.4**	5.4[D]	200*
AvCD-AR, 5 U/treat	48 h post	0/8	9.3 ± 1.2***	75.0 ± 0.0	5.6[D]	262
Ribavirin, 75 mg/kg	4 h pre	10/10***	>21.0 ± 0.0***	87.6 ± 5.2***	4.7**[f]	106***
Vehicle	–	0/18	7.2 ± 0.6	75.0 ± 0.0	6.2[f]	307
Normal control	–	–	–	90.4 ± 3.6	0.0[f]	115

[a] Study 1, twice-daily dosing for 7 days (14 doses total); study 2, once-daily dosing for 5 days (5 doses total); study 3, every-other-day dosing (3 doses total). treat, treatment.

[b] That is, before (pre) or after (post) viral challenge.

[c] Surv/total, number of survivors/total number of animals tested.

[d] Measurements were obtained on day 3 when the virus titer in the placebo group reached its peak.

[e] –, Insufficient numbers after day 3 due to anesthesia-related deaths.

[f] Superscripts A, B, and C: measurements taken on day 3 (A), 6 (B), or 9 (C) after viral challenge to reflect the treatment schedule. Superscript D: measurement taken on day 6 after viral challenge.

[g] *, $P < 0.05$; **, $P < 0.01$; ***, $P < 0.001$ (compared to vehicle [saline-treated controls]).

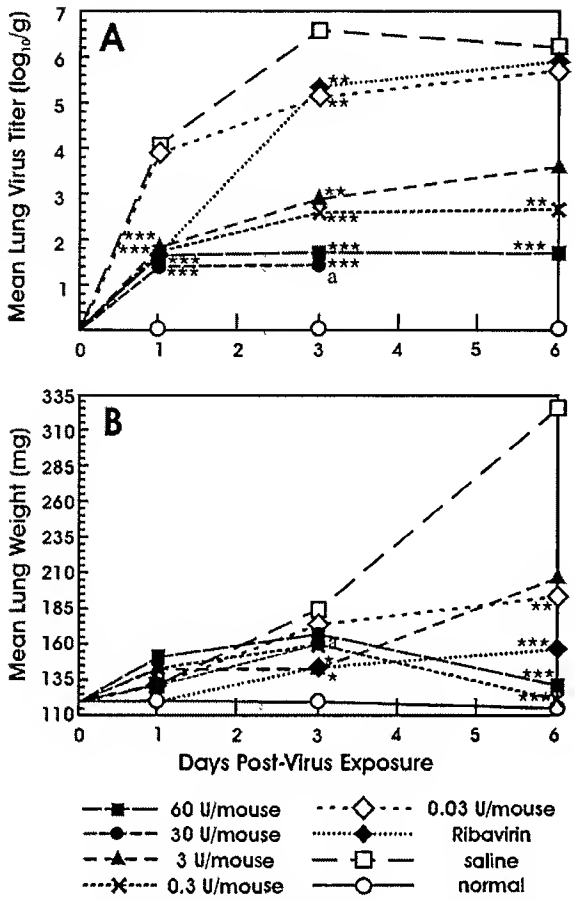

FIG. 4. Effects of DAS181 on lung virus titer (A) and lung weight (B) in infected mice. The results are part of experiment 1 in Table 5. The data at each time point were derived from three mice. Statistically significant values are labeled with one ($P < 0.05$), two ($P < 0.01$), or three ($P < 0.001$) asterisks. Ribavirin was used at 75 mg/kg.

creased 5,000 times (from 20 nM to 100 μM) when the compound was removed immediately prior to the virus infection (50). The efficacy of many antiviral compounds is influenced by the infectious dose of the virus; they are often more effective in cell culture at low MOIs and less active (or inactive) at higher virus-to-cell ratios. For the NAIs, such as oseltamivir and RWJ-270201, over the range of MOI 0.0002 to 0.02, every fivefold increase in MOI raised the EC_{50} of both compounds by 7 to 10 times (from 10 nM at an MOI of 0.0002 to >10 μM at an MOI of 0.02) (50). In contrast, DAS181 maintained a similar level of efficacy when the infectious dose was increased from an MOI of 0.001 to an MOI of 0.1 (Table 3).

Consistent with a previous report (52), 70 to 80% of the surface sialic acid was removed by DAS181 treatment (Fig. 2). Stray et al. reported that viral binding could occur in MDCK cells that were rid of about 70% of the cell surface sialic acid (52); however, in the sialidase-treated cells, multicycle amplification of IFVs was inhibited by 99 to 99.99% (52). Therefore, although enzymatic desialylation does not result in complete elimination of sialic acid, the viral infection that arises from residual sialic acid on the cell surface is negligible. Our own results fully corroborate the data of Stray et al. and demonstrate that it is unnecessary to completely eliminate cell surface sialic acid in order to achieve a desired therapeutic effect. In fact, further analysis of our in vitro results revealed that 50 to 70% cell surface sialic acid removal afforded >90% cell protection against all of the influenza viruses tested.

It was reported that cell surface sialic acids were primarily derived from glycoproteins (93%), and resialylation of the cell surface was mostly contingent upon de novo protein synthesis (41), even though at early time points a low level of sialic acid on the cell surface came from preexisting internal pools (41). Our observation on the surface sialic acid turnover after DAS181 treatment was consistent with this notion. A small but rapid rise in sialic acid level immediately after DAS181 treatment was most likely due to exchange with the internal pools of sialylated proteins (Fig. 2B). A slower return of sialic acid to the cell surface after the brief initial period probably reflected the rate of de novo protein synthesis that over time led to replenishment of sialylated proteins on the cell surface. The sialic acid turnover rate in the normal human respiratory epithelium is not known, but it is reasonable to expect that the sialic acid turnover is much slower in the normal respiratory epithelium than in the MDCK cells due to the lower cell

TABLE 6. Virus replication in the respiratory tract of DAS178 and vehicle-treated ferrets

Group and animal no.	Ferret tag no.	Virus titer (log_{10} $TCID_{50}$/ml) on day p.i.[a]: 1	2	3	4	5	Post challenge HI titers[c]
Vehicle-treated group							
1	228	5.7	4.2	4.2	1.7	–	640
2	784	3.9	4.9	1.9	1.9	–	640
3	793	4.4	4.2	2.4	3.9	–	640
4	794	4.9	5.9	1.4	–	–	160
5	789	4.4	4.2	3.4	3.4	–	640
6	799	3.7	4.4	3.4	–	–	320
7	811	4.4	4.4	–	–	–	1280
8	841	4.2	4.7	2.7	1.9	–	320
Mean[b]		4.4	4.7	2.7	3.7	–	
SD		0.4	0.7	1	0.4	–	
No. shed/total no.		8/8	8/8	7/8	5/8	0/8	
AR-AvCD-treated group							
1	780	–	–	–	NA	NA	NA
2	791	2.2	5.2	4.9	4.2	1.7	640
3	804	–	4.7	3.7	1.7	–	1280
4	803	–	–	–	–	–	≤01
5	805	–	–	–	–	–	≤01
6	806	–	–	–	–	–	≤01
7	810	2.2	4.7	3.2	2.9	–	160
8	812	–	–	4.4	–	–	640
9	813	–	3.2	4.4	4.7	–	160
10	819	2.7	5.2	–	–	–	320
11	828	–	4.9	1.9	1.7	–	320
12	843	–	4.4	4.9	4.9	3.4	320
Mean[b]		2.4	4.6	3.9	3.4	2.6	
SD		0.3	0.7	1.1	1.5	1.2	
No. shed/total no.		3/12	7/12	7/12	6/11	2/11	

[a] –, All nasal washes collected after day 5 postchallenge were negative for virus. Nasal washes recovered from the uninfected treated ferrets were negative for virus (not shown). NA, not applicable (the ferret died on day 4 postinfection due to an accident).

[b] That is, the mean value calculated for the ferrets that shed virus.

[c] HI, hemagglutination inhibition.

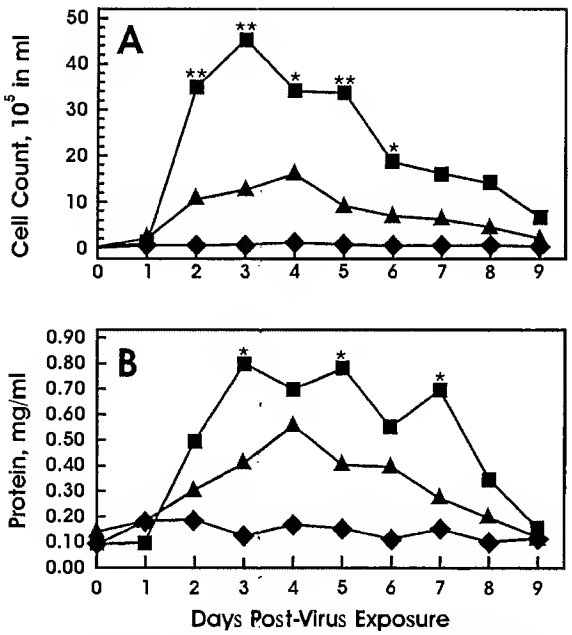

FIG. 5. Total inflammatory cell counts (A) and protein concentrations (B) in nasal washes from ferrets. Infected ferrets were vehicle treated (■) or were treated with DAS178 (▲). Uninfected animals were treated with DAS178 (◆) only. Statistically significant values are labeled with one ($P < 0.05$) or two ($P < 0.01$) asterisks. No that only the DAS178-treated ferrets that showed positive virus shedding were included in the analysis.

proliferation rate and slower protein synthesis in the differentiated epithelium. As a result, the treatment effect of DAS181 may last much longer than 2 days in the normal human airway as seen in the MDCK cells. Preliminary data with the HAE cultures indicated that desialylation by a single DAS181 treatment would last for more than 7 days in the respiratory epithelium (unpublished results). In spite of this reasoning, it should also be noted that faster sialic acid turnover may occur in the inflamed epithelia during influenza. Therefore, for influenza prophylaxis, infrequent dosing of DAS181 will likely be sufficient, whereas a relatively more frequent dosing regimen may be required for the treatment of an ongoing infection. It is, nevertheless, encouraging that once-every-other-day dosing of DAS181 resulted in significant therapeutic effects in mice even when the treatment was initiated at 48 h after virus infection (Table 5).

Generally, mice can only be infected by IFV strains that are previously adapted in mice, but ferrets can be infected with human unadapted influenza viruses and produce signs of upper respiratory tract diseases comparable to those seen in humans. Thus, ferrets are commonly used to evaluate influenza drug candidates (31, 42, 51). The lethal mouse model used in the present study represents influenza infection in the most severe form, whereas the self-limiting infection seen in the ferret model may mimic the more commonly encountered, milder form of influenza. Together, the two models cover a broad spectrum of influenza clinical manifestations. The ferret study reported here, however, was not optimal for evaluating the sialidase fusion protein candidate. To obtain full treatment effects, the sialidase fusion protein should evenly cover the surface of the upper and central respiratory tract, but this cannot be consistently achieved by the delivery method of nasal drops in larger animals such as ferrets. In spite of this, the sialidase fusion candidate still completely protected three animals as confirmed by negative seroconversion and significantly decreased the disease severity in the remaining eight ferrets. The animals also appeared to be more alert and active compared to the untreated ferrets that were invariably lethargic and feverish. Additional studies are being planned in which DAS181 will be formulated and delivered as dry powder inhalant, which is the designated delivery method in humans.

The sialic acids are negatively charged monosaccharides that are usually located at the outermost position of the polysaccharide chains attached to glycoproteins or glycolipids. Because of their negative charge, they may specifically or nonspecifically repel cell-cell interactions; they also serve as the ligands for various lectins (56). Selectins are the sialic acid-binding lectins that are found on blood cells or endothelial cells. It was proposed that interaction between sialic acids and selectins is involved in adhesion of leukocytes to the vascular endothelium (56). Another sialic acid-binding lectin is factor H that inhibits activation of the alternative complement pathway (35). Sialidase treatment of the cells has been shown to promote complement activation in vitro (14, 19, 33). However, in vivo, the apical surface of the airway epithelium does not have direct contact with the complement factors that are normally confined to the blood. It is therefore unclear what the physiological roles of sialic acids are on the airway surface other than serving as receptors for influenza virus, as well as parainfluenza virus (17).

Sialidase activities are normally present in many human tissues, including the salivary glands and the lungs (1); the in vivo effect of sialidase treatment has been previously evaluated in the context of airway hyperreactivity. *V. cholerae* sialidase was administered intratracheally in guinea pigs, and the sialidase treatment significantly reduced substance P-induced bronchoconstriction (21). Similar results were also obtained using *C. perfringens* sialidase and the isolated trachea and lungs from guinea pigs and rats. Again, sialidase treatment had no effect on smooth muscle contractions induced by acetylcholine, histamine, and 5-hydroxytryptamine, and it inhibited tracheal contraction induced by ovalbumin or compound 48/80 (22). Sialidase treatment did not change the rheological properties of respiratory mucus, nor did it affect the normal mucus transport activity on ciliated epithelium (25, 32). Extensive in vivo safety evaluations of DAS181 are being planned. Our current preliminary in vitro and in vivo data indicated a healthy safety margin for the drug candidate.

Cellular adhesion by some of the most important respiratory bacteria, including *Haemophilus influenzae* (10, 24, 55), *Streptococcus pneumoniae* (4), and *Pseudomonas aeruginosa* (3, 16, 28, 39, 40, 43), have been reported to be mediated by binding to the sialic acid receptors on the host cells. Sialidase treatment of human pharyngeal epithelial cells inhibited adherence by *H. influenzae* (24). Peltola et al. reported that mice infected with recombinant influenza viruses that carried higher neuraminidase (NA) activities were associated with a higher incidence of secondary pneumonia after inoculation with type 2 *S. pneumoniae* D39 strain. The authors hypothesized that desialylation by the viral NA may cause increased cell binding by *S. pneu-*

moniae (30, 36, 37). However, using a type 19 *S. pneumoniae* strain, Seki et al. failed to demonstrate potentiated secondary bacterial pneumonia following influenza virus infection unless the mice were chronically colonized with *P. aeruginosa* (45). In light of these conflicting reports, we performed several experiments in vitro to observe cell adhesion by different strains of *S. pneumoniae* and *H. influenzae* to A549 cells. Over a broad range of bacterial input, DAS181 treatment did not increase cell adhesion by four strains of *S. pneumoniae* (including the D39 strain), nor did it increase cell adhesion by three strains of *H. influenzae* (unpublished results). Further evaluations on this issue will be carried out in vivo.

The sialidase fusion protein DAS181 represents a novel, potentially broad-spectrum influenza therapeutic agent. Although DAS181 is designed to be nonimmunogenic to humans, immunogenicity remains an important issue to be evaluated by animal studies and clinical trials. By utilizing the *A. viscosus* sialidase that can effectively degrade receptor sialic acids for both human and avian IFVs, DAS181 potentially confers protection against a very broad range of influenza viruses, including the future pandemic viruses. It may also remain effective when viral strains change yearly. A recent report indicated that an IFV reassortant generated in the laboratory used a less common form of sialic acids, α(2,8)-linked sialic acid, as the receptor (58). Interestingly, *A. viscosus* sialidase can cleave the α(2,8)-linked sialic acid as well (54). Since DAS181 targets cellular receptors rather than a viral gene product, the chance of influenza viruses developing drug resistance is decreased. Besides serving as receptors for influenza virus, sialic acids are also used as receptors by parainfluenza virus, some bacteria, and bacterial toxins (57). Therefore, the potential therapeutic value of DAS181 may go beyond influenza prophylaxis and treatment and warrants further evaluation.

ACKNOWLEDGMENTS

This study was supported in part by NIH grant R43AI056786 and contracts NO1-AI-30048 and NO1-AI-15435 from the Virology branch, National Institute of Allergy and Infectious Diseases. M.P.M., L.M.A., D.H.K., A.I., E.R.C., M.Y., and F.F. declare that they have competing financial interests. D.F.S., M.K.W., R.W.S., L.V.G., V.P.M., and F.G.H. declare that they have no competing financial interests.

REFERENCES

1. **Achyuthan, K. E., and A. M. Achyuthan.** 2001. Comparative enzymology, biochemistry, and pathophysiology of human exo-α-sialidases (neuraminidases). Comp. Biochem. Physiol. B Biochem. Mol. Biol. **129**:29–64.
2. **Air, G. M., and W. G. Laver.** 1995. Red cells bound to influenza virus N9 neuraminidase are not released by the N9 neuraminidase activity. Virology **211**:278–284.
3. **Baker, N., G. C. Hansson, H. Leffler, G. Riise, and C. Svanborg-Eden.** 1990. Glycosphingolipid receptors for *Pseudomonas aeruginosa*. Infect. Immun. **58**:2361–2366.
4. **Barthelson, R., A. Mobasseri, D. Zopf, and P. Simon.** 1998. Adherence of *Streptococcus pneumoniae* to respiratory epithelial cells is inhibited by sialylated oligosaccharides. Infect. Immun. **66**:1439–1444.
5. **Beigel, J. H., J. Farrar, A. M. Han, F. G. Hayden, R. Hyer, M. D. de Jong, S. Lochindarat, T. K. Nguyen, T. H. Nguyen, T. H. Tran, A. Nicoll, S. Touch, and K. Y. Yuen.** 2005. Avian influenza A (H5N1) infection in humans. N. Engl. J. Med. **353**:1374–1385.
6. **Bergelson, L. D., A. G. Bukrinskaya, N. V. Prokazova, G. I. Shaposhnikova, S. L. Kocharov, V. P. Shevchenko, G. V. Kornilaeva, and E. V. Fomina-Ageeva.** 1982. Role of gangliosides in reception of influenza virus. Eur. J. Biochem. **128**:467–474.
7. **Chen, H., G. Deng, Z. Li, G. Tian, Y. Li, P. Jiao, L. Zhang, Z. Liu, R. G. Webster, and K. Yu.** 2004. The evolution of H5N1 influenza viruses in ducks in southern China. Proc. Natl. Acad. Sci. USA **101**:10452–10457.
8. **Drzeniek, R.** 1973. Substrate specificity of neuraminidases. Histochem. J. **5**:271–290.
9. **Els, M. C., W. G. Laver, and G. M. Air.** 1989. Sialic acid is cleaved from glycoconjugates at the cell surface when influenza virus neuraminidases are expressed from recombinant vaccinia viruses. Virology **170**:346–351.
10. **Fakih, M. G., T. F. Murphy, M. A. Pattoli, and C. S. Berenson.** 1997. Specific binding of *Haemophilus influenzae* to minor gangliosides of human respiratory epithelial cells. Infect. Immun. **65**:1695–1700.
11. **Gaskell, A., S. Crennell, and G. Taylor.** 1995. The three domains of a bacterial sialidase: a beta-propeller, an immunoglobulin module and a galactose-binding jelly-roll. Structure **3**:1197–1205.
12. **Gottschalk, A.** 1959. The Viruses. Academic Press, Inc., New York, N.Y.
13. **Griffin, J. A., S. Basak, and R. W. Compans.** 1983. Effects of hexose starvation and the role of sialic acid in influenza virus release. Virology **125**:324–334.
14. **Gutierrez, C., M. J. Martin, and K. A. Brown.** 1987. Complement activation by human lymphocytes from different lymphoid organs: role of sialic acid and lack of relationship to electrical surface charge. Complement **4**:99–109.
15. **Hassid, S., G. Choufani, N. Nagy, H. Kaltner, A. Danguy, H. J. Gabius, and R. Kiss.** 1999. Quantitative glycohistochemical characterization of normal nasal mucosa, and of single as opposed to massive nasal polyps. Ann. Otol. Rhinol. Laryngol. **108**:797–805.
16. **Hazlett, L. D., M. Moon, and R. S. Berk.** 1986. In vivo identification of sialic acid as the ocular receptor for *Pseudomonas aeruginosa*. Infect. Immun. **51**:687–689.
17. **Henrickson, K. J.** 2003. Parainfluenza viruses. Clin. Microbiol. Rev. **16**:242–264.
18. **Hierholzer, J. C., and R. A. Killington.** 1996. Virus isolation and quantitation, p. 25–46. *In* B. W. J. Mahy and H. O. Kangro (ed.), Virology methods manual. Academic Press, Ltd., London, England.
19. **Hirsch, R. L., J. S. Wolinsky, and J. A. Winkelstein.** 1986. Activation of the alternative complement pathway by mumps infected cells: relationship to viral neuraminidase activity. Arch. Virol. **87**:181–190.
20. **Ito, T.** 2000. Interspecies transmission and receptor recognition of influenza A viruses. Microbiol. Immunol. **44**:423–430.
21. **Jarreau, P. H., A. Harf, M. Levame, C. R. Lambre, H. Lorino, and I. Macquin-Mavier.** 1992. Effects of neuraminidase on airway reactivity in the guinea pig. Am. Rev. Respir. Dis. **145**:906–910.
22. **Kai, H., K. Makise, S. Matsumoto, T. Ishii, K. Takahama, Y. Isohama, and T. Miyata.** 1992. The influence of neuraminidase treatment on tracheal smooth muscle contraction. Eur. J. Pharmacol. **220**:181–185.
23. **Kannan, S., R. A. Lakku, D. Niranjali, K. Jayakumar, A. H. Steven, V. V. Taralakshmi, S. Chandramohan, R. Balakrishnan, C. Schmidt, and D. Halagowder.** 2003. Expression of peanut agglutinin-binding mucin-type glycoprotein in human esophageal squamous cell carcinoma as a marker. Mol. Cancer **2**:38.
24. **Kawakami, K., K. Ahmed, Y. Utsunomiya, N. Rikitomi, A. Hori, K. Oishi, and T. Nagatake.** 1998. Attachment of nontypable *Haemophilus influenzae* to human pharyngeal epithelial cells mediated by a ganglioside receptor. Microbiol. Immunol. **42**:697–702.
25. **King, M., A. Gilboa, F. A. Meyer, and A. Silberberg.** 1974. On the transport of mucus and its rheologic simulants in ciliated systems. Am. Rev. Respir. Dis. **110**:740–745.
26. **Kiso, M., Y. Sakai-Tagawa, K. Shiraishi, C. Kawakami, K. Kimura, F. G. Hayden, N. Sugaya, and Y. Kawaoka.** 2004. Resistant influenza A viruses in children treated with oseltamivir: descriptive study. Lancet **364**:759–765.
27. **Le, Q. M., M. Kiso, K. Someya, Y. T. Sakai, T. H. Nguyen, K. H. Nguyen, N. D. Pham, H. H. Ngyen, S. Yamada, Y. Muramoto, T. Horimoto, A. Takada, H. Goto, T. Suzuki, Y. Suzuki, and Y. Kawaoka.** 2005. Avian flu: isolation of drug-resistant H5N1 virus. Nature **437**:1108.
28. **Marcus, H., A. Austria, and N. R. Baker.** 1989. Adherence of *Pseudomonas aeruginosa* to tracheal epithelium. Infect. Immun. **57**:1050–1053.
29. **Matrosovich, M. N., T. Y. Matrasovich, T. Gray, N. A. Roberts, and H. D. Klenk.** 2004. Human and avian influenza viruses target different cell types in cultures of human airway epithelium. Proc. Natl. Acad. Sci. USA **101**:4620–4624.
30. **McCullers, J. A., and K. C. Bartmess.** 2003. Role of neuraminidase in lethal synergism between influenza virus and *Streptococcus pneumoniae*. J. Infect. Dis. **187**:1000–1009.
31. **Mendel, D. B., C. Y. Tai, P. A. Escarpe, W. Li, R. W. Sidwell, J. H. Huffman, C. Sweet, K. J. Jakeman, J. Merson, S. A. Lacy, W. Lew, M. A. Williams, L. Zhang, M. S. Chen, N. Bischofberger, and C. U. Kim.** 1998. Oral administration of a prodrug of the influenza virus neuraminidase inhibitor GS 4071 protects mice and ferrets against influenza infection. Antimicrob. Agents Chemother. **42**:640–646.
32. **Meyer, F. A., M. King, and R. A. Gelman.** 1975. On the role of sialic acid in the rheological properties of mucus. Biochim. Biophys. Acta **392**:223–232.
33. **Michalek, M. T., E. G. Bremer, and C. Mold.** 1988. Effect of gangliosides on activation of the alternative pathway of human complement. J. Immunol. **140**:1581–1587.
34. **Monti, E., A. Preti, C. Nesti, A. Ballabio, and G. Borsani.** 1999. Expression of a novel human sialidase encoded by the *NEU2* gene. Glycobiology **9**:1313–1321.
35. **Pangburn, M. K., K. L. Pangburn, V. Koistinen, S. Meri, and A. K. Sharma.**

2000. Molecular mechanisms of target recognition in an innate immune system: interactions among factor H, C3b, and target in the alternative pathway of human complement. J. Immunol. 164:4742–4751.
36. Peltola, V. T., and J. A. McCullers. 2004. Respiratory viruses predisposing to bacterial infections: role of neuraminidase. Pediatr. Infect. Dis. J. 23:S87–S97.
37. Peltola, V. T., K. G. Murti, and J. A. McCullers. 2005. Influenza virus neuraminidase contributes to secondary bacterial pneumonia. J. Infect. Dis. 192:249–257.
38. Potier, M., L. Mameli, M. Belisle, L. Dallaire, and S. B. Melancon. 1979. Fluorometric assay of neuraminidase with a sodium (4-methylumbelliferyl-α-D-*N*-acetylneuraminate) substrate. Anal. Biochem. 94:287–296.
39. Ramphal, R., and M. Pyle. 1983. Evidence for mucins and sialic acid as receptors for *Pseudomonas aeruginosa* in the lower respiratory tract. Infect. Immun. 41:339–344.
40. Ramphal, R., and M. Pyle. 1985. Further characterization of the tracheal receptor for *Pseudomonas aeruginosa*. Eur. J. Clin. Microbiol. 4:160–162.
41. Reichner, J. S., S. W. Whiteheart, and G. W. Hart. 1988. Intracellular trafficking of cell surface sialoglycoconjugates. J. Biol. Chem. 263:16316–16326.
42. Reuman, P. D., S. Keely, and G. M. Schiff. 1989. Assessment of signs of influenza illness in the ferret model. J. Virol. Methods 24:27–34.
43. Saiman, L., G. Cacalano, D. Gruenert, and A. Prince. 1992. Comparison of adherence of *Pseudomonas aeruginosa* to respiratory epithelial cells from cystic fibrosis patients and healthy subjects. Infect. Immun. 60:2808–2814.
44. Schauer, R. 1982. Chemistry, metabolism, and biological functions of sialic acids. Adv. Carbohydr. Chem. Biochem. 40:131–234.
45. Seki, M., Y. Higashiyama, K. Tomono, K. Yanagihara, H. Ohno, Y. Kaneko, K. Izumiknwa, Y. Miyazaki, Y. Hirakata, Y. Mizuta, T. Tashiro, and S. Kohno. 2004. Acute infection with influenza virus enhances susceptibility to fatal pneumonia following *Streptococcus pneumoniae* infection in mice with chronic pulmonary colonization with *Pseudomonas aeruginosa*. Clin. Exp. Immunol. 137:35–40.
46. Shoyab, M., G. D. Plowman, V. L. McDonald, J. G. Bradley, and G. J. Todaro. 1989. Structure and function of human amphiregulin: a member of the epidermal growth factor family. Science 243:1074–1076.
47. Sidwell, R. W., J. H. Huffman, E. W. Call, H. Alaghamandan, P. D. Cook, and R. K. Robins. 1986. Effect of selenazofurin on influenza A and B virus infections of mice. Antivir. Res. 6:343–353.
48. Sidwell, R. W., J. H. Huffman, J. Gilbert, B. Moscon, G. Pedersen, R. Burger, and R. P. Warren. 1992. Utilization of pulse oximetry for the study of the inhibitory effects of antiviral agents on influenza virus in mice. Antimicrob. Agents Chemother. 36:473–476.
49. Sinn, P. L., G. Williams, S. Vongpunsawad, R. Cattaneo, and P. B. McCray, Jr. 2002. Measles virus preferentially transduces the basolateral surface of well-differentiated human airway epithelia. J. Virol. 76:2403–2409.
50. Smee, D. F., J. H. Huffman, A. C. Morrison, D. L. Barnard, and R. W. Sidwell. 2001. Cyclopentane neuraminidase inhibitors with potent in vitro anti-influenza virus activities. Antimicrob. Agents Chemother. 45:743–748.
51. Smith, H., and C. Sweet. 1988. Lessons for human influenza from pathogenicity studies with ferrets. Rev. Infect. Dis. 10:56–75.
52. Stray, S. J., R. D. Cummings, and G. M. Air. 2000. Influenza virus infection of desialylated cells. Glycobiology 10:649–658.
53. Sutter, V. L. 1984. Anaerobes as normal oral flora. Rev. Infect. Dis. 6:S62–S66.
54. Teufel, M., P. Roggentin, and R. Schauer. 1989. Properties of sialidase isolated from *Actinomyces viscosus* DSM 43798. Biol. Chem. Hoppe-Seyler 370:435–443.
55. van Alphen, L., L. Geelen-van den Broek, L. Blaas, M. van Ham, and J. Dankert. 1991. Blocking of fimbria-mediated adherence of *Haemophilus influenzae* by sialyl gangliosides. Infect. Immun. 59:4473–4477.
56. Varki, A. 1992. Selectins and other mammalian sialic acid-binding lectins. Curr. Opin. Cell Biol. 4:257–266.
57. Varki, A. 1997. Sialic acids as ligands in recognition phenomena. FASEB J. 11:248–255.
58. Wu, W., and G. M. Air. 2004. Binding of influenza viruses to sialic acids: reassortant viruses with A/NWS/33 hemagglutinin bind to α2,8-linked sialic acid. Virology 325:340–350.
59. Yeung, M. K. 1993. Complete nucleotide sequence of the *Actinomyces viscosus* T14V sialidase gene: presence of a conserved repeating sequence among strains of *Actinomyces* spp. Infect. Immun. 61:109–116.
60. Zhang, L., M. E. Peeples, R. C. Boucher, P. L. Collins, and R. J. Pickles. 2002. Respiratory syncytial virus infection of human airway epithelial cells is polarized, specific to ciliated cells, and without obvious cytopathology. J. Virol. 76:5654–5666.